LUT UNIVERSITY
School of Energy Systems
Mechanical Engineering

Tuomas Kekki

AFFECTING FACTORS FOR LARGE RADIAL SHAFT SEAL LUBRICANT LEAK RATE

6.12.2021

Examiners: Professor Harri Eskelinen
M.Sc. (Tech.) Riku Liira

TIIVISTELMÄ

LUT-Yliopisto
LUT School of Energy Systems
LUT Mechanical Engineering

Tuomas Kekki

Suurikokoisen huulitiivisteen voiteluaineen vuotomäärään vaikuttavat tekijät

Diplomityö

2021

145 sivua, 94 kuvaa, 8 taulukkoa ja 6 liitettä

Tarkastajat: Professori Harri Eskelinen
DI Riku Liira

Hakusanat: Huulitiiviste, elastomeeri, vuotomäärä

Huulitiivisteet ovat hyvin yleisesti käytettyjä komponentteja koneenrakennuksessa – huulitiivisteitä käytetään suuressa osassa koneista, joissa on pyöriviä akseleita. Ideaalimaailmassa huulitiivisteet olisivat täysin vuodottomia, mutta tämä on harvoin todellisuutta varsinkaan operointituntien kasvaessa. Tyypillisesti tutkimukset keskittyvät suhteellisen pienikokoisiin tiivisteisiin ja täten suurikokoisten huulitiivisteiden suorituskyky eri olosuhteissa ei ole hyvin tunnettua.

Huulitiivisteen suorituskykyyn, elinikään ja vuotomäärään vaikuttaa monia eri tekijöitä olitpa ne sitten suuria tai pieniä. Diplomityön ensimmäisessä osassa tutustutaan huulitiivisteiden perusteisiin kuten materiaaleihin, tiivistysmekanismiin, voiteluominaisuuksiin, suorituskykyyn värähtelyssä sekä tyypillisiin vauriomekanismeihin.

Diplomityön jälkimmäisessä osassa muodostetaan syyseuraus kaavio, jossa arvioidaan mahdollisia syitä voiteluaineen vuodolle. Työssä suoritetaan myös sarja testejä vaihtelevissa käyttöolosuhteissa täysikokokoiselle suuren akselihalkaisijan tiivistejärjestelmälle, jossa eri tiivistehuulilla on erilaiset voiteluominaisuudet. Testeissä mitattua suorituskykyä vertaillaan asiakasyrityksen laitteista saatuihin tietoihin.

ABSTRACT

LUT University
LUT School of Energy Systems
LUT Mechanical Engineering

Tuomas Kekki

Affecting factors for large radial shaft seal lubricant leak rate

Master's thesis

2021

145 pages, 94 figures, 8 tables and 6 appendices

Examiners: Professor Harri Eskelinen
M.Sc. (Tech.) Riku Liira

Keywords: Radial sealing ring, elastomer, leakage rate

Radial sealing rings are very common machine elements, and they are used in majority of machines with rotating shafts. In ideal world the sealing rings would be leak-free, but that is rarely the case in reality especially when the number of operational hours increase. Typically, research focusing on sealing rings is considering only relatively small size sealing rings, and the performance of large radial shaft seals in different operational conditions is not well known.

In general, there are numerous different factors affecting the performance, lifetime and leakage rate of radial sealing rings whether they are large or small. The first part of this thesis introduces basic information regarding sealing rings, such as material properties, sealing mechanism, lubrication properties, performance under misalignment and failure mechanisms.

In the latter part of the thesis a cause-and-effect diagram for possible causes for lubricant leakage is created, and a series a tests with varying operational conditions are performed on a full scale large diameter seal system with several sealing rings with different lubrication conditions affecting the sealing rings. The seal system performance in different operational conditions is evaluated and the results are compared to available data of sealing rings used in customer company's applications.

ACKNOWLEDGEMENTS

I want to thank my thesis examiners Professor Harri Eskelinen and Riku Liira for their guidance throughout this project. I would also like to thank all the numerous experts who gave their insights for this work.

An especially warm thanks to my family, Marjo, Pihla and the little baby boy.

Porvoo 6.12.2021

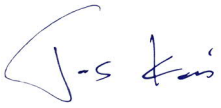

Tuomas Kekki

TABLE OF CONTENTS

SYMBOLS AND ABBREVIATIONS

Roman characters

b	Contact width	$[mm]$
F_{rtot}	Total radial force on the contact	$\left[\frac{N}{mm^2}\right]$
G	Hydrodynamic duty parameter	[-]
H	Hardness	[*Shore A*]
K	Seal specific wear coefficient	[-]
N	Rotation speed	$\left[\frac{m}{s}\right]$
P	Surface pressure	$\left[\frac{N}{mm^2}\right]$
R_s	Shaft radius	$[mm]$
s	Sliding distance	$[m]$
T	Frictional torque	$[Nm]$
u	Velocity in surface contact	$\left[\frac{m}{s}\right]$
V	Wear volume	$[m^3]$
Q	Radial force in seal – shaft contact	$\left[\frac{N}{mm^2}\right]$

Greek characters

ε	Radial misalignment	[mm]
η	Dynamic viscosity	$[Pa \cdot s]$
λ	Lambda ratio	[-]
μ	Friction coefficient	[-]
Φ	Seal specific proportionality factor	[-]

Abbreviations

ASTM	American Society for Testing and Materials
AW	Anti-wear
EHL	Elastohydrodynamic lubrication

EP	Extreme pressure
FKM, FPM	Fluorocarbon elastomer
FSR	Fluorosilicone rubber
GESAMP	Joint Group of Experts on the Scientific Aspects of Marine Environmental Protection
ISO	International Organization for Standardization
LIF	Laser Induced Fluorescence method
NBR	Nitrile rubber
NHBR	Hydrogenated nitrile rubber
NOAA	National oceanic and atmospheric administration
RMS	Root mean square

1 INTRODUCTION

Large radial shaft seals are used to seal large diameter ship propeller shafts in the case company's products. There are many different factors affecting to the leak rate of radial shaft seals. The main objective of this thesis is to gather the main affecting factors and their effect to the leak rate.

1.1 Motivation

Radial shaft seal design, lubrication and leak rate have been studied extensively as radial shaft seals are very commonly used in different fields of industry. However vast majority of the studies focus on the behavior of radial shaft seals that have very low or negligible pressure difference, oil, or other liquid present only on one side of the seal and relatively low diameter (typically under ø 100 mm). Factors behind the leak rate of large radial seals and especially pressurized seal systems are not fully available in literature which gives a challenge for the execution of this thesis but also great motivation for the research.

Excessive leakage rate on radial shaft seals used in the case company's product can lead to off-hire seal change either in dry-dock or underwater wet-dock. It goes without saying that off-hire seal changes create great costs for the case company and their customers when their vessels are out of duty on an unplanned repair. In addition, high leakage rates create material and labor costs for the ship owners when lubricant must be added constantly. Today, environmental aspects are getting more and more important also in the shipping industry, and thus it is also extremely important to prevent lubricant leakage to water.

1.2 Objectives

There are many assumptions and generalizations regarding the affecting factors for radial shaft seal lubricant leakage in the case company's products. Many of these are made without thorough research and thus they are found to be somewhat unreliable. The objective for the thesis is to gather state of the art knowledge regarding radial shaft seals, and to determine the main affecting factors for lubricant leakage in radial shaft seals used in the case company's product by performing a series of tests in a test device made for testing of the seals used by the case company.

A cause-and-effect diagram focusing on the affecting factors is created based on literature and testing to give the case company a tool to recognize some of the factors behind the seal leak rate. Knowing the factors behind the seal leak rate will help the case company to avoid conditions that increase the leak rate gratuitously.

1.3 Research problem

The research problem is related to the sealing rings response to different operational conditions present in the customer company's product. How does changing of one input parameter change the overall seal system response and most importantly the lubricant leakage rate.

1.4 Research questions

Four research questions were defined to answer one larger upper-level research question "What are the main factors behind leak rate of a large radial shaft seal?". The research questions are listed below with a brief explanation of how this thesis aims to answer these questions. For all the questions, a literature review is performed to find existing research data to find out if there is correlation between the variable and leakage rate. It is also good to understand that the variables in each research question have an influence on each other. For example, shaft surface speed will influence the heat generation of the seal and thus it is difficult to perform testing that will only change one variable.

1. How does the surface speed and viscosity of the used lubricant affect the leak rate? Testing with different shaft speeds and lubricant temperatures are performed on the test device to see the lubricants viscosity and surface speed effect on the leak rate.
2. How does the pressure difference between the two sides of the seal affect the leak rate? Tested seal system has many different pressure differences effecting over the sealing rings which will help to answer this research question.
3. How does shaft misalignment, static or dynamic, affect the leak rate? Testing with different shaft misalignments, both static and dynamic, are performed to answer this question.
4. How does the wearing or damage of the sealing ring affect the leak rate?

sealing rings are visually inspected, and leakage rate reports form operating vessels with the case company's products are reviewed.

1.5 Research methods

In the first part of this thesis the theory behind radial shaft seal lubrication and leakage is studied to better understand the phenomena that are present in the actual application and in the test device. A survey of reported amount of oil leakages in the shipping industry is performed to understand why lubricant leakages are an issue worth looking into in the first place.

In this thesis, quantitative methods are used, and they are focused on the tests performed on the test device and in analyzing the test results. Suitable distribution plots and curve fittings are created to analyze correlation between different inputs' effect on the seal leak rate. Well controlled and repetitive test conditions are produced to receive reliable test results.

1.6 Scope

This thesis is restricted to cover sealing ring designs that is relevant for the case company's products. Based on the cause-and-effect diagram and performed tests, the existing design can be developed in future to minimize leakage. Concept creation and actual product development are ruled out from this thesis.

Mathematical models and simulations are also ruled out from this thesis even though some are reviewed as they are relevant when comparing literature findings to obtained test results. In addition, some simulations were done by the case company based on information obtained from testing. Some of these simulation results are used in this thesis but performing the simulations are not on the scope of this thesis.

2 METHODS

As the subject for the thesis is relatively large and complex, a thorough literature review is required together with testing. The research was performed by performing a thorough literature review, examining of operating vessel reports, case company data, operating environment and used sealing rings, and by performing a series of tests with a test device. A cause-and-effect diagram was created based on the literature review and information from the case company. Test parameters were chosen based on the available information of the case company's product. Test data and the used sealing rings were analyzed, and the results are compared with available studies and with assumptions made in the cause-and-effect diagram so that causes for lubricant leakage can be verified or discarded.

2.1 Literature review

As one of the goals of the thesis is to gather state of the art knowledge regarding radial shaft seals, the literature review is executed as an exploratory literature review. Studies and textbooks related to radial shaft seals and materials used in the seals are reviewed to compose an up-to-date summary of the subject. LUT Primo scientific library together with Springer and Elsevier databases are used as the main sources for searching information for the literature review. General internet search engine searches are also used.

2.2 Seal system, operating environment, and reports from operating vessels

The seal system used in the case company's product is explained in a general level. Relevant drawings, system- and function descriptions and tacit knowledge are used to give the overall understanding of the seal system.

The operating environment of the case company's product is relatively well known in the case company when the shaft speeds and pressure differences are considered. The relevant data are extracted from relevant technical documents available in the case company. The vibration conditions present in the case company's product is based on research performed in one of vessels that use the case company's products.

Reports given by ship crews together with available sensor data are used in defining the baseline for the lubricant leakage rate.

2.3 Test arrangements

The test arrangements for the tests performed with the test device are divided into temperature tests, static misalignment and dynamic misalignment tests.

2.3.1 Temperature test arrangements

A series of tests with different shaft speeds and pressure differences over sealing rings 3 and 4 are performed to find the overall system temperature and system response to different operational conditions.

Two shaft speed sweep tests with increasing shaft speeds are performed on two different water pressures, 1,14 bar and 1,57 bar. In these tests seal chamber 4 pressure is not adjusted, so only the radial load of sealing ring 4 is changed. The purpose of the sweep tests is to find the systems overall temperature behavior with two different water pressures and shaft speeds. In the sweep tests the shaft speed is increased gradually. One shaft speed is kept until the sealing ring and seal chamber temperatures have evened.

The effect of radial force on sealing ring 3 is tested with three different pressure differences and shaft speeds to find the effect of radial load to the temperature and shaft torque.

The effect of radial force on sealing ring 4 is tested with four different pressure differences and two shaft speeds to find the effect of radial load to the temperature. The effect of the radial force on sealing ring 4 to the shaft torque is tested with three different pressure differences at one shaft speed.

The temperature tests help answering how radial force affects the temperature of the seal system and give an answer if high temperature related causes in the cause-and-effect diagram can be confirmed or discarded. A baseline of the lubricant leakage rate for vibration testing can also be defined.

2.3.2 Static misalignment test arrangements

Static misalignment tests are divided into two parts – to tests with a standstill shaft and to tests with rotating shaft.

In the first part, the static misalignment tests are performed to find the sealing rings ultimate performance under static misalignment. These tests are performed with non-rotating shaft at room temperature. The static misalignment is increased gradually until lubricant leakage occurs, or mechanical limits for shaft misalignment are reached. The first test is performed without water in the water tank and the other test is performed with water in the water tank.

In the second static misalignment test the shaft is rotated with a constant speed and misalignment is increased gradually to see the effect of static misalignment on the temperature of the sealing rings.

The static misalignment tests answer the question whether static misalignment caused by manufacturing and assembly tolerances can cause leakage or excessive temperature. The static misalignment test results also help when analyzing the dynamic misalignment test results – is the systems capability to follow dynamic misalignment the same than static misalignment.

2.3.3 Dynamic misalignment test arrangements

The seal system response to dynamic misalignment on radial direction is tested with several different vibration amplitudes at 5 Hz vibration frequency. Tests were run also with two other frequencies, but the results are not reported on this thesis.

In the first test vibration amplitude is increased gradually with steady shaft speed until heavy leakage to find the seal system’s ultimate performance against dynamic radial misalignment.

In the following tests the effect of shaft speed and sealing ring 3 pressure difference with constant vibration amplitude is tested. The purpose of these tests is to find how shaft speed and sealing ring 3 pressure difference affects the seal system leak rate.

The dynamic misalignment tests help to answer the questions related to dynamics in the cause-and-effect diagram.

3 OIL LUBRICATED PROPELLER SHAFT SEALS

Propeller shaft seals are referred usually as stern tube seals, which refers to ships equipped with a shaft line that is supported with a slide bearing. The stern tube is a hollow tube where the slide bearing and other related components such as the stern tube seals are located. The term propeller shaft seal is used in this thesis because it does not rule out propeller shafts that do not have a stern tube. This thesis is also limited to the seals having water – oil interface and seals that are preventing lubrication oil from entering the ship are ruled out.

Typical oil lubricated propeller shaft seals consist of several sealing rings, usually four. Two of the sealing rings are separating water from the lubrication oil, and two seals are used to prevent oil from entering water. Typically, a wear element, a liner, is used on the shaft under the sealing rings. (Flitney 2007, p. 147.) Several suppliers are providing seals fitting this description. In addition, they have some variation in the direction of which the seals are, but all have at least two seals facing water and one facing the seal oil. They all also provide a system where oil and water are separated with an air chamber that can be drained. There are two variations in the working principle of the air chamber, one variation has higher pressure in the air chamber than in water, which makes air to constantly leak out to water. In the other variation the air pressure is lower than water pressure and thus air does not leak out. (Kemel Eagle Industry 2021a; Kemel Eagle Industry 2021b; Lagersmit 2020; SKF 2016a; SKF 2016b; Wärtsilä 2020.) Section views of typical propeller shaft seal arrangements are presented in **Figure 1**.

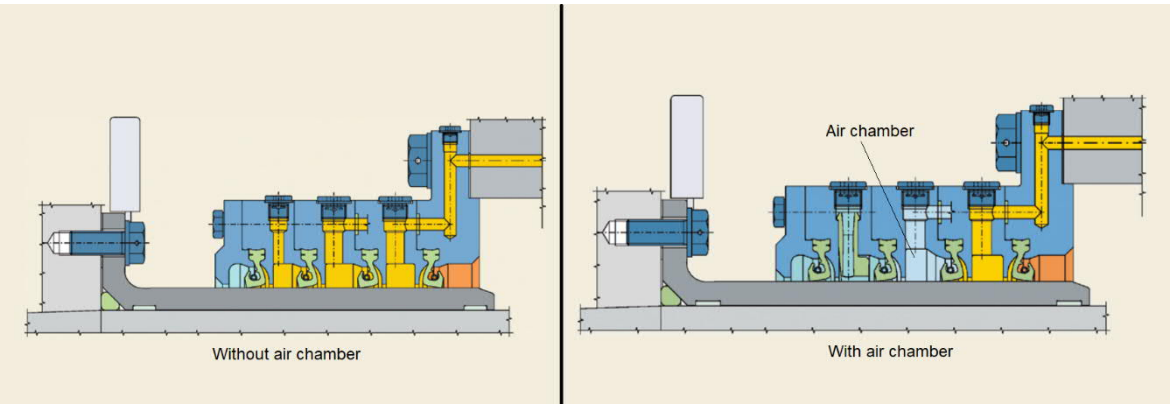

Figure 1. Typical propeller shaft seal arrangements (Mod. SKF 2016a; SKF 2016b).

As ship shaft lines are submerged relatively deep into water, the hydrostatic pressure of water creates radial load on the sealing rings. The pressure differences over individual seals are balanced using hydrostatic pressure of the seal oil. In cases where the design has an air chamber air pressure can also be used to balance pressure differences over the sealing rings. (Kemel Eagle Industry 2021a; Kemel Eagle Industry 2021b; Lagersmit 2020; SKF 2016a; SKF 2016b.) A schematic view of a typical propeller shaft seal system with air chamber is presented in **Figure 2**.

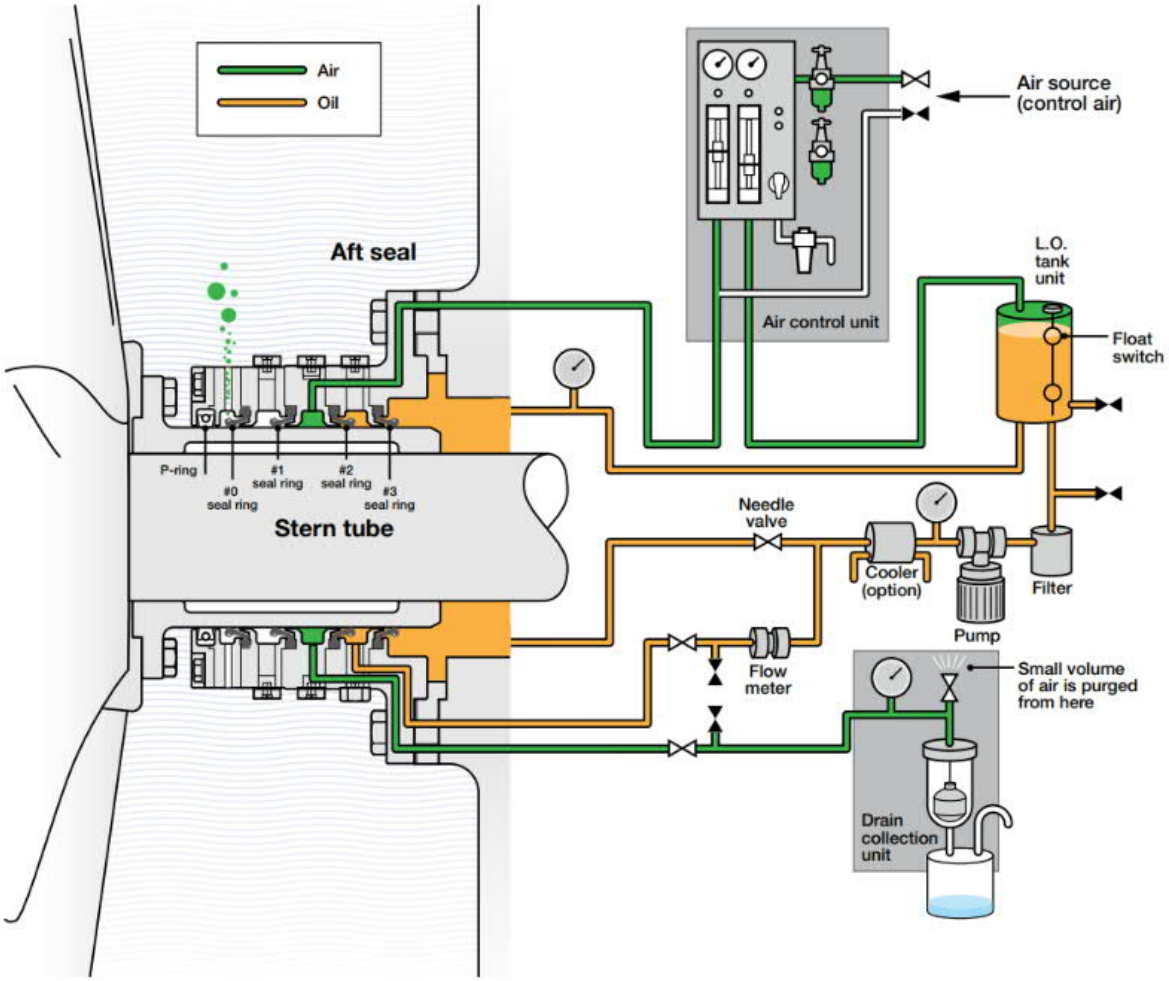

Figure 2. Schematic view of a typical propeller shaft seal system with air chamber (Wärtsilä 2020, p. 8).

3.1 Lubricant leakage from propeller shaft seals

Lubricant leakage from sealed compartments is naturally an unwanted event from whatever device the lubricant leaks out from. Lubricant leakage is even more harmful in some applications as in the application in subject of the thesis – ship propeller shaft seals, as lubricant leaking out from the propeller shaft ends up to marine waters.

Most ships that operate in the world's oceans are equipped with propeller shaft seals that use oil as a lubricant (Etkin 2008, p. 1). A study on lubricant leakage from ships to sea, focusing on lubricant leakage to the Mediterranean Sea showed that even though there are several of potential sources of lubricant leakage in sea-going ships, such as rudder bearings, thrusters, controllable pitch propellers etc., the largest source of lubricant leakages is the ships propeller shaft seals (Pavlakis et al. 2001, p. 13). Based on the study by Pavlakis et. al. (2001, p. 13), the majority of the leakage is not due to accidents but as a result of normal ship operation. Lubricant leakage from the propeller shaft seals is widely seen as operational consumption, which is considered normal (Etkin 2008, p. 1; Carter 2009, p. 1; Seal manufacturer 1, 2021).

A study of focusing on oil discharges to sea was performed by Joint Group of Experts on the Scientific Aspects of Marine Environmental Protection (GESAMP) on 2007. The study revealed that normal ship operation causes 457 million liters of oil entering marine waters annually (GESAMP 2007, p. 8). The GESAMP study did not separate propeller shaft leakages as an own source within the ships' total leakage, and there are no exact numbers for the total amount of lubricant lost to sea from propeller shaft seals, but there are a few estimates available. Both Carter (Carter 2009, p. 1) and (Thornhill 2014, p. 2) estimate that up to 80 million liters of oil from propeller shaft seals leak to marine waters. Based on the study performed by Etkin (2008, p. 14), the total annual propeller shaft leakage is between 4,6 to 32,6 million liters. Even though there is a big difference between the numbers provided by Carter and Thornhill compared to the ones presented by Etkin, based on these numbers it is easy to say that the lubricant leakage from the propeller shaft seals is a quite lager portion of the total quantity of the lubricant discharges.

4 RADIAL SHAFT SEALS

This chapter introduces basic radial shaft seal design and theory behind sealing ring lubrication, leak rate and failure mechanisms. Only spring-loaded seals are being covered as that is the case in the experimental part of this thesis. The seals in the case company's product are very large compared to the common radial shaft seals used in industry. As radial shaft seals are very commonly used in different applications, there are several standards focusing on them, for example ISO 6194, which covers nominal dimensions and tolerances, vocabulary, storage, handling and installation, performance test procedures and identification of visual imperfections (ISO 6194-1 2007; ISO 6194-2 2009; ISO 6194-3 2009; ISO 6194-4 2009; ISO 6194-5 2008). ISO 6194 limits to 200 mm diameter in the shaft size and most of the literature available focus on seals that are considered small compared to the case company's products. For that reason, some of the dimensions given in the following chapters apply on smaller size seals and differ from the case company's seals.

4.1 Shaft sealing

Müller & Nau (1998, p. 1) state the overall sealing problem as *"the control of fluid interchange between two regions sharing a common boundary"*. When considering dynamic sealing conditions, as in radial shaft seals, where there is relative motion in the interface of the static and moving component, a small gap will inevitably exist as presented in **Figure 3**. Therefore, fluid molecules will transfer between the regions that are sealed either by diffusion, convection or pressure flow. (Müller & Nau 1998, pp. 1-2.)

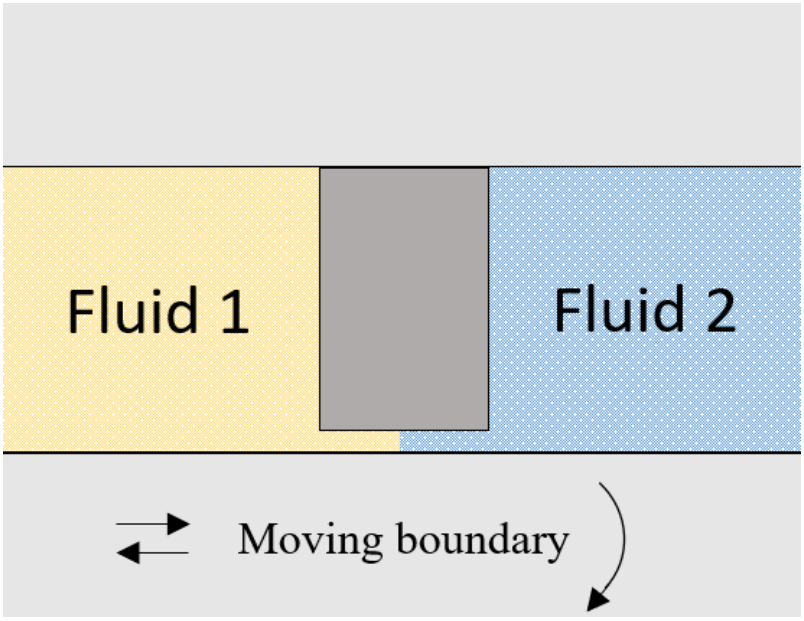

Figure 3. Sealing problem (Mod. Müller & Nau 1998, p. 2).

Radial shaft seals are also referred as for example radial lip seals, rotating shaft seals or sealing rings. They are a very common component in machine building as good sealing capability is obtained with low cost. Basically, every application that has a rotating, oscillating or reciprocating shaft can have a radial shaft seal installed. Typically, the purpose of a radial shaft seal is to seal a component – usually a bearing – so that the lubricant used in the bearing does not leak out, and on the other hand ensure that dirt or other impurities does not contaminate the lubricant. (Parker Hannifin 2018, p. 10.) In some applications radial shaft seals are used in separating different fluids from each other or to maintain system pressure or detain external pressure (SKF 2019, p. 8). As radial shaft seals are very typical machine elements, they are used in a large variety of different operating conditions. For example, the surface speed of a shaft can vary greatly between different applications. Many of the applications might be in a well-known and controlled environment, but radial shaft seals are also used in applications that face quickly changing conditions, such as cars. (Parker Hannifin 2018, pp. 10-11.)

4.2 Elastomers for radial shaft seals

Radial shaft seals are typically made of an elastomeric material. Elastomers are viscoelastic materials, meaning that their behavior under deformation shows both viscous and elastic behavior. (R.L. Hudson & Company 2005, p. 18.) Natural rubber is the first elastomeric

material, and it still provides the highest elasticity and resilience of any material. Unfortunately, the temperature range and resistance against aging are not on a good enough level for most industrial sealing applications. (Flitney 2007, p. 362.) Nowadays, several different types of synthetic rubbers are available for different purposes (Cardarelli 2018, p. 1039).

The material properties of different elastomers vary even inside a certain elastomer type based on its chemical composition and manufacturing process. Identifying different types or grades of elastomers is basically impossible with only visual methods as two materials looking the same can have very different properties. (Flitney 2007, p. 358.)

4.2.1 Material basics

Cardarelli (2018, p. 1014) explains the usual basic structure of polymers to be *"a long linear chain of thousands of monomers but the monomers can also be linked together by cross-linking or reticulation to form large two- or three-dimensional molecular structures"*.

Polymers are divided to three groups:

1. Thermoplastics, which are the simplest polymers consisting of a long, unconnected chains of monomers.
2. Thermosetting plastics, that are polymers made by polymerization of soft or viscous monomers that are cured into an infusible and insoluble three-dimensional polymer network.
3. Elastomers, which consist of long coiled, asymmetric linear polymer chains created by the cross-links between the polymer chains. Due to the cross-links elastomers withstands high deformations without braking. (Cardarelli 2018, p. 1014.)

Elastomers can be divided into thermoset elastomers and thermoplastic elastomers. Majority of elastomers are thermosets, which are vulcanized i.e., subjected to heat and pressure to create their material properties. The cross-links in thermoset elastomers are irreversible after vulcanization. Thermoplastic elastomers have weaker cross-links compared to vulcanized thermosets, and thus they can be turned back to liquid state by heating. Therefore, thermoplastic elastomers are more like plastic materials but with the elastomer's elasticity

properties. (James Walker 2017, pp. 5,7.) Elastomers relevant to this thesis are thermoset elastomers.

The bulk polymer unit of the elastomer is defining the basic properties of the elastomer and therefore for example hydrocarbon polymers and fluorocarbon polymers will have significantly different chemical resistance properties (Flitney 2007, p. 362). If a material would consist only of the basic polymer without the cross-links, it would be easily distorted without the ability to recover because of the lack of a chemical bond between the polymer chains (James Walker 2017, p. 5). The material properties can be increased by curing and creation of cross-links between the polymer chains. Curing agent is added to the polymer and it is exposed to heat and pressure to crate the cross-links. (Flitney 2007, pp. 362-363.) To further improve the material properties of the elastomer, a filler chemical is added to the material. Fillers do not take part in the actual polymer chain but are mixed inside the polymer matrix. (Cardarelli 2018, p. 1015.) The effect of cross-links and filler are illustrated in **Figure 4**.

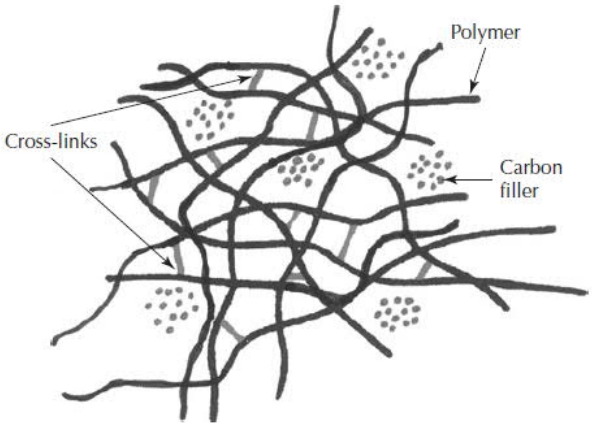

Figure 4. Effect of cross-links and filler in elastomeric material (Flitney 2007, p. 364).

When an elastomeric material is distorted due to an outside force, the cross-links enables that the material returns to its initial state when the outside force is removed (James Walker 2017, p. 5). A lot of different factors, such as polymer type, temperature, formulation of the elastomer compound, filler type and proportion affect the materials strain properties, its resilience and residual strain (Flitney 2007, pp. 363-364).

Poisson's ratio of elastomeric materials is high, close to 0,5 which means that they are close to being incompressible. The high Poisson's ratio being combined with low shear and elastic modulus makes elastomeric materials to be both easily deformable and incompressible. (Müller & Nau 1998, p. 18.)

Elastomers are widely used in sealing because their suitable material properties for sealing. Elastomers' modulus of elasticity is very low, and they elongate typically 100% or more before braking. (Müller & Nau 1998, p. 18.) Even though the tensile strength of elastomeric materials is relatively low, the materials will not usually creep even at elongations that are close to their braking point. These properties enable use of large strains during installation of the seals and provide good seal interference. Same properties make sealing rings accommodate to quite large range of shaft tolerances and misalignment with low contact stresses. (Flitney 2007, p. 359.)

Elastomers have low hysteresis, and they are very resilient at the same time when they are used in a suitable temperature range (Flitney 2007, p. 359). Hysteresis in this context means the difference between energy input and outputs on elastic deformation. Resilience describes the elastomers speed of recovery to its original state after deformation. (James Walker 2017, pp. 5, 43.) These properties provide the sealing rings capability to withstand pressure changes, shaft vibrations and runout (R.L. Hudson & Company 2005, p. 28). Temperature and loading amplitude the elastomer encounters have great effect on the hysteresis loss (Hanhi et al. 2007, p. 12). Hysteresis loss can be represented by variable tan δ, which presents the elastomers ability to absorb and return energy subjected on the material. High tan δ value means that the materials response to changing conditions is worse compared to low tan δ value. Tan δ curves show a clear peak at a material specific temperature. On the lower temperature side of the peak, the material has low tan δ value but at the same time the material has become significantly stiffer than in higher temperatures. This means that that the material has reached its glass transition temperature and even though the material is resilient, the strain area it can work with is very narrow as the material is very stiff. (Flitney 2005, pp. 7-9.) Graphs showing two fluorosilicone rubber (FSR) compounds and one fluorocarbon (FKM) compounds modulus of elasticity and tan δ values in the function of temperature is presented in **Figure 5**.

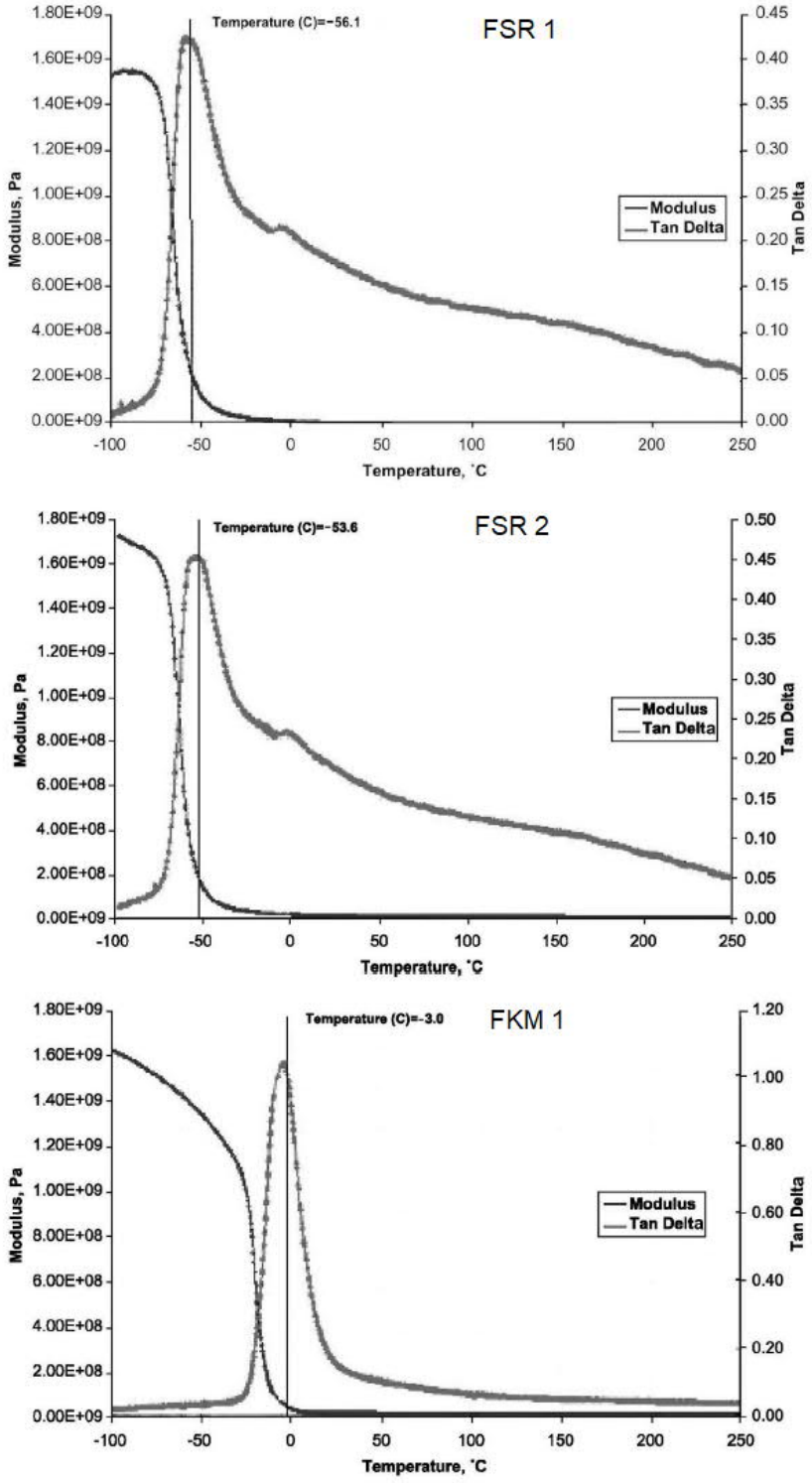

Figure 5. Modulus and tan δ of different elastomers retell (Flitney 2005, p. 9).

The glass transition temperature can vary greatly inside one material grade and thus the glass transition temperature is unknown if only the elastomer grade is known as can be seen in **Figure 6**.

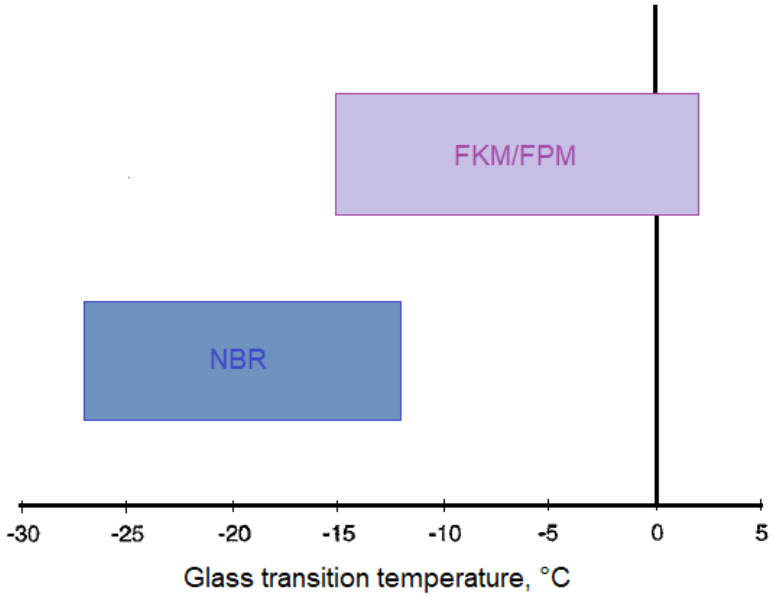

Figure 6. Glass transition temperatures for different elastomer compounds (Mod. Müller & Nau 1998, p. 19).

Elastomeric materials are easily torn as they are soft (Flitney 2007, p. 360). Applicable temperature range of elastomeric materials also vary between different types of elastomers. For example, nitrile rubber (NBR) has a general temperature range from -50 °C up to 100 °C. Comparably for FKM, the temperature range is from -40 °C up to 205 °C and for hydrogenated nitrile rubber (NHBR) -30°C 150°C (Freudenberg Sealing Technologies 2015, p. 36; James Walker 2017, pp. 8-9; R.L. Hudson & Company 2005, pp. 42-47). The temperature range varies slightly between different manufacturers especially when considering the lowest permissible temperature, but values given above give the good overall view of temperature limits of the different materials.

Chemical resistance of elastomers is greatly dependent of both the elastomer type and individual grades within the material types. Also, enhancing of one material property often leads to weakening of another property. For example, a composition leading to high temperature resistance can lead to poor chemical resistance. (James Walker 2017, p. 6.) Swelling of elastomers can be very large due to permeation of the fluid to the material. On the other hand, ingredients of the material can also be dissolving from the base material, and the elastomer could shrink due to the contact to some fluids. Contact with water or acids

might also cause the tensile strength properties of the material to weaken due to hydrolysis. (Hanhi et al. 2007, p. 13.)

Elastomers are sensitive to permeation and diffusion when they are subjected to the substances present in their operating environment. Even if the speed of permeation is small, it can make a difference in many cases, as even a small addition or loss in the material might be important for the application the material is being used in. (Brown 2018, p. 253.) Diffusion rate defines the speed of the fluids permeation into the material, and solubility determines the amount of fluid that remains dissolved in the material. The diffusion rate of liquids is typically increased when the application temperature rises but inhibited when the application pressure rises. (Flitney 2007, p. 378.)

The stress-strain properties of elastomers are non-linear. The stress-strain behavior can be divided into three regimes. In the first regime, elastomers roughly follow Hooke's law, and the strain is proportional to stress and the modulus of elasticity is constant. However, when the load applied on the material is further increased, and the material reaches the second regime, modulus of elasticity decreases. In the third regime the modulus of elasticity increases again with increasing slope. (Müller & Nau 1998, p. 26.) Diagram explaining the stress-strain behavior is presented in **Figure 7**.

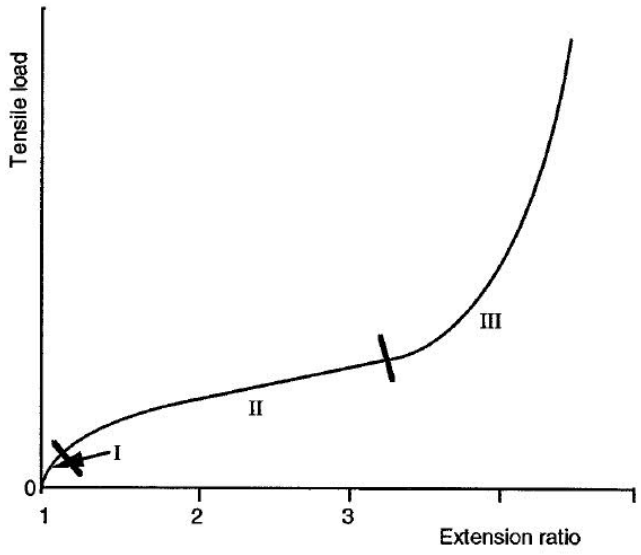

Figure 7. Stress-strain behavior of elastomeric materials (Müller & Nau 1998, p. 27).

The stress-strain curves of elastomers are material, cross-section, and temperature dependent. The nonlinearity presented in **Figure 7**, can be reduced by increasing the proportion of filler in the material. This will however increase hysteresis loss and have a harmful effect considering radial shaft seals as the seals capability to follow shaft dynamics is reduced when hysteresis loss increases. (Flitney 2007, pp. 361-362.) Stress-strain curves of different materials is presented in **Figure 8**. From the curves it can be clearly seen that the materials stress-strain properties cannot be known by just looking at the upper-level material grade. For example, the curves 3, 4 and 6 are all for FKM material but the curves differ greatly from each other.

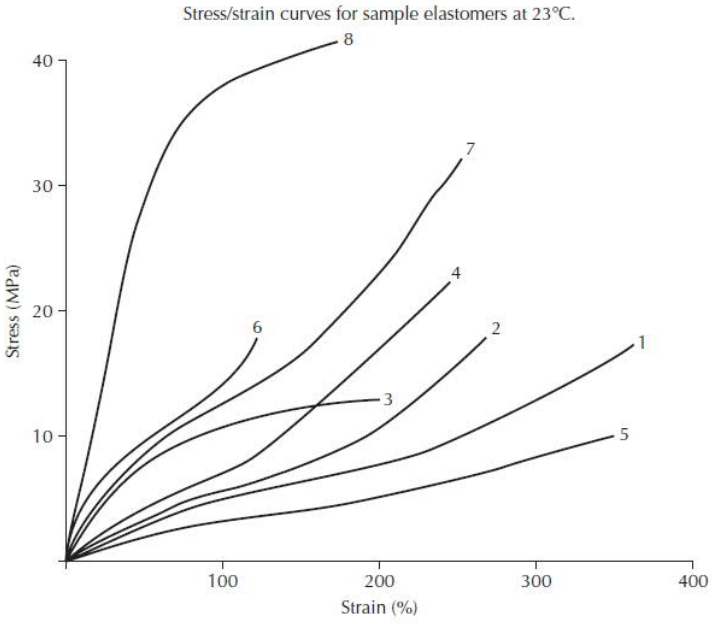

Key:

No.	Material type	Hardness (IRHD)
1	Nitrile	65
2	Nitrile	70
3	Fluorocarbon type A	75
4	Fluorocarbon, terpolymer, peroxide cure	70
5	Fluorosilicone	60
6	Fluorocarbon, type B	90
7	Hydrogenated nitrile	90
8	Polyurethane	95

Figure 8. Stress-strain curves of different elastomers (Flitney 2007, p. 361).

4.3 Effect of temperature to elastomer materials

It is very important to measure material properties of elastomers in different temperatures to fully understand the behavior of the material. Temperature has short-term and long-term effects on the elastomer. Short-term effects, such as thermal expansion, are physical and they are reversible when temperature comes back to ambient temperature. Long-term effects, on the other hand are chemical effects and they are irreversible. Those long-term effects are often referred as ageing of the material. (Brown 2018, p. 305.) The material properties are degraded due to chemical reactions between the base material and fluid they as exposing liquids and gases permeates into the material. The degrading chemical reactions are accelerated when the temperature increases. When the material is being compressed in operation, new cross-links are formed in the material due to residual curing agent in the material. Additional cross-linking causes hardening of the material, and it typically causes cracks or material removal on the surface of the elastomer. Further chemical activity can also be initiated due to the other chemical species in the elastomer. Another type of degrading chemical reaction breaks the cross-links and thus causes softening of the material. (James Walker 2017, p. 25.)

Lubricant – elastomer combination is crucial when considering the elastomers durability in the application it is used in. Both the elastomer and the lubricant consist of numerous different components, such as fillers, cross-linking additives, plasticizers etc. when elastomers are considered, and extreme pressure (EP) or anti-wear (AW) additives, viscosity improvers, corrosion protection additives etc. when lubricants are considered. Polarity of the lubricant and the elastomer is the most significant factor when considering solubility. Polarity for different elastomer types and lubricants are significantly different between different grades. This means that oil components can diffuse to the elastomer and vice versa when the polarity of the elastomer and the oil are similar. Non-polar lubricant combined with non-polar elastomer will lead to shrinking, and polar – polar combination will lead to swelling. It is also possible that chemical action does not lead to net volume change in the elastomer or oil, but the elastomers' chemical structure has still changed. (Adler et al. 2018, pp. 31-32.) A schematic view of changes in the elastomer and lubricant is presented in **Figure 9**.

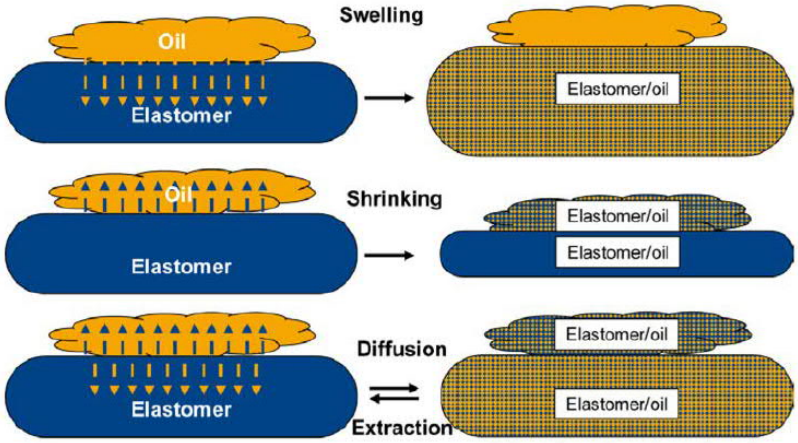

Figure 9. Diffusion processes between elastomer and lubricant (Adler et al. 2018, p. 32).

Application temperature can have a significant effect on the material properties, but it is good to note that each material behaves differently. For example, fluoroelastomers, which have good chemical resistibility, tensile strength properties will typically be reduced a lot more when the temperature increases compared to fluorosilicone rubber. (Flitney 2005, p. 7.) Comparison of tensile strength in the function of temperature between three different FKM compounds and two FSR compounds is presented in **Figure 10**.

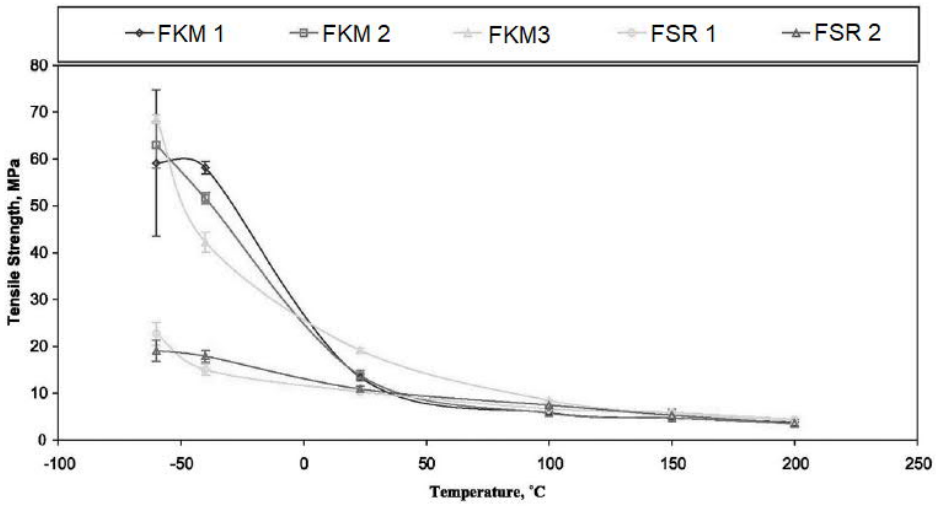

Figure 10. Tensile strength of different elastomers in the function of temperature (Mod. Flitney 2005, p. 7.)

Temperature has also a large effect on the elongation at brake, 100% modulus and tear strength. The 100% modulus represents a temperature where the elongation at brake is larger

than 100%. (Flitney 2005, p. 7.) Graphs showing different elongation and tear strength properties of same materials shown in **Figure 5** and **Figure 10** are presented in **Figure 11**.

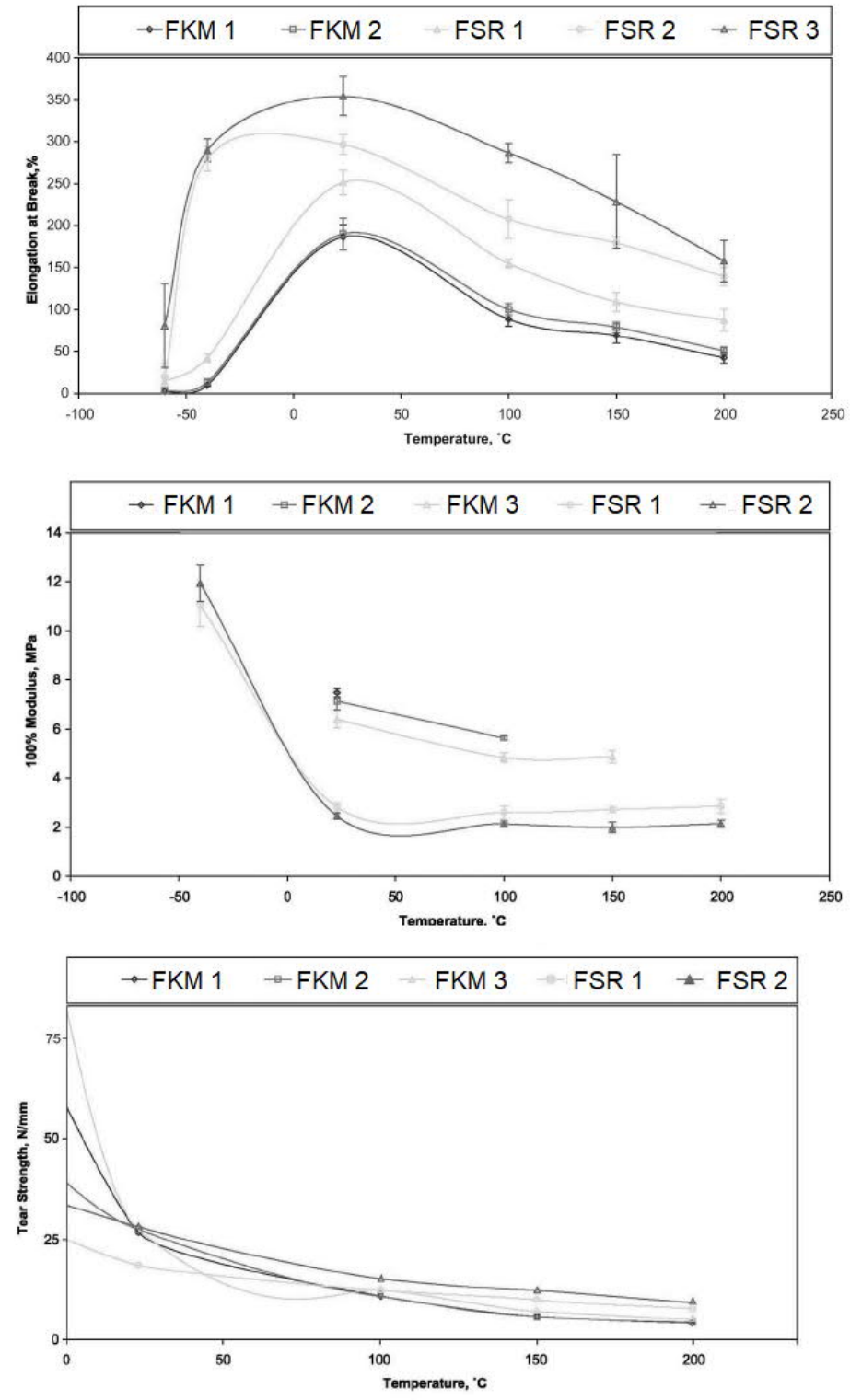

Figure 11. Elongation at brake, 100% modulus and tear strength in the function of temperature (Mod. Flitney 2005, p. 8).

The graphs show that each material has largest elongation at brake at approximately room temperature and it is decreased in lower or higher temperature. The 100% modulus shows that FSR materials have larger 100% modulus value compared to FKM materials when they show over 100% elongation, but on the other hand, they do not elongate over 100% at a very broad temperature scale. FKM materials on the other hand have over 100% elongation at brake even at relatively low temperatures. The materials tear strength is lower at high temperatures compared to low temperatures. (Flitney 2005, pp. 7-8.)

4.4 Fluorocarbon elastomer material properties

Fluorocarbon elastomer material properties are presented in more detail because the material of the radial shaft seals in subject of this thesis are made of fluorocarbon.

One quarter of the annual use of fluoroelastomer materials are used to produce radial shaft seals. However, fluorocarbon polymer chains are relatively stiff and thus their resilience is not as good as in many other elastomer grades. Because of this, fluorocarbon elastomers have been used traditionally in static than dynamic seals. Still, because of the good temperature and oil resistance of fluorocarbon elastomers, they are used commonly in radial shaft seals. (Drobny 2016, pp. 3, 5, 10.)

Fluorocarbon elastomers has two abbreviations, FKM and FPM and it can be referred also as fluoroelastomer. FKM is the abbreviation used in American Society for Testing and Materials (ASTM) standards and FPM is used in International Organization for Standardization (ISO) standards. Fluorocarbon has good stability due to good strength of the chemical bond between fluorine and carbon. No other elastomer grade show as good temperature and oil resistance than fluoroelastomers. They can be used in high temperatures, up to 200 °C and even up to 300-315 °C temporarily. FKM materials have good resistance against different chemicals, oxygen and ozone even in elevated temperatures (Cardarelli 2018, p. 1043; Drobny 2016, p. 3; Hanhi et al. 2007, pp. 41, 43). Fluoroelastomers also have good resistance against chlorinated solvents, but limited resistance against polar solvents (Flitney 2007, p. 389). Other advantage of fluorocarbons is that they are incombustible and generally have good abrasion resistance (Hanhi et al. 2007, pp. 41, 43). Fluoroelastomers good temperature and oil resistance compared to other elastomers is presented in **Figure 12**.

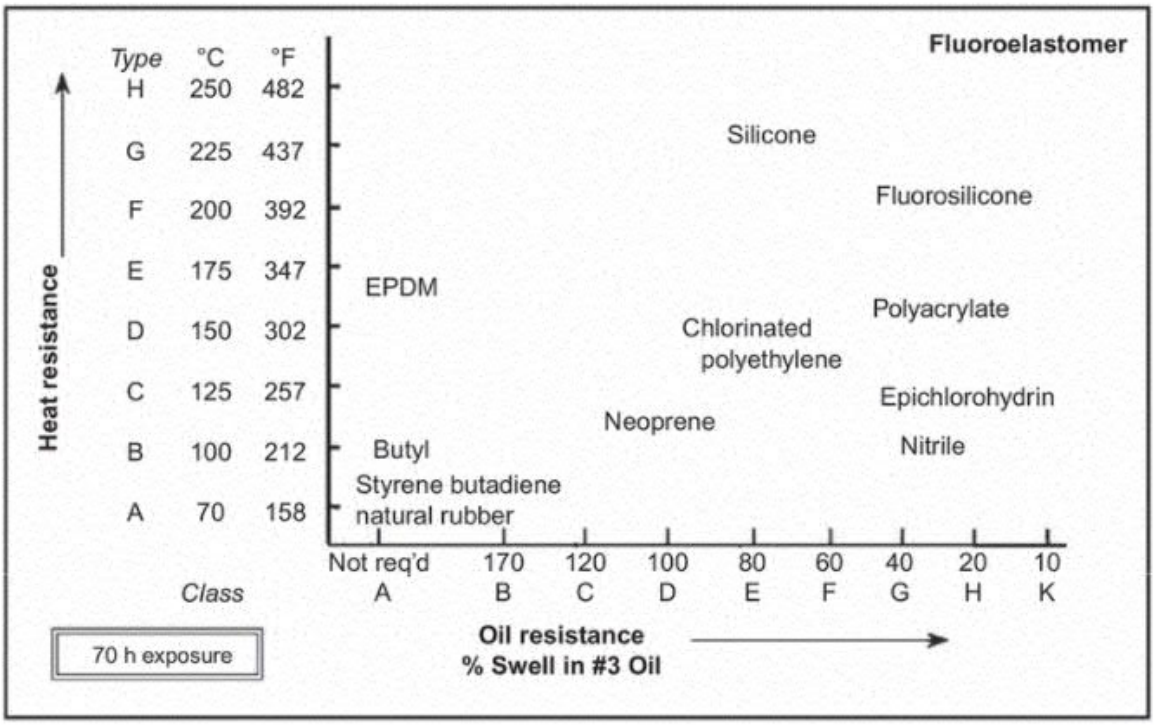

Figure 12. Temperature and oil resistance of different elastomers (Drobny 2016, p. 4).

Commonly, fluoroelastomer compounds reduction in tensile strength is less than 30%, elongation at break less than 50% and change in hardness only 15 points after being immersed in 250 °C oil for 70 hours. Good oil and temperature resistance provides excellent service life even at elevated temperatures as presented in **Figure 13**. (Drobny 2016, p. 4.)

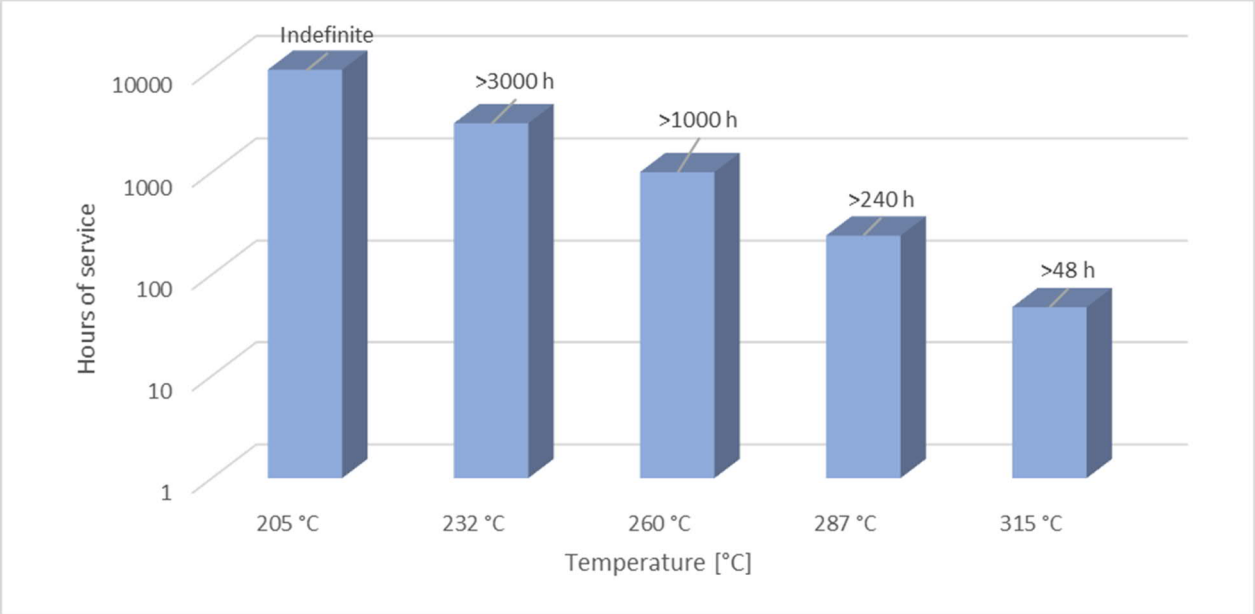

Figure 13. Fluoroelastomer service life in elevated temperatures (Mod. Drobny 2016, p. 4).

On the downside, there is also a list containing a good number of disadvantages. Fluoroelastomers alkali resistance is not good, and their mechanical properties are low compared to many other elastomers. Fluorocarbons elasticity is also poor at low temperatures and their tensile strength decreases significantly in high temperatures as was shown in **Figure 10**. (Hanhi et al. 2007, p. 43.) Even though fluoroelastomers have good oil resistance, it does not generally apply for gear oils with EP-additives and in applications that use such gear oils must have an FKM material specially made compatible with EP-additives. Fluoroelastomers durability is also reduced in above 100 °C water or steam. (Flitney 2007, p. 389.)

4.5 Radial shaft seal design in general

Most common radial shaft seal designs have a bonded metal case, or an otherwise rigid frame and a flexible component that is fitted around the shaft to be sealed. There is also a variety of radial shaft seal designs, especially in large diameter seals, that does not utilize the bonded case design but require the sealing ring to be assembled into the case. (Parker Hannifin 2018, pp. 12-14.) The key part of the radial shaft seal is the flexible part made of an elastomeric material. The design of this part has the greatest influence for the performance of the seal. Cross-section of a radial shaft seal is presented in **Figure 14**. Dimension H, or beam length, is the distance from tip of the lip to the thinnest part of the sealing ring. The flexibility of the seal decreases when the dimension H is reduced, or the flex thickness t is increased. Stiffer sealing ring will lead into a larger radial force when the seal is mounted on the shaft, which creates more frictional heat and will also reduce the seals capability to withstand offset between the shaft and the seal housing in radial direction. On the other hand, stiffer designs are more robust against deformation caused by high pressure. (R.L. Hudson & Company 2005, p. 77.) When pursuing for a flexible seal design, decreasing the flex thickness may lead to stick-slip phenomena as the sealing ring starts to twist when the shaft is rotating (Horve 1996, p. 124).

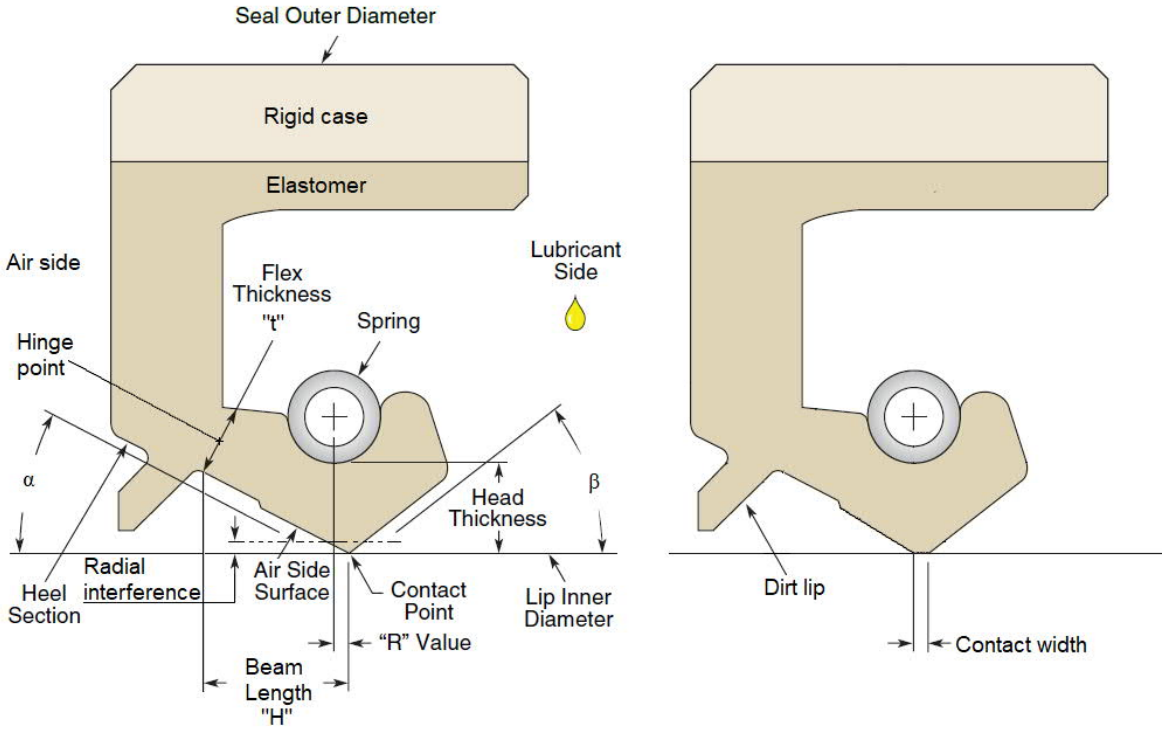

Figure 14. Typical radial shaft seal design (Mod. Parker Hannifin 2018, p. 14).

The angles on the lubricant side and air side are usually referred as α and β angles. In a typical sealing ring design, the angle β is larger compared to the air side angle (R.L. Hudson & Company 2005, p. 78). According to Flitney (2007, p. 106) the angle β is in rage of 40-50 ° and the angle α is in the range of 25-30° on a typical radial shaft seal design. The angle must be greater on the oil side compared to the air side because this will create a suitable pressure gradient between the sealing ring and the shaft (Horve 1996, p. 124). The sealing ring also has an interference fit on the shaft meaning that when the sealing ring is not mounted on the shaft, its inner diameter is smaller than the shaft's outer diameter (R.L. Hudson & Company 2005, p. 78). As for the stiffness of the sealing ring, changing the interference to larger or smaller will enhance some of the properties on the cost of others. Increased interference will increase the radial force on the lip tip creating more frictional heat, but on the other hand it will enhance the sealing rings capability to withstand radial movements of the shaft, such as vibration or dynamic runout (R.L. Hudson & Company 2005, p. 78). The dimension from the sealing ring lip tip to the spring groove bottom is the seals head thickness. Too thin head thickness can cause the lip tip contact to lift off from the shaft or make the seal to fluctuate with the shaft motion, which will cause excessive leakage (Horve 1996, p. 124).

Many radial shaft seal designs also have a radial spring, typically a garter spring, to create more force between the shaft seal lip tip and the shaft. This additional loading is needed to compensate the change in the preload crated by the interference when the elastomers' temperature changes. (Horve 1996, p. 122.) The springs' distance from the lip tip, dimension R in **Figure 14**, is approximately 10% of the beam length H and it is good to note that the dimension is outwards from the oil side to prevent tilting of the sealing ring towards the oil side. With the location of the spring, the asymmetric geometry of the sealing ring can be adjusted together with the extra load on the lip tip. (Flitney 2007, p. 107.)

In propeller shaft seals in addition to the radial force created by the interference fit and the garter spring, a radial force is created by the pressure difference over the sealing ring. This additional radial force twists the sealing ring and the contact area between the seal and the shaft increases and eventually the maximum contact pressure is reduced even though the total radial force is further increased. Due to the twisting of the sealing ring under pressure, a back-up ring is used on the back side of the seal to prevent the sealing ring from inverting to the wrong side. (Borras et al. 2020, pp. 26-27.) The effect of the pressure difference on the orientation of the sealing ring and the contact pressure is presented in **Figure 15**.

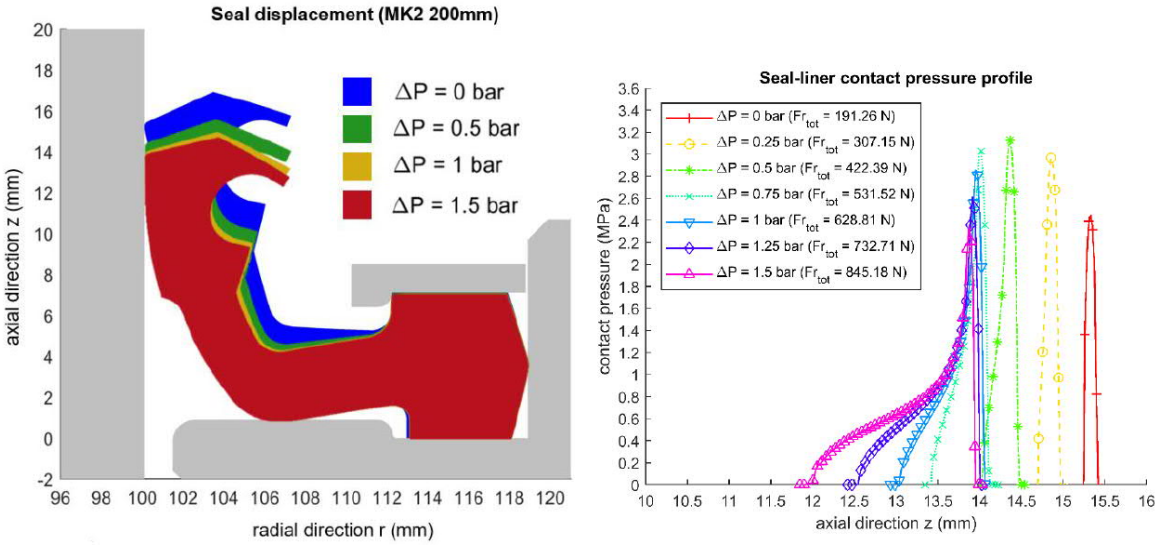

Figure 15. Effect of pressure difference on the seal-shaft contact (Mod. Borras et al. 2020, pp. 26-27).

In the study performed by Borras et al. (2020, pp. 26-27) the influence of the radial force created by the interference fit and the garter spring on the total radial force is larger than the radial force created by the pressure difference over the sealing ring profile until the pressure difference is more than 0,5 bar, which indicates that the interference and the garter spring play a significant role in the contact properties especially when the pressure difference is less than 0,5 bar. A graph showing the radial force in the function of the pressure difference is presented in **Figure 16**.

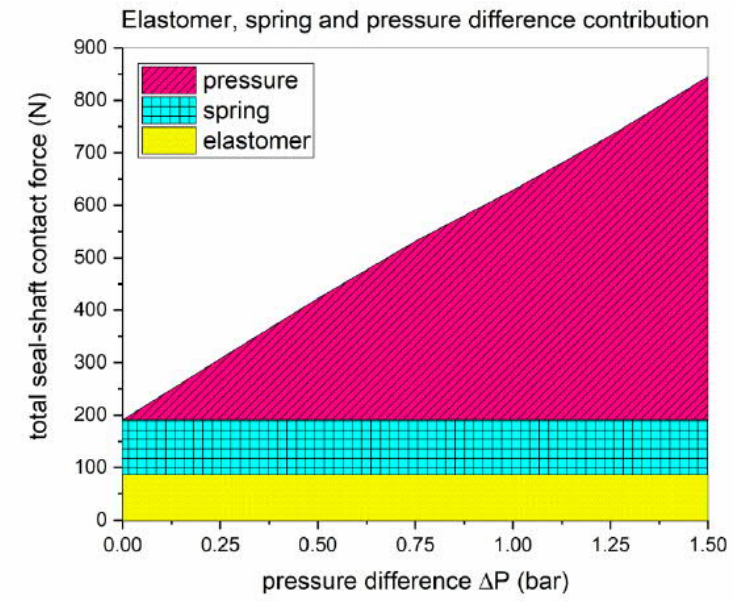

Figure 16. Seal-shaft contact force in the function of pressure difference (Borras et al. 2020, p. 28).

The contact width of the seal also increases significantly from its original value when the seal wears down. In the most common shaft seal diameters (such as described in ISO 6194) the contact width can increase from 0.1 mm to 0.7 mm or even as high as 2.5mm. (Horve 1996, p. 126; Müller & Nau 1998, p. 76.)

4.6 Sealing mechanism

When radial shaft seals were introduced in the 1930s it was thought that the sealing mechanism of the radial shaft seals is based on sufficient contact force between the seal lip tip and the rotating shaft, but the actual sealing mechanism was found in the 1950s (Borras 2020, p. 41). The sealing mechanism of radial shaft seals is based on a thin lubrication film between the shaft and the seal (Salant 1997, p. 92) (Stakenborg 1988a, p. 336) (Guo et al.

2013, p. 195), but there are still unclear tribological characteristics related to the sealing mechanism of radial shaft seals (Wennehorst 2016, p. 27). The physical parts involved in the shaft sealing are quite simple and thus the sealing mechanism might seem quite simple at first, as the first impression is that the elastic seal is just forming a tight barrier on the shaft (Horve 1996, p. 163). In reality, the tribological system formed by the shaft, oil film and seal is very complex (Salant 2009, p. 2637; Stakenborg 1988a, p. 336). There are multiple variables such as oil viscosity and temperature, shaft diameter and surface speed, sealing ring material properties, contact force between the seal and the shaft and its' distribution, contact width etc. that all have an influence on the behavior of the lubrication film (Stakenborg 1988a, p. 336).

The lubrication film forms when small asperities on the sealing rings surface deform when the sealing ring is distorted as the shaft is rotating (Guo et al. 2013, p. 195). When this happens, the asperities orient at an angle compared to the shaft and form into vane-like shapes. When liquid flows through these vanes, the liquid lifts the lip surface and pumps oil towards the lip creating the lubrication film. (Salant 2009, p. 2638; Stakenborg 1988b, p. 10.) When considering hydrodynamics in for example bearing lubrication, a lubrication film formed between two moving parts would lead into leakage (Horve 1996, p. 163). This is not the case in radial shaft seals as their primary function is to seal liquid. The reason for the sealing performance is due to asymmetric contact pressure in the sealing ring lip area and it has the greatest influence in the sealing capacity of the seal. (Freudenberg Sealing Technologies 2015, p. 27; Guo et al. 2013, p. 195.) The highest pressure gradient is on the spring side of the sealing ring because the angle between the shaft and the seal is smaller on the air side than on the oil side, and also the spring is located on the air side of the sealing ring (Salant 2009, p. 2638). As the asperities on the seal material distort, forming the vanes as described earlier, the angle of the vanes is smaller on the air side, which leads into higher pump rate from the air side to the oil side resulting in leak-free seal (Horve 1996, p. 163). The pumping rate form the back side of the seal to the spring side of the seal is often referred as inward pumping (Flitney 2007, p. 110; Müller & Nau 1998, p. 7). In case both sides of the seal are filled with liquid, the net pump rate will still be from the back side of the seal to the spring side of the seal. Because of this radial lip seals are not very good in separating two liquids from each other. (Bavel 1997, pp. 25-26, 75; Müller & Nau 1998, pp. 85-86.) It is also good to note that lubricant viscosity also plays a role in the

pumping rate and the pumping direction can change if the lubricant viscosity on one side of the seal changes (Borras et al. 2020, p. 9). As the inward pumping is dependent on the asymmetric contact pressure, spring force on the seal also influences the pumping rate – the larger the spring force, the larger the pumping rate (Jia et al. 2014, p. 1181). A schematic view of the pressure distribution and lubricant flow between the shaft and the sealing ring is presented in **Figure 17**.

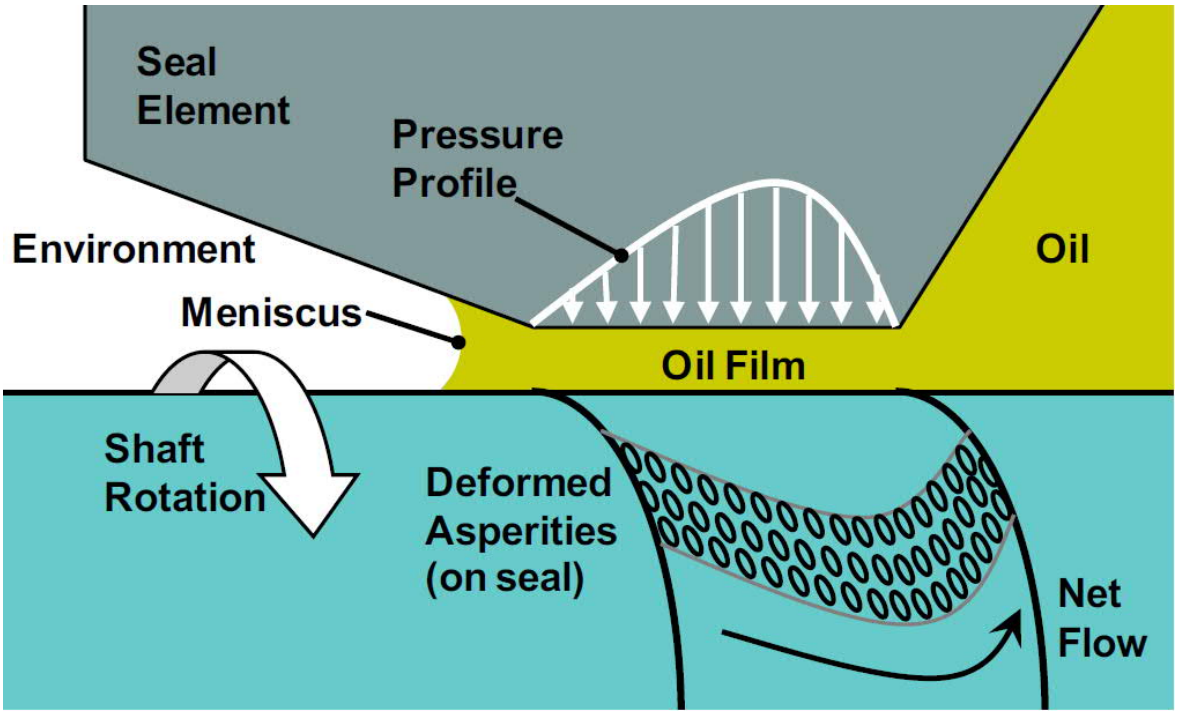

Figure 17. Pressure distribution and lubricant flow in the lip-tip area (Wenk et al. 2016, p. 290).

The asperities that greatly contribute to the hydrodynamic pressure that lifts the seal contact from the shaft are formed when the shaft starts to rotate against a new seal. The amount of the asperities that form on the seal surface is also important – if there are too few asperities, the lubrication under the sealing ring does not work as it should, which will lead into premature wearing and excessive leaking. (Salant 2009, p. 2638.) Whether a sufficient number of asperities are formed is up on the material properties of the elastomer from what the seal is manufactured of (Horve 1996, p. 163; Müller & Nau 1998, p. 77). Pictures of sealing ring surfaces with insufficient and sufficient number of asperities are presented in **Figure 18**. The surface on the left side has insufficient number of asperities

while the number is sufficient on the surface presented on the right side (Flitney 2007, p. 113).

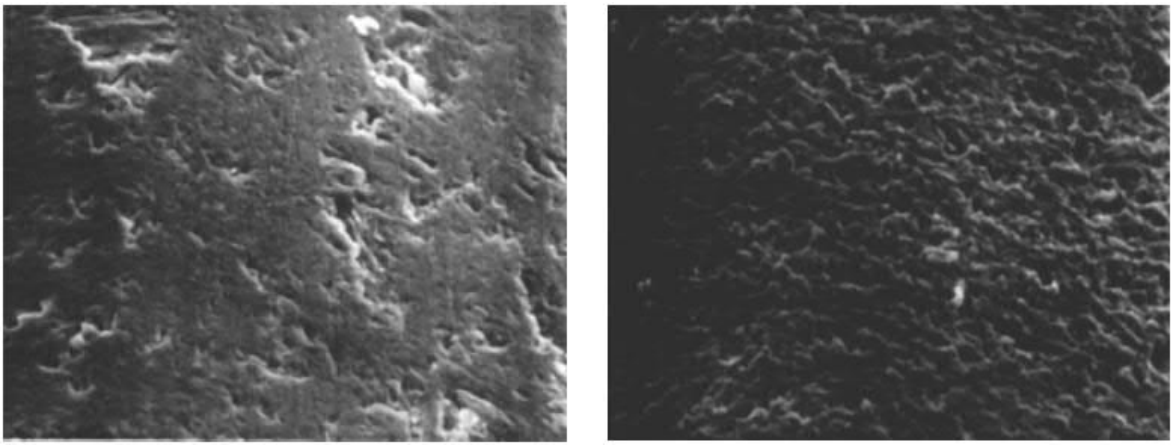

Figure 18. Asperities on seal contact surface after run-in period (Flitney 2007, p. 113).

If artificial asperities are generated on a seal surface of a seal that has such material characteristics that surface asperities are not formed naturally, the seal lubrication will function as it should until the artificial asperities disappear due to seal wear (Müller & Nau 1998, p. 79). As the asperities distort when the shaft is rotating, over time the asperities become directionally oriented because the elastomer loses some of its flexibility on the surface, and the asperities do not return to their original shape when the shaft rotation stops. Because of this, the seals tend to leak more if the shaft is turned in reverse direction. (Flitney 2007, p. 111.)

Interestingly, the sealed shaft surface has to be smooth so that the seal won't wear down too fast, but if the shaft surface is too smooth, the essential asperities do not form on the shaft surface. The shaft surface also has to be treated, e.g. grinded, so that there is no machining lead on the shaft as lubricant can be transferred even on a small machining lead. As a rule of thumb, the surface roughness Ra value should be on the range of 0,2-0,6 μm. (Müller & Nau 1998, p. 79.)

There is also a second phenomenon contributing to the inward pumping rate from the air side to the oil side and outward pumping rate from the oil side to the air side. This phenomenon is based on geometrical imperfections on the shaft such as roundness of the

shaft and dynamic runout. Because of the described imperfections there is small radial movement between the shaft and the seal when the shaft rotates, and the radial movement then makes the lip tip to move axially. The axial movement will make the seal to act as a very small-scale pump enhancing the lubricant pumping rate. (Flitney 2007, p. 113.) Installation of the sealing ring into the housing and the housing's manufacture tolerances also makes the seal not to be perfectly perpendicular to the shaft. This makes the seal to axially wipe on the shaft creating similar enhancement on the lubricant pumping rate as the small pumping produced by the radial displacement (Horve 1996, p. 167). There are seals available on the market that utilize the enhancement in the pumping rate caused by geometrical imperfections by making the seal profile to have several sine waves on the contact surface as presented in **Figure 19** (SKF 2005, p. 20).

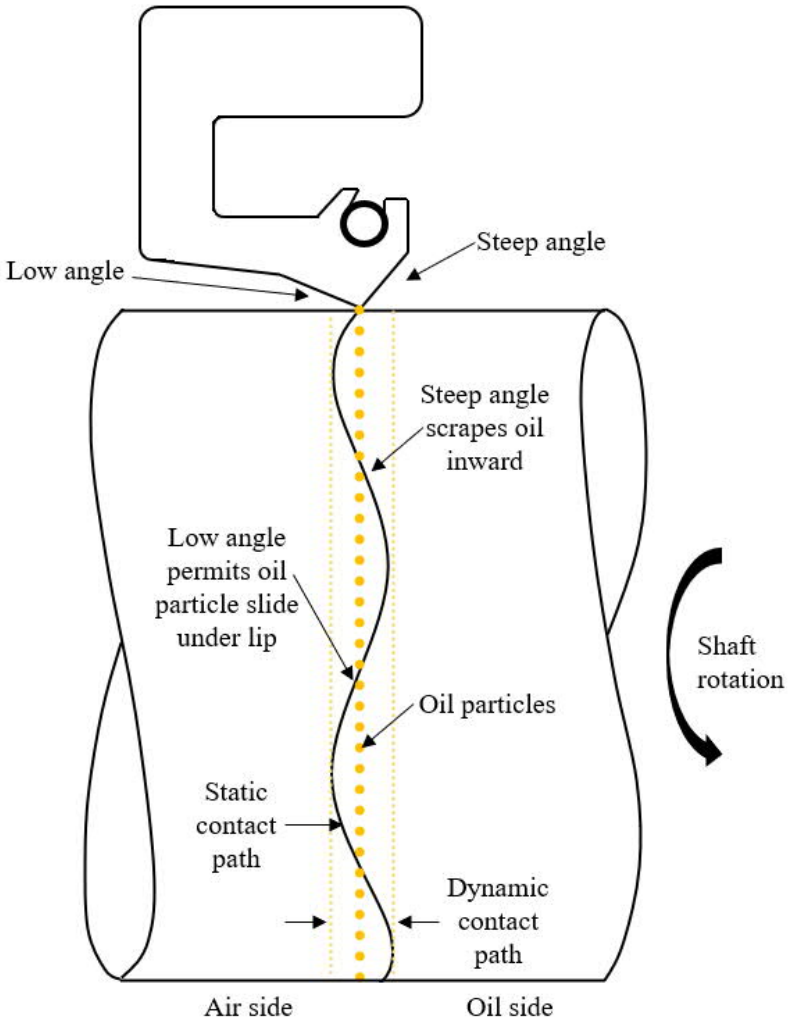

Figure 19. Radial shaft seal with waved shaft contact (Mod. SKF 2005, p. 20).

4.7 Lubrication film properties

When the sealing mechanism was studied for the first time in the 1950s, it was expected that there would be a dry contact pair between the shaft and the seal, and the seal must cut the lubricant film to enable leak-free contact (Borras 2020, p. 41; Wennehorst 2016, p. 5). However, in one of the first ever tests, it was found that that a significant frictional torque was created between the shaft and the seal even when the radial force was close to zero (Wennehorst 2016, p. 9). The frictional force in a dry contact pair would have been proportional to the radial force, and because this was not the case here, it suggested that the contact between the shaft and seal lip tip is continuously lubricated (Borras 2020, p. 43). One of the first ever tests that aimed to further determine the sealing mechanism were performed with a test rig that allowed the radial load on the seal to be changed. A series of tests with different radial forces were performed so that with lower radial forces the seal would leak. It was also thought that there would be a distinct change in the slope of the frictional torque between a leaking and non-leaking seal, but the testing revealed that such change in slope does not exist. (Borras 2020, pp. 42-43.) Figure showing radial force, frictional torque and frictional coefficient from these tests is presented in **Figure 20**.

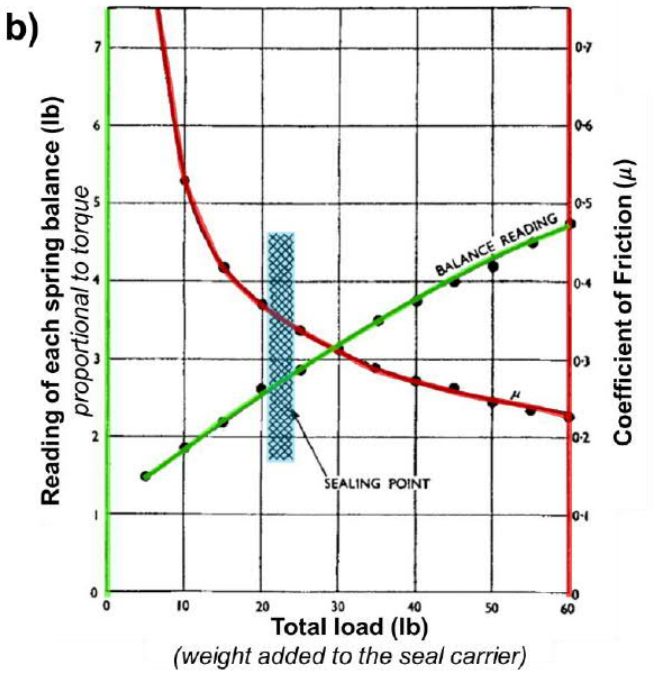

Figure 20. Effect of radial force on sealability and frictional torque (Borras 2020, p. 43).

The same tests revealed that the lubrication film thickness is in the range of being approximately ten times thinner than in plane journal bearings. This leads to significantly larger, at least one order of magnitude larger, frictional coefficients than in journal bearings. (Wennehorst 2016, p. 9.)

4.7.1 Lubrication regimes and film thickness

Lubrication regimes in sliding contacts can be divided into four different types – boundary, mixed, elastohydrodynamic and hydrodynamic lubrication. The conditions for each regime is shown in the two graphs on **Figure 21**. The first graph shows the lubrication regime in the function of the lubricant film parameter h/σ. The second graph shows the friction coefficient μ as a function of $\eta N/P$, and is also known as a Stribeck curve. On the top of **Figure 21** is a visual representation of the different lubrication regimes. (Bhushan 2013, p. 400.)

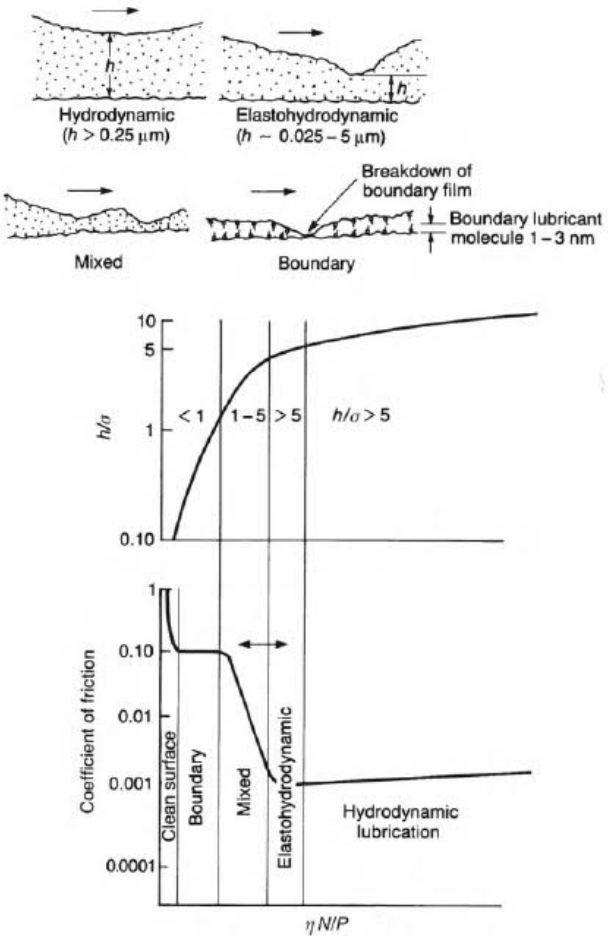

Figure 21. Lubrication regimes and Stribeck curve (Bhushan 2013, p. 400).

The h/σ compares the mean lubrication film thickness and the composite standard deviation of the surface heights of the two surfaces against the lubrication film. The bottom graph in **Figure 21** presents friction coefficient μ as a function of the product of absolute viscosity η and shaft rotation speed N divided by the surface pressure P acting on the contact. (Bhushan 2013, p. 401.) The h/σ is often referred as lambda ratio λ and the $\eta N/P$ as a dimensionless hydrodynamic duty parameter G (Borras 2020, p. 45-46; Horve 1996, p. 186). Borras (2020, p. 45) gives the parameter G in a perhaps more convenient form than Bhushan (2013, p. 400).

$$G = \frac{\eta u b}{F_{rtot}} \tag{1}$$

In Equation 1, η is the dynamic viscosity of the fluid, u is the velocity in the contact, b is the contact width and F_{rtot} is the total radial force on the contact. There is also a linear correlation between the friction coefficient and the hydrodynamic duty parameter which strengthens the assumption that there is a hydrodynamic lubrication film in the contact between the seal and the shaft. The friction coefficient can be derived as follows. (Wennehorst 2016, p. 10.)

$$\mu = \frac{\Phi}{G^{\frac{1}{3}}} \tag{2}$$

In Equation 2, μ is the friction coefficient, Φ is a seal specific proportionality factor and G is the hydrodynamic duty parameter. When the hydrodynamic duty parameter is low with low shaft speeds, the seal operates in dry friction contact or boundary lubrication zone (Borras 2020, p. 45; Horve 1996, p. 186; Wennehorst 2016, p. 10). The suitability of the Stribeck curve and the hydrodynamic duty parameter is however found to be insufficient to fully describe the lubrication state when radial shaft seals are in question, as it does not take the seal and shaft surface quality into consideration (Borras 2020, p. 46; Wennehorst 2016, p. 12). The friction coefficient can also be calculated if the seal specific proportionality factor and the hydrodynamic duty factor are unknow by determining the seals frictional torque and radial load as presented below (Horve 1996, p. 183).

$$\mu = \frac{\mathrm{T}}{2\pi R_S^2 F_{rtot}} \quad (3)$$

In Equation 3, T is the frictional torque of the seal, R_s is the radius of the shaft and F_{rtot} is total radial force on the contact.

In radial lip seals the hydrodynamical forces creating the lubrication film are relatively low but on the other hand, the seal material is relatively soft and will deform under these low forces and move the seal away from the shaft in the radial direction. As in typical contacts that fall under elastohydrodynamic lubrication (EHL) the fluid forces are much higher, the radial shaft seal contact is referred as soft elastohydrodynamic lubrication (soft EHL). (Salant 2009, p. 2637.) When soft EHL is in question, the lambda ratio λ varies between 1 to 5, which makes it hard to define reliably on which lubrication regime the seals operate in (Borras 2020, p. 46). When the lambda ratio is between 1-5, according to **Figure 21**, the lubrication regime is mixed lubrication. Mixed lubrication regime is a transition regime between boundary lubrication and elastohydrodynamic regimes and it is a sort of a gray area where two different lubrication mechanisms may be functioning simultaneously. This means that the two surfaces that should be separated by the lubrication film might have intermittent material-to-material contacts, but some areas in the contact have a fluid film between the separated surfaces. (Bhushan 2013, p. 403.) Radial shaft seals have been found to operate in the mixed lubrication regime (Borras 2020, p. 46; Wennehorst 2016, p. 57). This means that the friction force in the contact is determined by a constant and a velocity dependent term (Borras 2020, p. 46).

Multiple studies have been made to define the lubrication film thickness between the radial shaft seal and the shaft. Horve (1996, p. 184) also gives a way to calculate the lubrication film thickness h as presented below.

$$h = \frac{R_S G}{\mu} \quad (4)$$

In Equation 4, h is the lubrication film thickness, R_s is the shaft radius, G is the dimensionless hydrodynamic duty parameter and μ is the friction coefficient in the contact.

Horve (1996, pp. 187-190) reported the lubrication film thickness in different operating conditions based on tests performed on one specific seal design with different oil sump temperatures. Test conditions and results are presented in

Table 1, *Table 2*, *Table 3* and *Table 4*.

Table 1. Seal data and test parameters (Mod. Horve 1996, p. 187).

Seal material	FKM		
Shaft diameter [mm]	76.2		
Seal outer diameter [mm]	101.6		
Oil	Mobil 1		
Oil pressure	0		
Oil sump level	Full		
Contact width [mm]	0.36		
	Oil sump temperature [°C]		
	93	121	149
Radial load [N/mm]	0.102	0.0985	0.0854

Table 2. Test results at 93° oil sump temperature (Mod. Horve 1996, p. 188).

Shaft speed [m/s]	Torque [Nm]	Contact temperature [°C]	Oil viscosity in the contact [cp]	Friction coefficient (μ)	Duty parameter (G)	Lubrication film thickness [μm]
0.2	0.28	94.4	9.46	0.297	0.000000171	0.0219
0.4	0.26	95.6	9.25	0.282	0.335	0.0453
0.8	0.27	98.9	8.65	0.286	0.626	0.0834
0.8	0.28	104.4	7.78	0.301	0.845	0.107
1.6	0.29	107.8	7.3	0.309	1.058	0.13
2.0	0.30	108.9	7.17	0.324	1.298	0.153
4.0	0.37	113.9	6.56	0.391	2.37	0.231
6.0	0.42	119.4	5.97	0.444	3.24	0.278
8.0	0.46	125.6	5.4	0.485	3.91	0.307
10.0	0.49	132.2	4.87	0.527	4.41	0.319
12.0	0.54	135.0	4.67	0.572	5.07	0.367
14.0	0.58	137.8	4.48	0.613	5.68	0.378
16.0	0.61	140.6	4.3	0.651	6.23	0.359
18.0	0.65	142.8	4.17	0.696	6.79	0.372
19.9	0.68	145.6	4	0.726	7.24	0.38
21.9	0.73	147.2	3.91	0.779	7.78	0.38

Table 3. Test results at 121° oil sump temperature (Mod. Horve 1996, p. 189).

Shaft speed [m/s]	Torque [Nm]	Contact temperature [°C]	Oil viscosity in the contact [cp]	Friction coefficient (μ)	Duty parameter (G)	Lubrication film thickness [μm]
0.2	0.31	121.1	5.8	0.35	0.000000109	0.0119
0.4	0.29	122.8	5.65	0.322	0.214	0.0253
0.8	0.27	125.6	5.4	0.303	0.43	0.0541
0.8	0.26	131.1	4.95	0.295	0.561	0.0725
1.6	0.27	133.3	4.79	0.299	0.724	0.0923
2.0	0.27	134.4	4.71	0.303	0.89	0.112
4.0	0.32	140.0	4.34	0.354	1.64	0.177
6.0	0.36	143.3	4.13	0.405	2.34	0.22
8.0	0.40	146.7	3.94	0.44	2.98	0.258
10.0	0.43	150.6	3.74	0.479	3.53	0.281
12.0	0.46	153.3	3.6	0.515	4.08	0.302
14.0	0.49	156.7	3.45	0.55	4.56	0.316
16.0	0.53	160.0	3.3	0.593	4.99	0.321
18.0	0.56	161.7	3.23	0.629	5.49	0.333
19.9	0.61	163.3	3.16	0.676	5.97	0.336
21.9	0.64	165.0	3.1	0.715	6.44	0.343

Table 4. Test results at 149° oil sump temperature (Mod. Horve 1996, p. 190).

Shaft speed [m/s]	Torque [Nm]	Contact temperature [°C]	Oil viscosity in the contact [cp]	Friction coefficient (μ)	Duty parameter (G)	Lubrication film thickness [μm]
0.2	0.39	146.7	3.94	0.499	0.00000008580	0.00655
0.4	0.36	149.4	3.8	0.462	0.166	0.0137
0.8	0.33	153.3	3.6	0.426	0.314	0.0281
0.8	0.32	158.9	3.35	0.408	0.438	0.0409
1.6	0.31	163.9	3.14	0.399	0.548	0.0523
2.0	0.31	165.6	3.08	0.399	0.671	0.0641
4.0	0.32	168.9	2.95	0.417	1.28	0.117
6.0	0.35	172.2	2.83	0.453	1.85	0.156
8.0	0.37	176.7	2.69	0.481	2.35	0.186
10.0	0.40	180.0	2.58	0.517	2.81	0.207
12.0	0.43	183.9	2.47	0.558	3.23	0.221
14.0	0.46	187.2	2.38	0.589	3.63	0.235
16.0	0.49	190.0	2.31	0.635	4.03	0.242
18.0	0.53	192.2	2.25	0.676	4.41	0.249
19.9	0.56	194.4	2.2	0.716	4.8	0.255
21.9	0.59	195.6	2.17	0.753	5.2	0.263

From the tables above it can be seen that the contact temperature, friction coefficient and frictional torque all rise when the shaft speed is increased. Lubrication film thickness is increased when the shaft speed is increased, but it is lower with high oil sump temperatures than with low ones. Stribeck curves of the test results with each oil sump temperature are presented in **Figure 22** and a graph showing lubrication film thickness in the function of shaft speed is presented in **Figure 23**.

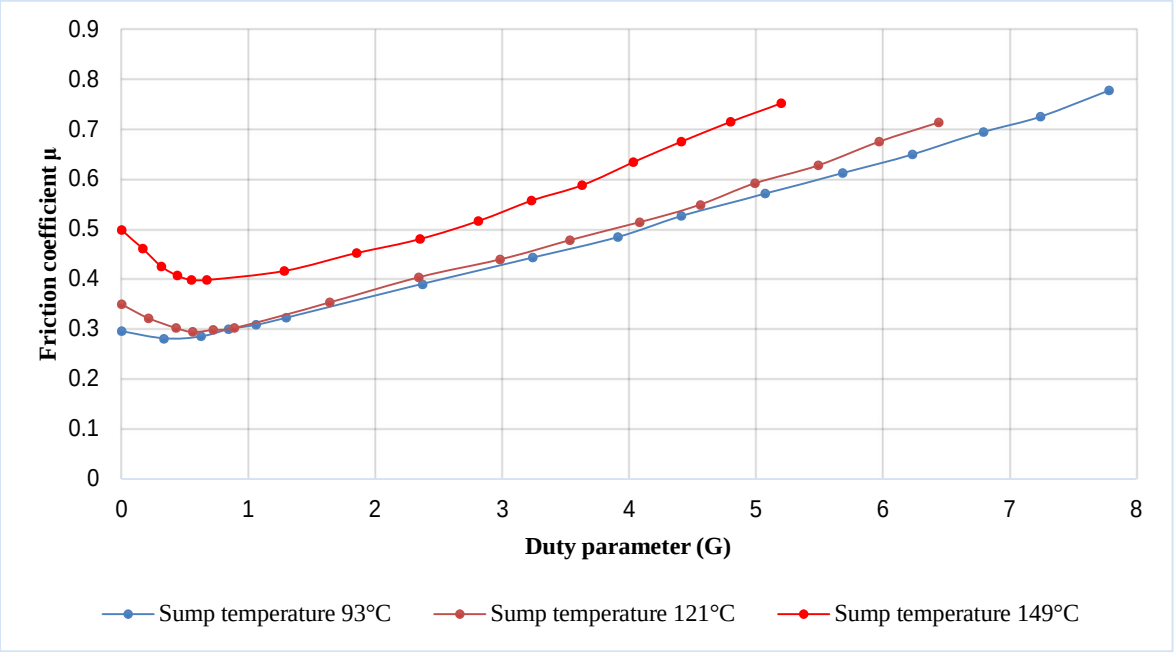

Figure 22. Stribeck curves for different oil sump temperatures (Mod. Horve 1996, p. 192).

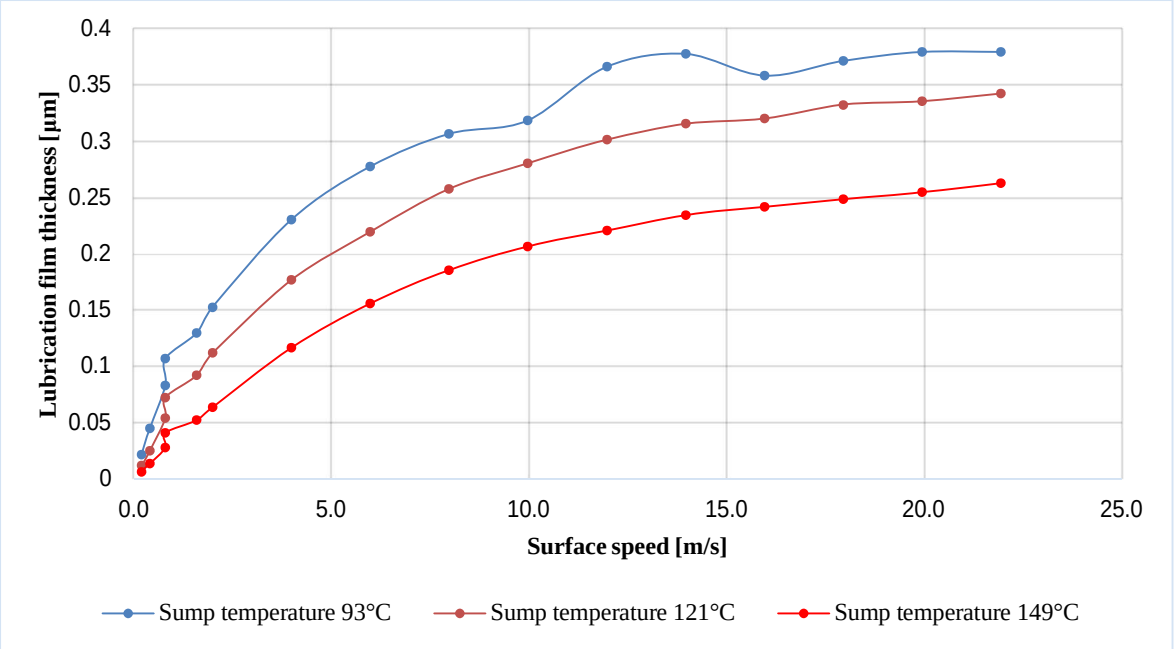

Figure 23. Lubrication film thickness in the function of shaft surface speed based on test results presented in Tables 2, 3 and 4.

From the Stribeck curves it can be concluded that the seal operates in different lubrication regimes. All the curves have a minimum value which indicates that the seals operate in boundary lubrication regime when the shaft surface speed is low and transfers to mixed lubrication as the surface speed is increased (Horve 1996, p. 187). With oil sump temperatures 121 °C and 93 °C the seals reach elastohydrodynamic regime with very high shaft speeds but with the highest oil sump temperature 149 °C the seal does not practically reach elastohydrodynamic lubrication regime. From **Figure 23** it can be seen that the lubrication film thickness increases in a steeper slope with lower shaft speeds. It is also good to note that the lubrication film thickness is very thin even with the highest shaft surface speeds.

From the torque – surface speed graph presented in **Figure 24** it can be seen that when the lubrication of the seal is in the mixed lubrication regime the friction torque increases steadily.

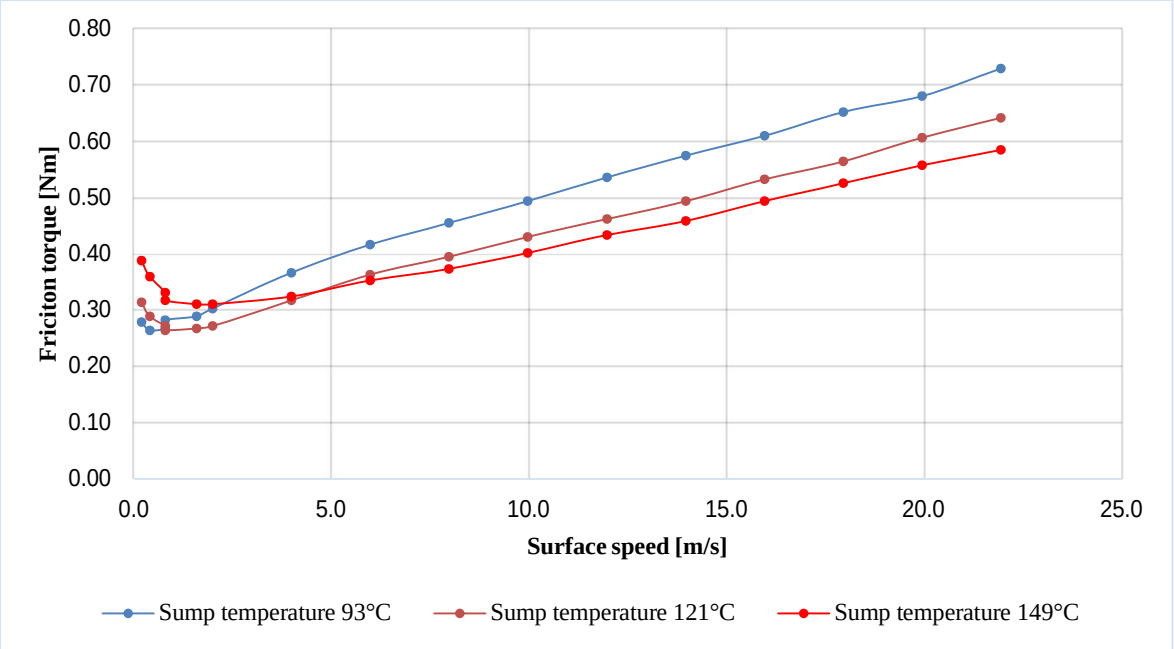

Figure 24. Frictional torque as a function surface speed based on test results presented in Tables 2, 3 and 4.

Different studies show similar behavior. Wennehorst (2016) studied the lubrication conditions and lubrication film thickness with different shaft surface speeds. He also measured the lubrication film thickness in different locations on the seal cross-section. As in the test results reported by Horve (1996, pp. 187-190), the tests performed by Wennehorst (2016) show that the friction coefficient starts from a non-zero value, which strengthens the conclusion that the frictional force of the seal is determined by a constant and velocity dependent terms (Borras 2020, p. 46) . A graph showing the frictional torque in the function of rotation speed based on tests performed by Wennehorst (2016, p. 72) is presented in **Figure 25**.

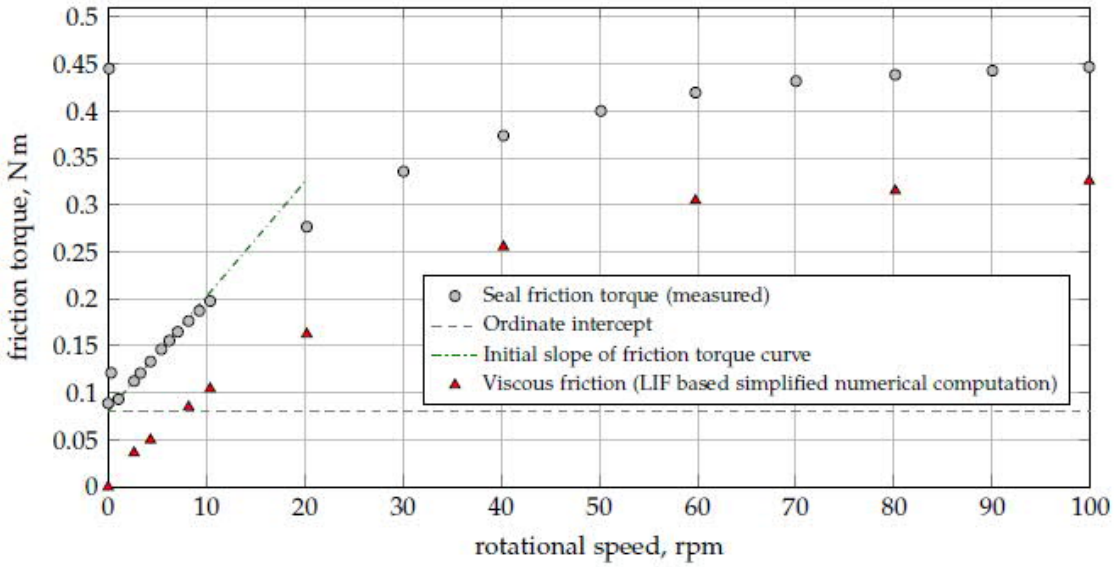

Figure 25. Friction torque in the function of rotational speed (Wennehorst 2016, p. 72).

The lubrication film thickness – rotational speed graphs presented by Wennehorst (2016) show similar behavior than tests reported by Horve (1996, pp. 187-190) – the film thickness increases with a steeper slope in the lower rotational speeds and the slope becomes less steep with higher rotational speeds. The lubrication film thickness values differ between Horve and Wennehorst, but when comparing the test conditions between the two studies the conditions – and of course the seal cross section– are different. Especially the oil sump temperature and radial force differs greatly between the two studies. It is also good to note that as in Horve's work the lubrication film thickness is a calculated value, Wennehorst utilized Laser Induced Fluorescence method (LIF) to measure the lubrication film thickness and distribution in the contact (Wennehorst 2016, p. 33). The seal and test properties used by Wennehorst (2016, pp. 30, 43, 48-49) are presented in *Table 5*, the oil sump temperature and the contact width are approximate values extracted from graphs presented by Wennehorst. The minimum film thickness in the function of rotational speed determined by Wennehorst (2016, p. 57) is presented in **Figure 26**.

Table 5. Seal data and test parameters (Mod. Wennehorst 2016, pp. 30, 43, 48-49).

Seal material	FKM
Shaft diameter [mm]	82
Oil	Mineral
Oil kinematic viscosity at 40°C [mm^2/s]	172

Table 6 continues. Seal data and test parameters (Mod. Wennehorst 2016, pp. 30, 43, 48-49).

Seal material	FKM
Shaft diameter [mm]	82
Oil	Mineral
Oil kinematic viscosity at 40°C [mm^2/s]	172
Oil pressure	N/A
Sump level	N/A
Contact width [mm]	approx. 0.15
Oil sump temperature [°C]	20-30
Radial load [N/mm]	0.0555

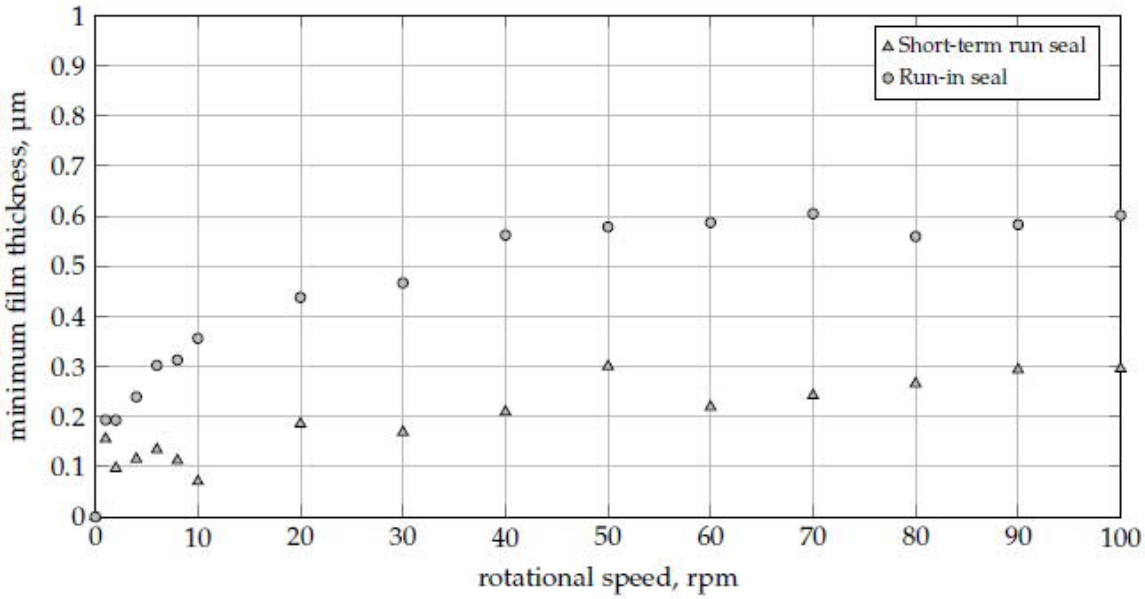

Figure 26. Minimum lubrication film thickness in the function of rotational speed (Wennehorst 2016, p. 57).

One of the key findings in the tests performed by Wennehorst (2016, pp. 55-56) were that the lubrication film thickness and its behavior is different when comparing a run in and a "new" seal. He found that that when considering a new seal, the lubrication film thickness increase caused by increasing surface speed occurs mainly close to the start and end of the contact area where the contact stress is low. Wennehorst explains this to happen by viscous drag flow of the lubricant around the surface asperities on the sealing ring contact surface, as pressure build-up caused by viscous drag flow is highly dependent on the local contact

pressure distribution. (Wennehorst 2016, pp. 48, 55-56.) Lubrication film thickness in different areas of the contact in a new seal is presented in **Figure 26**.

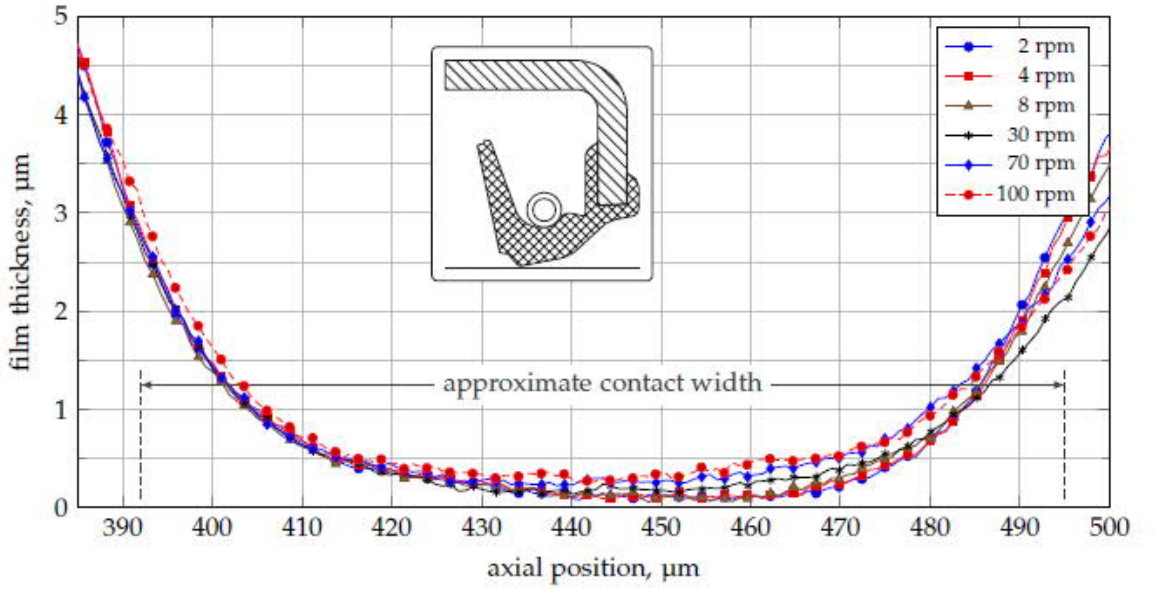

Figure 27. Lubrication film thickness in different areas of the contact in a new seal (Wennehorst 2016, p. 55).

With a run-in seal, the surface speed related lubrication film build-up occurs on the whole contact area, and the lubrication film thickness is significantly larger, excluding very low surface speeds when the seal has not reached the mixed lubrication region. The lubrication film thickness is also increased more in the middle area of the contact when the shaft speed was increased, which was contrary compared to a new seal. The lubrication film thickness was also found to always be lower than the combined surface roughness of the seal contact face and the shaft surface. The maximum local film thickness was measured from the areas that contained the deepest cavities in the seal material and the cavities oriented in circumferentially around the shaft when the shaft rotation was started. (Wennehorst 2016, pp. 56-57.) This strengthens the sealing and lubrication theory explained in Chapter 4.6. Lubrication film thickness in different areas of the contact in a new seal is presented in **Figure 28**.

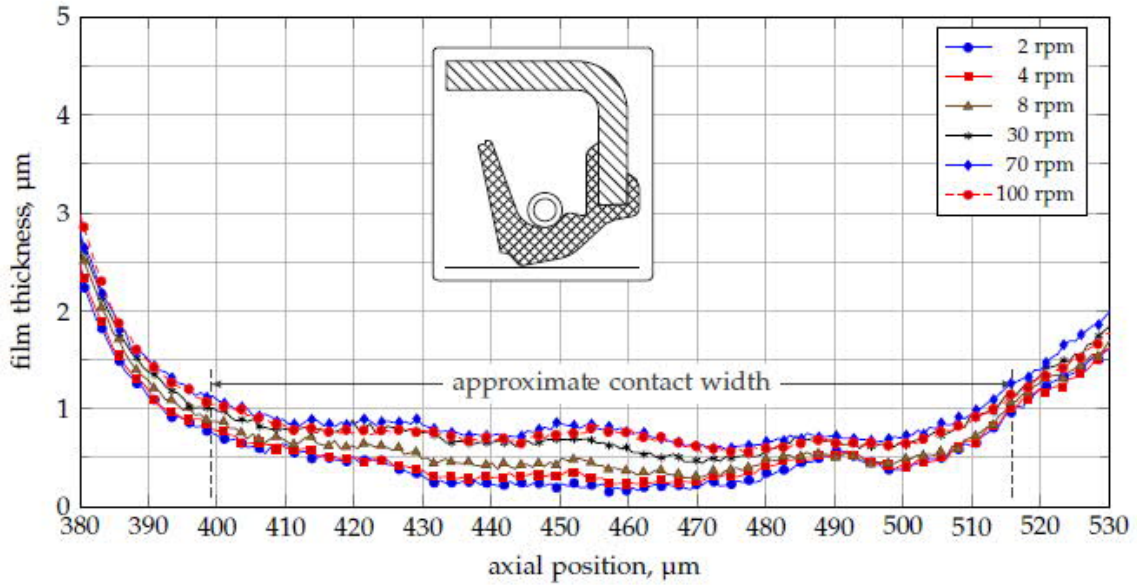

Figure 28. Lubrication film thickness in different areas of the contact in a run-in seal (Wennehorst 2016, p. 56).

The lubricant also cavitates on the seal-shaft contact when the surface speed of the shaft is increased sufficiently. Cavitation first occurs on the back side of the seal on a small region, but when the surface speed is further increased, lubricant cavitation also occurs on the spring side of the seal. When the shaft surface speed is increased even further, the intensity and width of the cavitating regions increases. (Stakenborg 1988b, p. 12.)

4.7.2 Seal followability in static and dynamic misalignment

Considering the case company's products, the seals ability to follow the shaft's dynamics is essential due to relatively large radial displacements present in the case company's application. The seals capability to follow shaft movement is also important basically in every operating condition as the seals practically always see static misalignment and dynamic excitation due to geometrical imperfections on the shaft, seal, and other components of the system in question (Stakenborg & Leeuwen 1990a, p. 578). Dynamic misalignment is also known to have a significant effect on the seal wear and lifetime (Horve 1996, pp. 227-228).

Misalignment can be divided into static and dynamic misalignment, and they can yet again be divided into radial and angular misalignment. In addition to static and dynamic

misalignment created by the components on the system, the source of misalignment can be for example due to outside forces or speed-induced wobbling. (Borras 2020, pp. 278-279.) A schematic view showing different types of misalignment is presented in **Figure 29**.

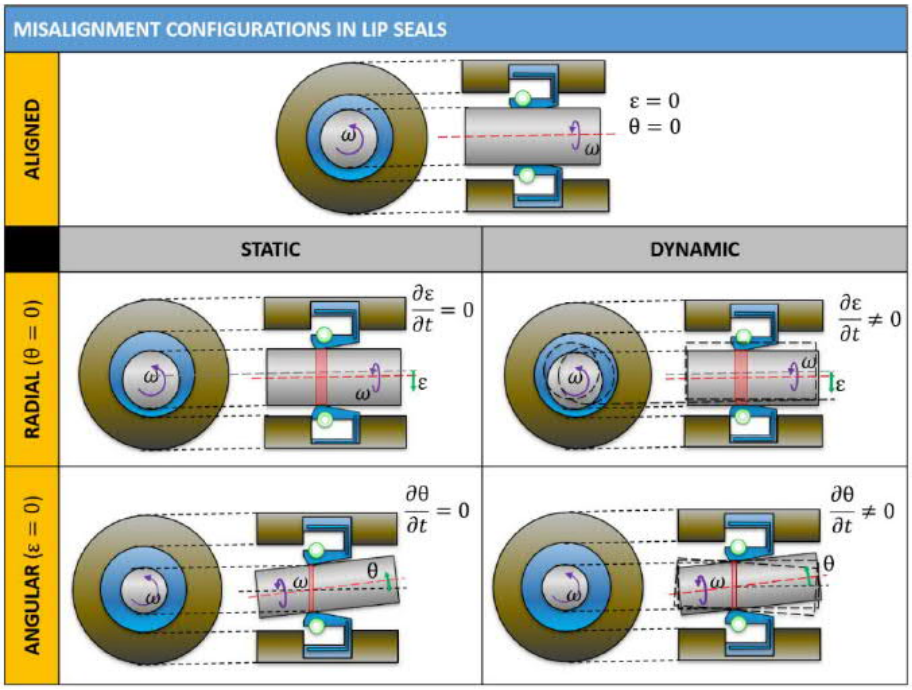

Figure 29. Different types of misalignment (Borras 2020, p. 279).

Stakenborg and Leeuwen (1990b) studied how dynamic runout effects the lubrication film between the seal and the shaft and found that when the shaft speed, and thus the frequency of the harmonic excitation on the seal created by the shaft runout, exceeds a certain limit, the seal material won't be able to follow the radial movement of the shaft. Due to the materials incapability to follow the radial movement, a gap is formed between the seal and the shaft. (Stakenborg & Leeuwen 1990b, pp. 585-586.) A schematic view showing how a gap is formed between the seal and the shaft in vibrating conditions and how lubricant flows to the formed clearance is presented in **Figure 30**.

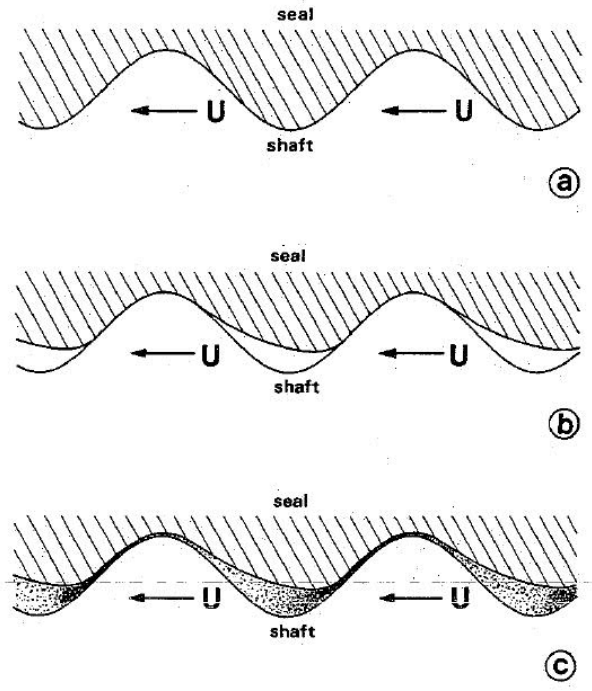

Figure 30. Seal followability on shaft surface (Stakenborg & Leeuwen 1990b, p. 586).

Forming of the gap is dependent on the viscoelastic material behavior of the seal. Elastomeric materials show glass transition, which leads to a significant increase on the material stiffness and thus the materials capability to follow shaft movement. The dynamic stiffness of the seal can be orders of magnitude higher in the glassy state at high frequencies compared to rubbery state at low frequencies. (Stakenborg & Leeuwen 1990a, p. 578.) As the seal material behavior is temperature and time dependent, and so the temperature that the seal is operated on together with the frequency of the excitation the seal faces is essential. Thus, the seals ability to follow the shaft is a combination of material properties, operating temperature, shaft speed and the type and magnitude of the misalignment. Seals are also found to follow dynamic misalignment better when the shaft is rotated and thus the seal is lubricated due to suction effect created by the lubricant cavitation on the seal-shaft contact. (Borras 2020, p. 56.) A study by Borras et. al. (2020, p. 26) also revealed that seals will start to leak before contact pressure between the seal and the shaft is zero. Graph showing the sealing limit pressure of a seal is presented in **Figure 31**.

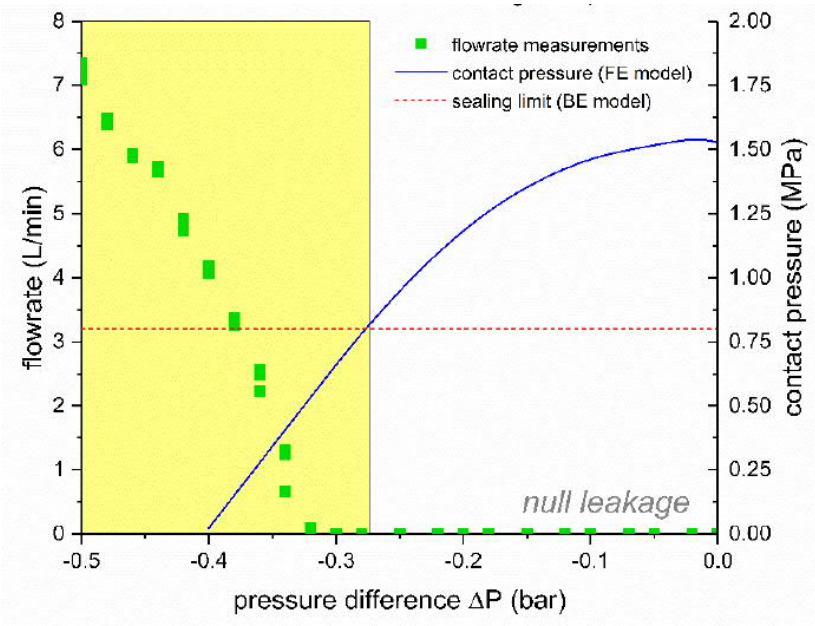

Figure 31. Sealing limit pressure (Borras et al., 2020, p. 26).

As the stiffness of the elastomer depends on temperature, applied load amplitude and frequency, the material stiffness of the elastomer is significantly higher at higher than in low frequencies. Temperature has also a significant meaning on the material stiffness in the frequency range of 0 to 100 Hz but is in less significance in lower frequencies. (Stakenborg 1988b, pp. 59-60.) A schematic presentation of the dynamic stiffness behavior of an elastomer in different temperatures is presented in **Figure 32**.

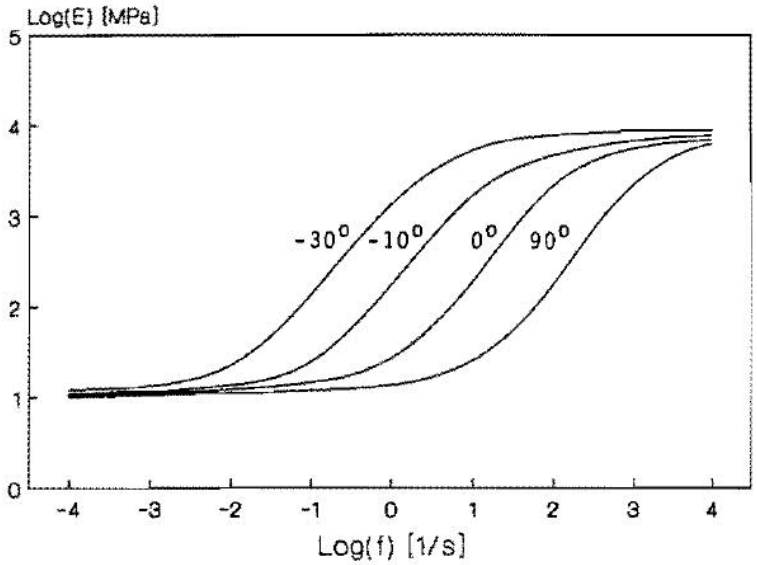

Figure 32. Dynamic stiffness of an elastomer as a function of excitation frequency (Stakenborg 1988b, p. 60).

Deformation of the seal profile can be considered non-significant as when examining the cross-section of the radial shaft seal during radial displacement, the seal flexes from its hinge point (see **Figure 14**) and the movement of the sealing ring tip can be considered as rigid body rotation. Naturally, the α and β angles and the location of the hinge point and different parts of the sealing change in respect to the shaft due to radial misalignment ε as presented in **Figure 33**. (Borras et al. 2020, pp. 4-5.)

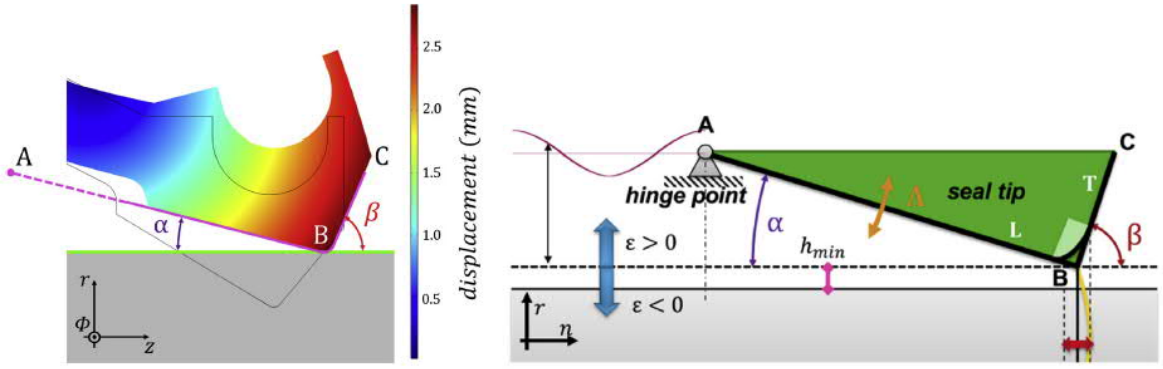

Figure 33. Seal cross-section movement due to radial displacement (Mod. Borras, Rooij, & Schipper, 2020, pp. 5-6).

When the shaft is misaligned radially and the seal deforms, the contact profile of the seal on the shaft become sinusoidal forming two convergent and two divergent gaps on the seal contact on the circumferential direction. When the shaft is rotated, two areas will experience increasing pressure, and two regions will experience decreasing pressure. This leads to unsymmetric conditions for the lubrication film build-up, and thus the liquid flow rate becomes larger on one direction compared to the other. Without misalignment, the flow rate is typically greater from the back side of the seal to the spring side, but due to misalignment the direction of liquid flow can change. The unsymmetric pressure distribution in different areas of the seal is shown in **Figure 34**. (Borras et al. 2020, pp. 3-4, 8.)

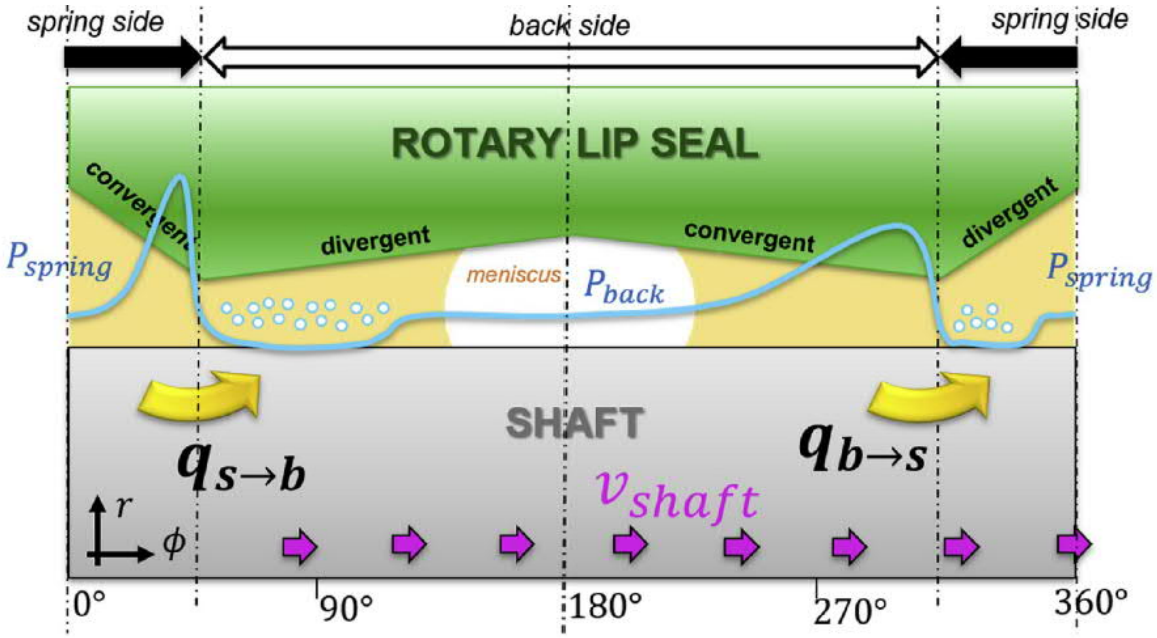

Figure 34. Pressure build-up due to radial misalignment (Borras, Rooij, & Schipper 2020, p. 4).

When the misalignment is dynamic, e.g. when the shaft is vibrating, the location of the high and low pressure regions will vary accordingly. If the hydrodynamic load induced by the misalignment is sufficiently large, some areas of the seal can intermittently operate on boundary lubrication region, or on the other hand, on full film lubrication region. (Borras et al. 2020, p. 9.)

4.8 Heat generation in the radial lip seals

Frictional heat is generated on the seal-shaft contact. The heat generation is also relatively large and thus the heat density is high, and the contact temperature is considerably higher compared to the oil temperature (Flitney 2007, p. 116). Temperature of the seal and the lubricant also affects the seals contact force, width, and stress distribution. Above-mentioned changes in the contact conditions happen because the seal material and shaft have different heat expansion properties and the stiffness of the seal material is also affected by temperature. Length and stiffness of the garter spring is also temperature dependent. (Stakenborg & Ostaijen 1988, p. 79.) Power consumption of a radial shaft seal can be calculated as presented below (Frölich et al. 2014, p. 75).

$$P = \mu p v \pi d b \tag{5}$$

In Equation 5, μ is the friction coefficient, p is the average contact pressure, v is surface velocity, d is the shaft diameter and b is the contact width.

The friction torque of a radial shaft seal is practically speaking proportional to the product of the viscosity of the lubricant and surface speed of the shaft, and when the surface speed is low, the surface speed is the main factor impacting on the friction torque. When the shaft surface speed is increased, the lubricant in the contact heats and its viscosity gets lower and thus a maximum value in frictional torque is reached even if the shaft speed is increased further as presented on the left side of **Figure 35**. (Jia et al. 2014, p. 1180.) After reaching the peak value, the friction torque decreases slightly as presented on the right side of **Figure 35** (Guo et al. 2013, p. 198).

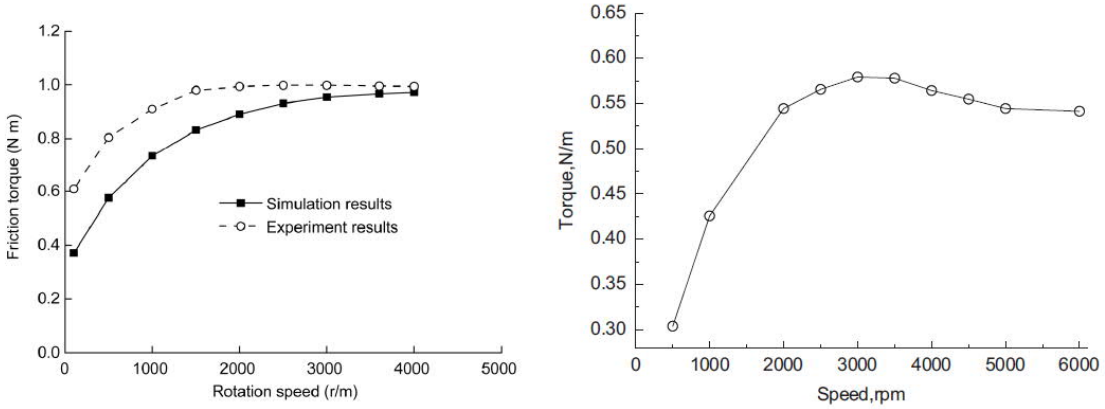

Figure 35. Frictional torque in the function of rotational speed (Jia et al. 2014, p. 1180; Guo et al. 2013, p. 198).

As the frictional coefficient is related to the lubricant viscosity, the friction torque and power consumption of a radial lip seal is reduced when the oil sump temperature is increased (Horve 1996, p. 220). Contact temperature is also reduced if all other parameters but the base oil viscosity are kept stabile (Frölich et al., 2014, p. 75). Graphs showing the contact temperature, friction torque and power consumption with different shaft speed and oil sump temperatures for a radial lip seal is presented in **Figure 36**.

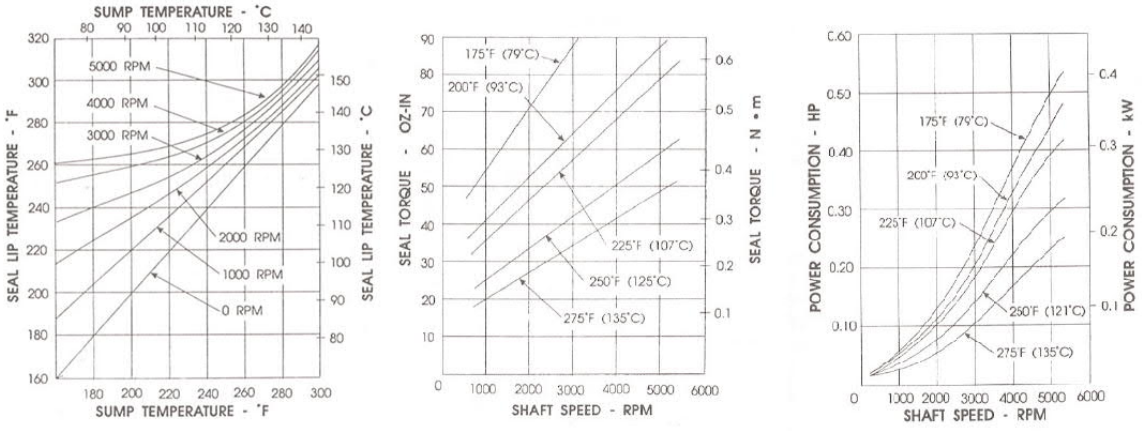

Figure 36. Contact temperature, torque and power consumption with different shaft speeds and oil sump temperatures (Mod. Horve 1996, p. 221).

The contact temperature is higher than the sump temperature as can be seen from **Figure 36**. The span between the contact temperature is dependent on the lubricant type, viscosity and oil sump fill level as presented in **Figure 37**. Lower curves for the two oils in the **Figure 37** are for a seal with full oil sump, and the upper curves are for seals with oil sump level being 25% of the shaft diameter. (Freudenberg Sealing Technologies 2015, p. 39.)

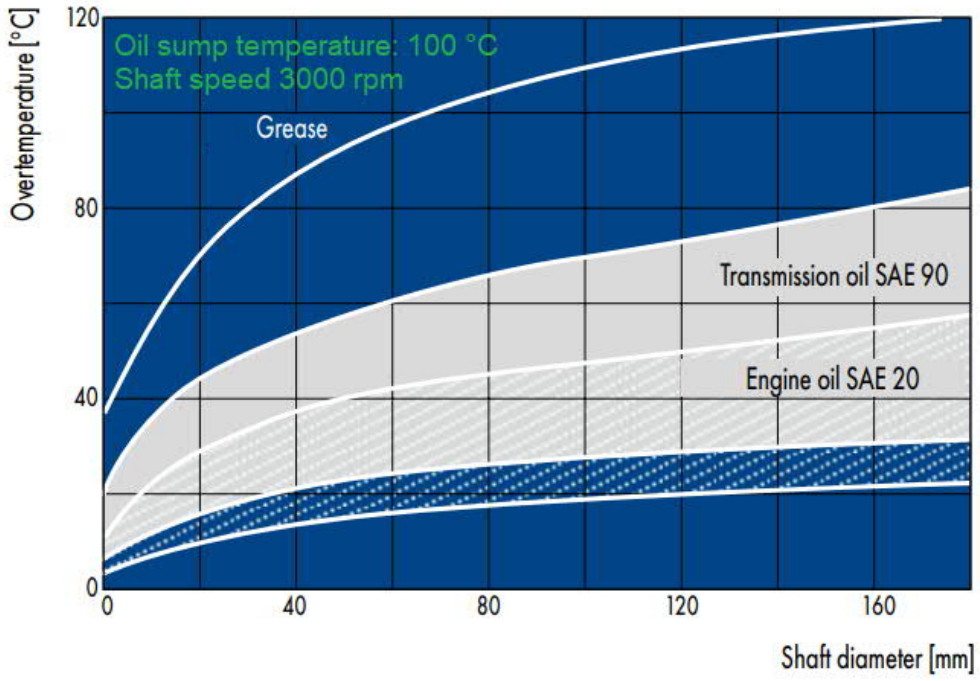

Figure 37. Overtemperature on the seal contact (Mod. Freudenberg Sealing Technologies 2015, p. 39).

Radial force affecting on the seal contact has great effect on the contact temperature. The highest contact stress is concentrated into a small area on the sealing ring tip. (Kim & Shim 1996, p. 113.) Temperature distribution on the sealing ring develops accordingly as presented on the left side on **Figure 38**. A graph presenting the rise in the contact temperature as a function of the radial force is presented on the right side of **Figure 38**.

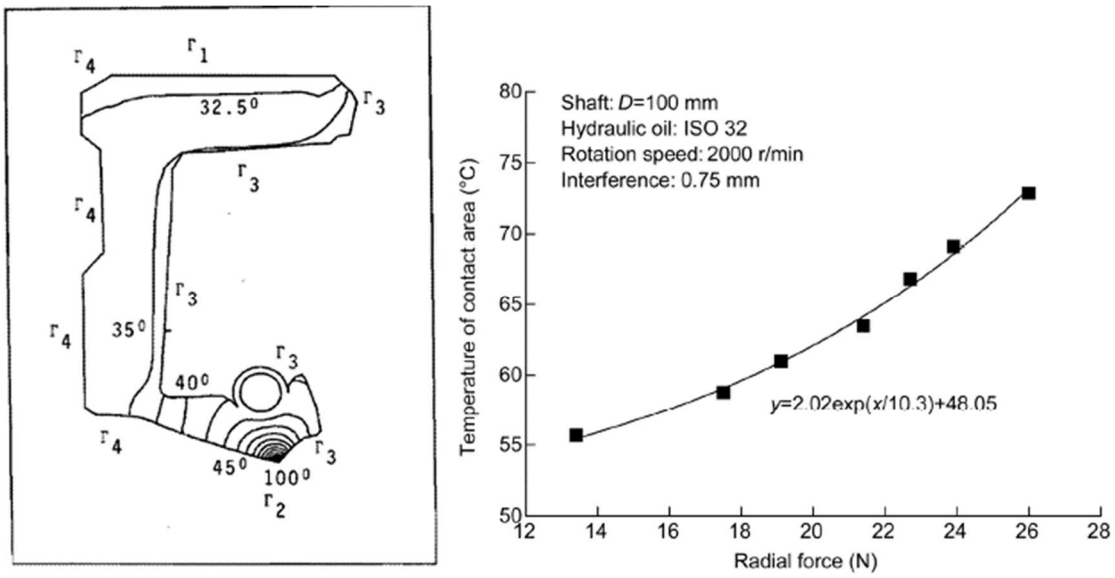

Figure 38. Left side: Steady-state temperature distribution (Stakenborg & Ostaijen 1988, p. 86). Right side: Contact temperature in the function of radial stress (Jia et al. 2014, p. 1181).

4.9 Leakage, wear, and seal lifetime

As described in the previous chapters, shaft seals can lose their sealing capability temporarily or permanently for following reasons:

- Inward pumping mechanism is disturbed or the pumping rate from the spring side to the back side is higher than the inward pumping rate.
- Seal is not able to follow shaft dynamics and lubricant leaks through gaps between the shaft and the seal.

Radial shaft seals can also start to leak irreversibly if the seal material is excessively worn or damaged. Hardening and thus cracking of the seal material is one of the main reasons for seal leakage. Hardening affects the seals ability to follow shaft dynamics and it will also have a negative effect on the inward pumping mechanism. When the hardening of the material is advanced further, cracks allowing lubricant leakage will also be formed on the

seal material. Blisters on the seal material can also cause leakage. (Müller & Nau 1998, pp. 86-87.)

The seal material will age when it is in contact with the lubricant, and it will eventually swell due to absorption of the lubricant. The increased volume of the seal will loosen the interference between the seal and the shaft. Swelling also softens the material leading to reduction on the elastic modulus of the material. These changes in the seal material will affect the pumping phenomena on the seal contact. The pumping rate can decrease quite substantially in a relatively short time as presented in **Figure 39**. (Guo et al. 2014, p. 193.)

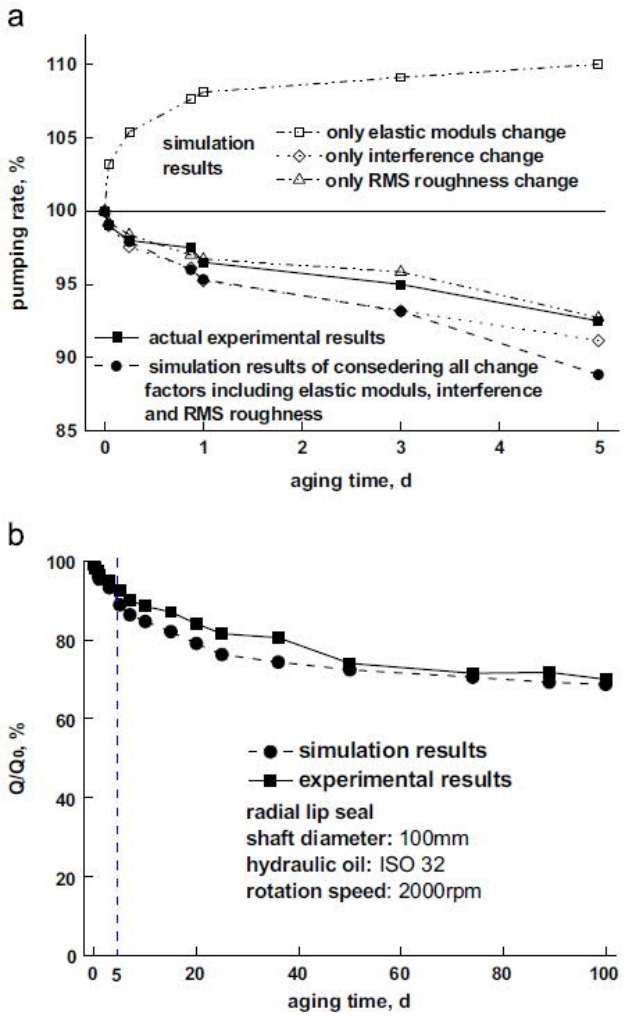

Figure 39. Seal pumping rate reduction in the function of time (Guo et al. 2014, p. 193).

Interestingly, if only the elastic modulus of the sealing ring is reduced, the pumping rate is actually increased rather than decreased. The reduction of the pumping rate is thus caused

by reduction in the interference fit and decreasing surface root mean square (RMS) roughness of the seal material. (Guo et al. 2014, p. 193.)

Dynamic runout is also found to have a significant effect in the seal lifetime (Flitney 2007, p. 118; Horve 1996, p. 228; R.L. Hudson & Company 2005, p. 131). For example, tests performed by Horve (1996, p. 228) show that every 0,1 mm increase in the dynamic runout decreases seal lifetime by approximately 16 %.

4.9.1 Wear mechanisms and lifetime estimation

There are three wear mechanisms relevant to seal wear:

- Adhesive wear causes changes on the seal or shaft surface due to material transfer from one surface to the other induced by physical bonding forces.
- Abrasive wear is especially relevant when radial shaft seals are considered as typically abrasive wear occurs in soft–hard contact pairs as surface roughness of the harder material causes wear on the softer material. Abrasive wear can also occur on both surfaces in case there are hard particles on the sliding contact.
- Erosive wear is caused by impact of solid particles on liquid stream on the material surface. (Frölich et al. 2014, p. 74.)

There are multiple different methods to try to calculate seal wear. A common method is to use contact pressure in the calculation as presented below. (Frölich et al. 2014, p. 74.)

$$V = K\frac{Q}{H}s \tag{6}$$

In Equation 6, V is the volume of the wear, K is an empirically defined seal specific wear coefficient, Q is the radial force in the contact, H is the hardness of the seal material and s is the sliding distance. A simplified version of the method presented in Equation 6 ignores the seal material hardness as presented below. (Frölich et al. 2014, p. 74.)

$$V = KQs \tag{7}$$

In Equation 7, V is the volume of the wear, K is the empirically defined seal specific wear coefficient, Q in the radial force in the contact and s is the sliding distance. Temperature has a significant influence on the seal rate, and thus an empirically defined temperature–wear coefficient is also often added to the equations. (Frölich et al. 2014, p. 74.)

4.9.2 Seal wear in FKM seals

Excessive seal and shaft wear has been reported in systems that use fluoroelastomer seals with synthetic lubricants (Burkhart et al. 2020, p. 2). It has also been found that some synthetic oil – elastomer combinations does not show regression in the elastomers' mechanical properties in immersion tests, but in dynamic testing conditions excessive wear is found (Adler et al. 2018, p. 30). Wear rate in a seal system is connected to wetting properties of the elastomer – lubricant combination. Fluoroelastomers are found to have worse wetting properties than for example NBR, and thus fluoroelastomer seals operate more on the mixed lubrication regime. In fact, a portion of the contact between the shaft and the seal is continuously on mixed lubrication regime and thus has rigid body contact. The area of the contact that is on the mixed lubrication regime is dependent on the surface speed as presented in **Figure 40**. (Burkhart et al. 2020, pp. 2-9.)

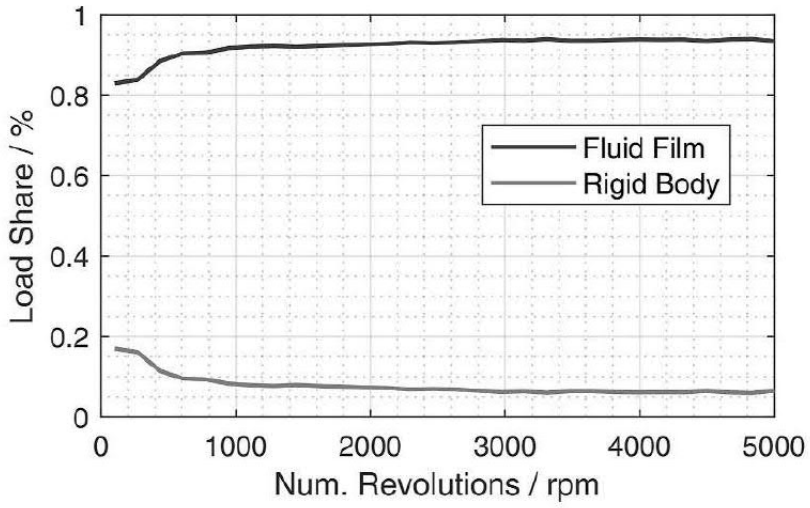

Figure 40. Load share between mixed lubrication and elastohydrodynamic lubrication (Burkhart et al. 2020, p. 10).

The used lubricant has a significant effect on the wetting properties of the elastomer – lubricant combination. If the wetting properties are not sufficient, the lubricant does not

reach the whole contact area of the shaft and seal leading to poor lubrication and high wear rate. Polarity difference of the elastomer and oil is one of the main factors when wetting properties are considered – the higher the polarity difference, the worse are the wetting properties. (Adler et al. 2018, p. 34.) Polarity of different elastomers and oils and the effect of wetting properties are presented in **Figure 41**.

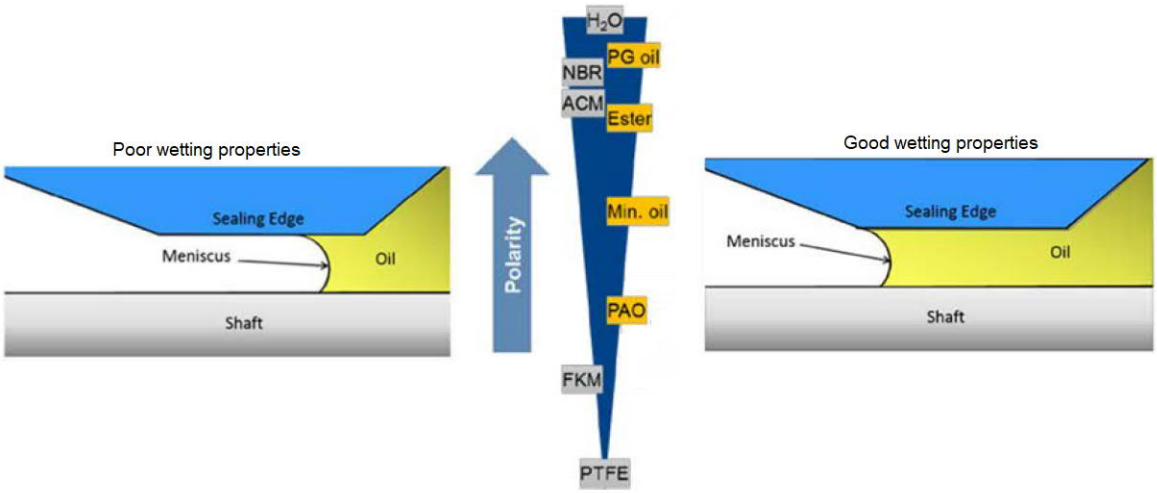

Figure 41. Polarity and wetting properties (Mod. Adler et al. 2018, pp. 31, 34).

Fluorocarbon elastomers have also significantly higher filler proportion compared to NBR, which is also found to have an impact on the wear rate as the hard filler particles cause abrasive wear on the seal. Especially silica fillers are reported to cause excessive wear. The size of the filler particles can be on the range of 10 to 50 µm, which is significantly higher than the lubricant film thickness. However, even though FKM seals used together used with synthetic polyalphaolefin (PAO-I) lubricants are found to cause excessive wearing, it cannot be generalized that FKM seals and PAO-I lubricants automatically cause wear issues, as not all seals and/or shafts run with same conditions show signs of wear. Uneven filler distribution in the elastomer can explain why some seals wear fast and also groove the shaft. (Burkhart et al. 2020, pp. 2-11.)

4.9.3Temperature and seal wear

Effect of temperature on the contact between the seal and the shaft and on the seal material can be divided into reversible and irreversible effects (Stakenborg & Ostaijen 1988, p. 79). Reversible effects were covered in Chapter 4.8. The irreversible effects are:

- Effect of temperature on seal aging which hardens the elastomer.
- Effect of temperature on the chemical reactions between the lubricant and the elastomer.
- Effect of temperature on the elastomers lubricant absorption rate. (Stakenborg & Ostaijen 1988, p. 79.).

Excessive temperature on the seal is one of the main reasons for premature seal failure (Kim & Shim 1996, p. 113). Seal manufacturers give a maximum temperature that should not be exceeded to prevent excessive wear (Stakenborg & Ostaijen 1988, p. 81). Heat accelerates breakdown of the lubricant and varnish starts to form on the hot spots of the sealing ring. Eventually, the varnish changes to carbon and builds in thickness near the sliding contact between the shaft and the seal. The rate of the varnish building is highly dependent on temperature. If varnish forms in an unfavorable area, it can accelerate seal wear or even lift the sealing lip causing leakage. Heat also accelerates the hardening of the rubber, especially at the contact surface between the seal lip and the rotating shaft. (Müller & Nau 1998, p. 87.)

4.10 Common causes for seal damage and leakage

As described in the earlier chapters, multiple reasons can lead to seal failure and leak. Some of the most common causes for damage and leaking seals are listed in this chapter. The mechanisms are being covered in more detail in the previous chapters and they are only briefly summarized here.

4.10.1 Blisters near or on the contact surface

Blisters can be caused by excessive heat especially on the back side of the seal. Blisters make the seal deform and thus lift the lip tip from the shaft causing leakage. In some cases, blisters are present only when the seal is hot, which can make diagnosing difficult. (R.L. Hudson & Company 2005, p. 226.) Blisters can be also caused by chemical incompatibility of the elastomer and lubricant, or if the seal is exposed to other chemicals such as cleaning solvents. Incompatible elastomer – lubricant combination can also cause the seal to swell and distort. (Flitney 2007, p. 433.) An example of blisters on the seal surface is presented in **Figure 42**.

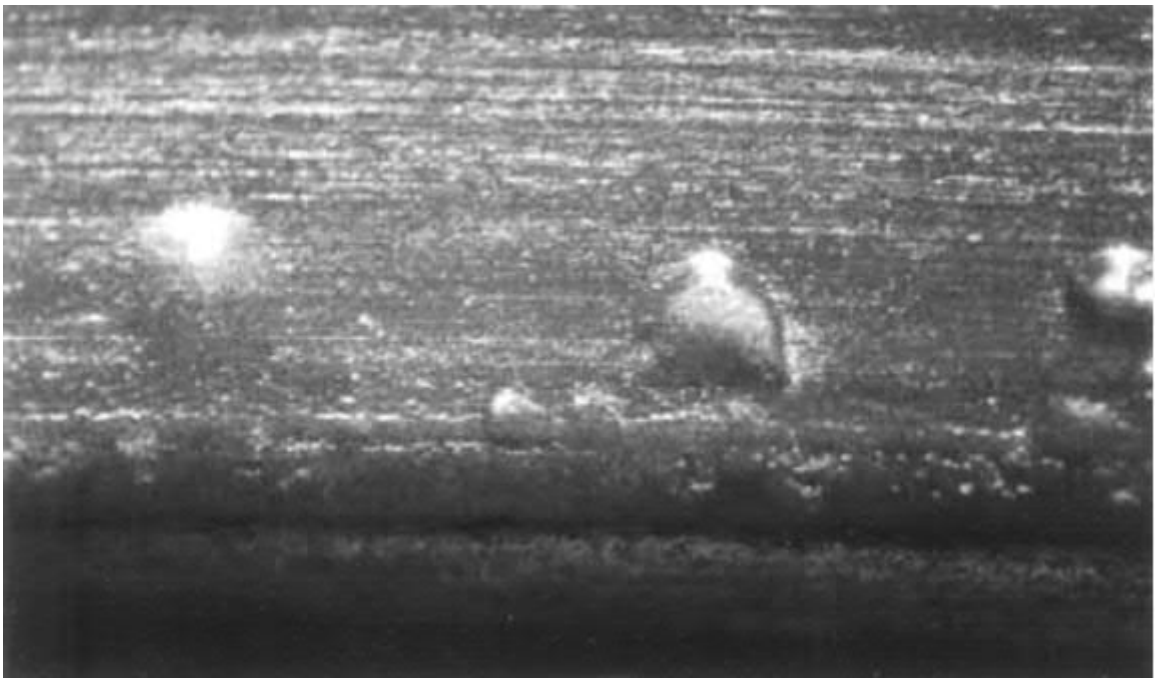

Figure 42. Blisters on seal surface (Flitney 2007, p. 434).

4.10.2 Excessive unsymmetric wear

Excessive unsymmetric wear can occur if the seal is not installed perpendicularly against the shaft or if the shaft is misaligned in relation to the seal housing. In addition to unsymmetric seal wear, risk for the garter spring to dislodge from its groove if the sela is misaligned. (R.L. Hudson & Company 2005, p. 226.) A schematic view of an unsymmetrically worn seal is presented in **Figure 43**.

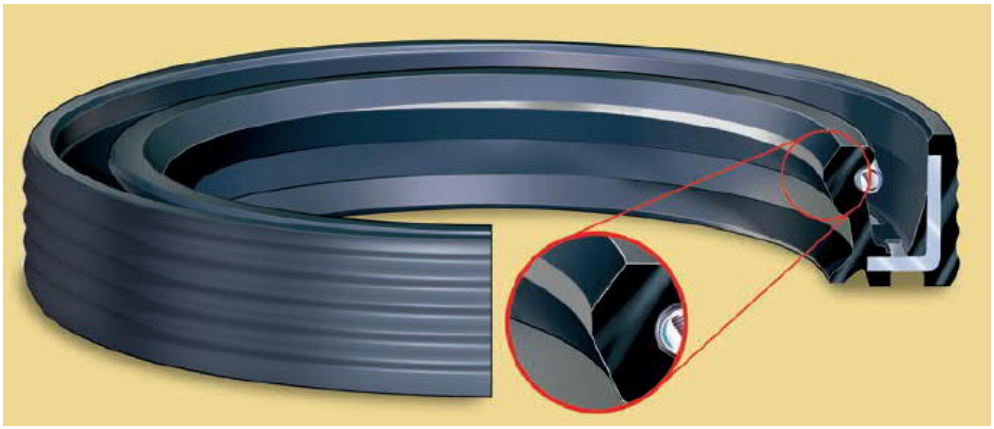

Figure 43. Unsymmetrically worn seal (R.L. Hudson & Company 2005, p. 226).

4.10.3 Broken lip

Dynamic runout or shaft vibration in low operating temperatures can cause seal lip breakage if the elastomer is not applicable to be used in low temperatures (Horve 1996, p. 287). An example of a broken lip is presented in **Figure 44**.

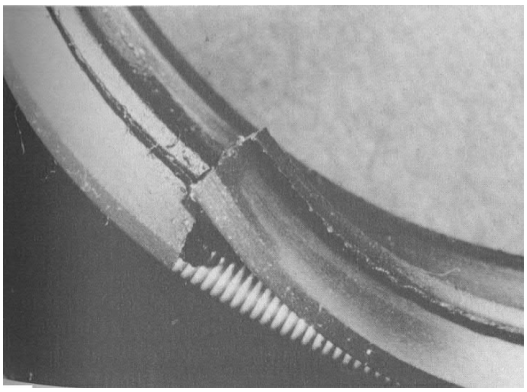

Figure 44. Broken lip due to dynamic runout in low operating conditions (Horve 1996, p. 287).

4.10.4 Axially cracked lip

Axial cracking on the contact surface can be caused by various reasons such as high pressure, high shaft speed, incompatible elastomer - lubricant combination, excessive temperature, or poor lubrication (SKF 2019, p. 51). Cracks are formed due to hardening of the elastomer and the seal might leak even before the cracks form as the hardened sealing ring is not able to follow shaft dynamics (R.L. Hudson & Company 2005, p. 228). An example of an axially cracked lip is presented in **Figure 45**.

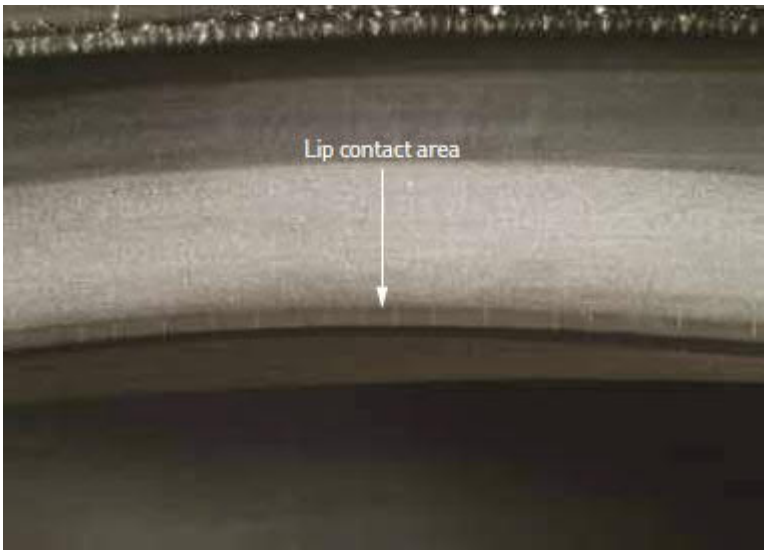

Figure 45. Axially cracked lip (SKF 2019, p. 51).

4.10.5 Nicks, cuts, or scratches on the seal surface

Nicks, cuts, or scratches on the seal surface are typically originated to assembly of the seal. Such surface defects are typically caused by installation tools or discontinuities, such as keyways or splines on the shaft. (SKF 2019, p. 50; R.L. Hudson & Company 2005, p. 229.) An example of a cut seal surface is presented in **Figure 46**.

Figure 46. Cut seal surface (SKF 2019, p. 50).

4.10.6 Leakage trough the static seal surface

Leakage trough the static sealing surface can be caused by various reasons such as scratches and dents on the metal casing of the seal (R.L. Hudson & Company 2005, pp. 230-232). Examples of different types of damage on the casing are presented in **Figure 47**.

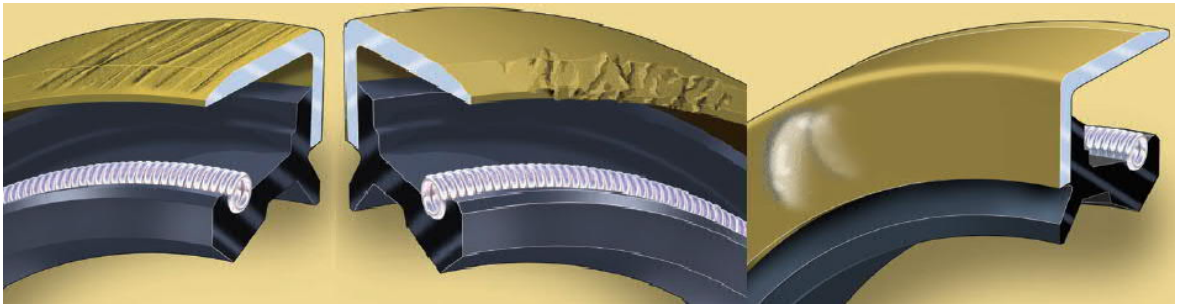

Figure 47. Damaged seal casings retell (R.L. Hudson & Company 2005, pp. 230-232).

It is good to note that when considering large diameter seals, metal casing is not usually used (Parker Hannifin 2018, p. 14). However, seals could still leak trough the static seal surface if the seal or the casing is damaged.

4.11 Excessive wear

Excessive wear can be caused by high operating pressure, abrasive particles in the seal system, excessive radial load, poor lubrication, incompatible elastomer – lubricant combination, too rough shaft surface or high static misalignment or dynamic runout. In case of multiple causes for excessive wear the wear rate can be very fast. It is also good to note that the seals wear also in normal operating condition, so seal wear is cannot always be considered as a failure. (SKF 2019, p. 50.) A schematic view of an excessively worn seal is presented in **Figure 48**.

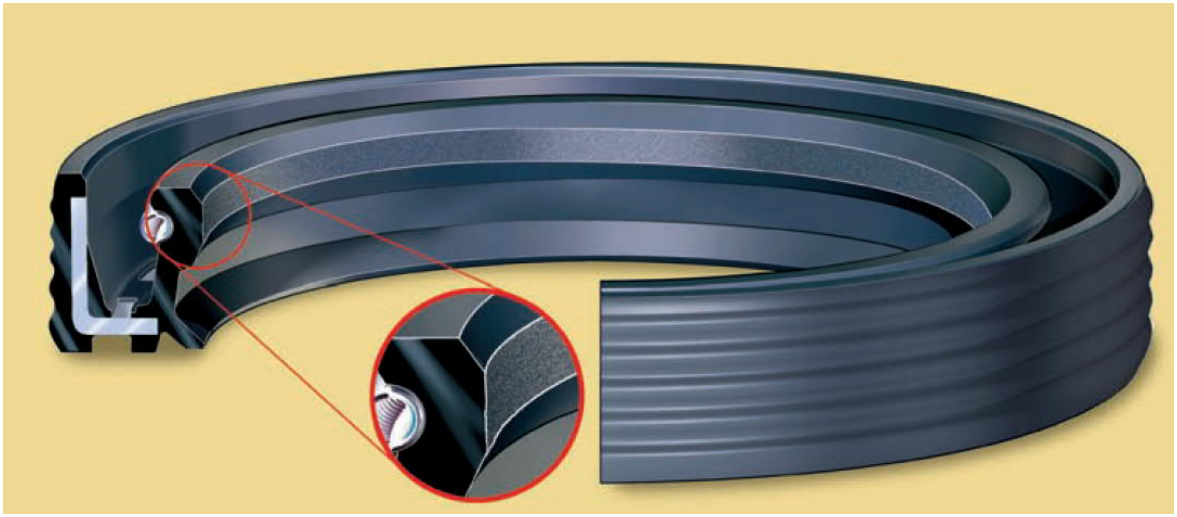

Figure 48. Excessive seal wear (R.L. Hudson & Company 2005, p. 233).

Especially when there is excessive wearing of the seal, the shaft itself can also be worn. The shaft can be worn due abrasive particles on the seal – shaft contact which grind the shaft surface. In some cases, debris can enter the seal system causing excessive shaft wear or seal damage. (R.L. Hudson & Company 2005, p. 236.)

4.11.1 Oil cocking on the seal surface

High contact temperatures lead to hard carbon layer build-up on the seal surface as the oil "burns" on the shaft surface on the air side of the seal. The hard carbon layer prevents the seals lubricant pumping mechanism from working normally leading to other damage. The carbon build-up can also lift the seal off from the shaft leading to leakage. (Horve 1996, p. 285.) An example of oil cocking is presented in **Figure 49**.

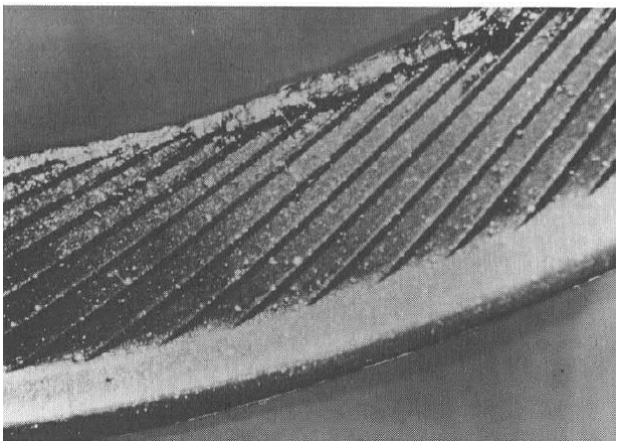

Figure 49. Oil cocking on seal surface (Horve 1996, p. 288).

4.11.2 Stick-slip

Stick-slip phenomena in radial shaft seals is caused by poor lubrication. The used lubricant can have poor lubrication capability with the elastomer it is used with, or the lubricant viscosity can be too low due to excessive temperature on the seal – shaft contact. (Horve 1996, p. 286.) Splash-lubricated seals suffer from the stick-slip phenomena more commonly than sump lubricated seals (R.L. Hudson & Company 2005, p. 245.) An example of a damaged seal due to stick-slip is presented in **Figure 50**.

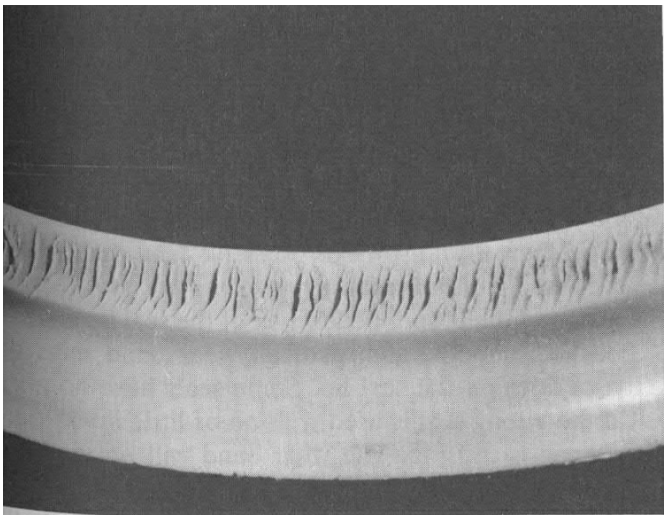

Figure 50. Seal damaged due to stick-slip phenomenon (Horve 1996, p. 289).

4.12 Summary of Chapter 4

There are numerous factors influencing the radial seal performance. Elastomers have a lot of good properties for sealing purposes, such as low modulus of elasticity, good resiliency and high elongation before braking. On the other hand they also offer a list of disadvantages, such as non-linear stress-strain properties and temperature related material properties. The material properties also vary greatly between different elastomer grades, and their performance and suitability for use must be evaluated case by case. Fluorocarbon elastomers are often used in radial shaft seals due to their good temperature and chemical resistance even though they are stiffer compared to many other elastomers. However, increased seal wear have been reported in FKM seals due to poor wetting properties formed with the elastomer - lubricant combination and large filler particle size. The lubricant to be sealed has naturally an effect on the material itself, but it essential to understand that the material –

lubricant combination also has an effect on the lubrication film properties between the seal and the shaft.

Not only the seal material properties have an effect in the radial shaft seal performance, but numerous other factors in the radial shaft seal design further determine their performance. The location of the spring and the angles on the spring side and on the back side of the seal are crucial parts of the design as they are used to create suitable pressure gradient between the seal and the shaft. Mistakes in the geometry or radial force will result in prematurely leaking seals as will poor materials.

The sealing mechanism of radial shaft seals is much more complex than could be assumed at first sight. Radial shaft seals seal liquid because a thin, typically under 0,5 µm, lubrication film is formed between the seal and the shaft. Lubricant flows in both directions in the contact, but due to the asymmetric design of the sealing ring, higher flowrate is generated from the back side of the seal compared to the flowrate form the spring side of the seal, resulting in a non-leaking seal. The lubrication film properties are dependent on numerous different factors starting from the composition of the used elastomer. The lubrication film thickness increases when the shaft speed is increased, but still usually the seals operate in mixed lubrication regime or even boundary lubrication regime when the shaft speeds, or the viscosity of the lubricant is very low.

In rotating machines, it is important that the seal is capable to withstand static dynamic misalignment even if the application would have low vibration levels as the seals usually face both static and dynamic misalignment due to geometrical imperfections of the seal, shaft or other components. In dynamic misalignment a gap forms between the seal and the shaft making it possible for the lubricant to leak out through the gap. Dynamic misalignment also changes the lubrication film properties and is found to reduce seal lifetime.

Temperature affects the seals performance greatly as it affects both the seal material properties and lubricant properties. The friction torque is proportional to the product of the viscosity of the lubricant and surface speed of the shaft. As the lubricant viscosity is temperature dependent, the friction torque will not increase endlessly even if the shaft surface speed is increased. The lubrication film properties naturally have a great influence

in the heat generation, but radial force is another main factor influencing the heat generation. Temperature is also found to accelerate seal wear and high temperature is related to many of the common failure mechanisms of radial shaft seals.

5 SEAL SYSTEM AND OPERATING ENVIRONMENT IN CASE COMPANY'S PRODUCT

The prevailing conditions present in the case company's application are explained in this chapter so that the reader can better understand the matters related to the sealing ring leakage rate in the case company's application. The basic system design of the shaft seal system in question is also being explained on a general level.

5.1 Seal system

The seal system in the case company's product is similar to the ones explained in Chapter 3 but it has five sealing rings instead of four. The five sealing rings are numbered from 1 to 5 starting from the one closest to water, and they form four seal chambers which are numbered from 1 to 4, but to avoid mixing with the sealing rings, roman numerals I, II, III and IV are used to identify the seal chambers. The seal system is equipped with an air chamber, chamber II, that separates lubrication oil and water. The air chamber can be drained. The air chamber has higher pressure than water, so air is constantly leaking to water. The air is also constantly flowing through the drain tank so that liquid entering the seal chamber II is constantly drained from it. Four of the five sealing rings, 1, 2, 4 and 5, are oriented so that the spring side of the seal is towards the water side of the seal system, and only the sealing ring number 3 is oriented the other way. The sealing ring three is oriented the other way to prevent oil leaking to the seal chamber II as seal chamber III has higher pressure than seal chamber II. On the back side of the sealing ring 5 is a bearing oil sump which is half filled with oil. Oil in the seal system is the same brand and grade as the oil used in the bearing. The bearing oil quality is monitored and maintained, so impurities should not enter the seal system from the bearing oil. Case company products have different seal and liner sizes. The liner size relevant to this thesis is ø mm. A schematic view of the sealing rings and seal chambers is presented in **Figure 51**.

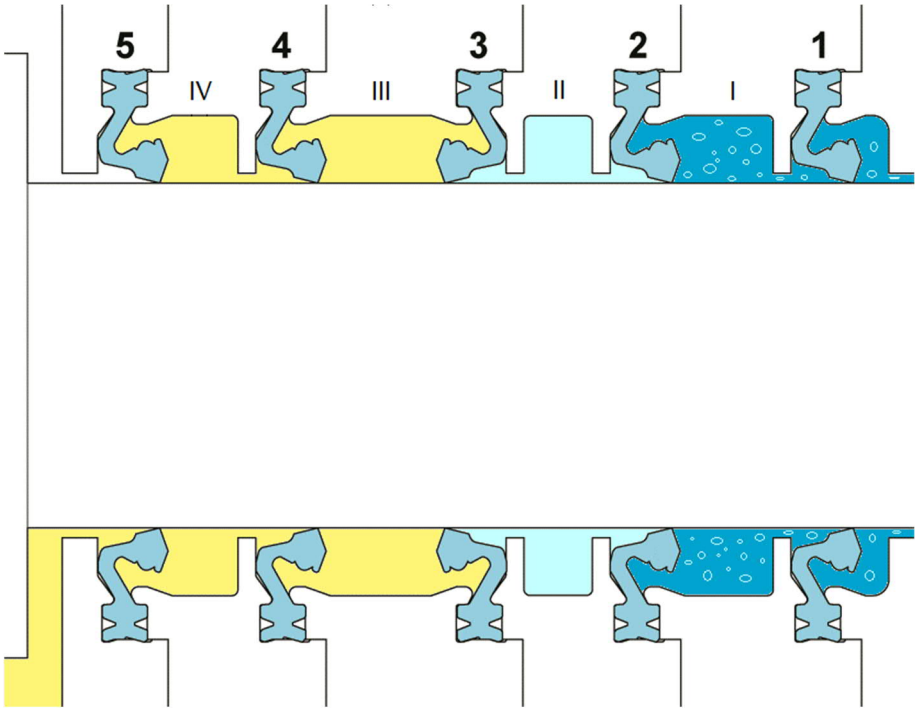

Figure 51. Schematic view showing the sealing rings and seal chambers.

Air pressure together with the hydrostatic pressure of the lubrication oil is used to provide suitable pressure difference over the sealing rings three, four and five. Same air pressure is fed to the seal chamber II making the pressure difference over the sealing ring three stay stable even if the pressure in the seal chamber II changes. Seal chamber IV lubrication oil tank is equipped with an adjustable pressure regulator so the pressure can be balanced between sealing rings four and five. Pressure difference over sealing rings one and two is very low because of the overpressure in the seal chamber II. A schematic view showing the seal system is presented in **Figure 52**.

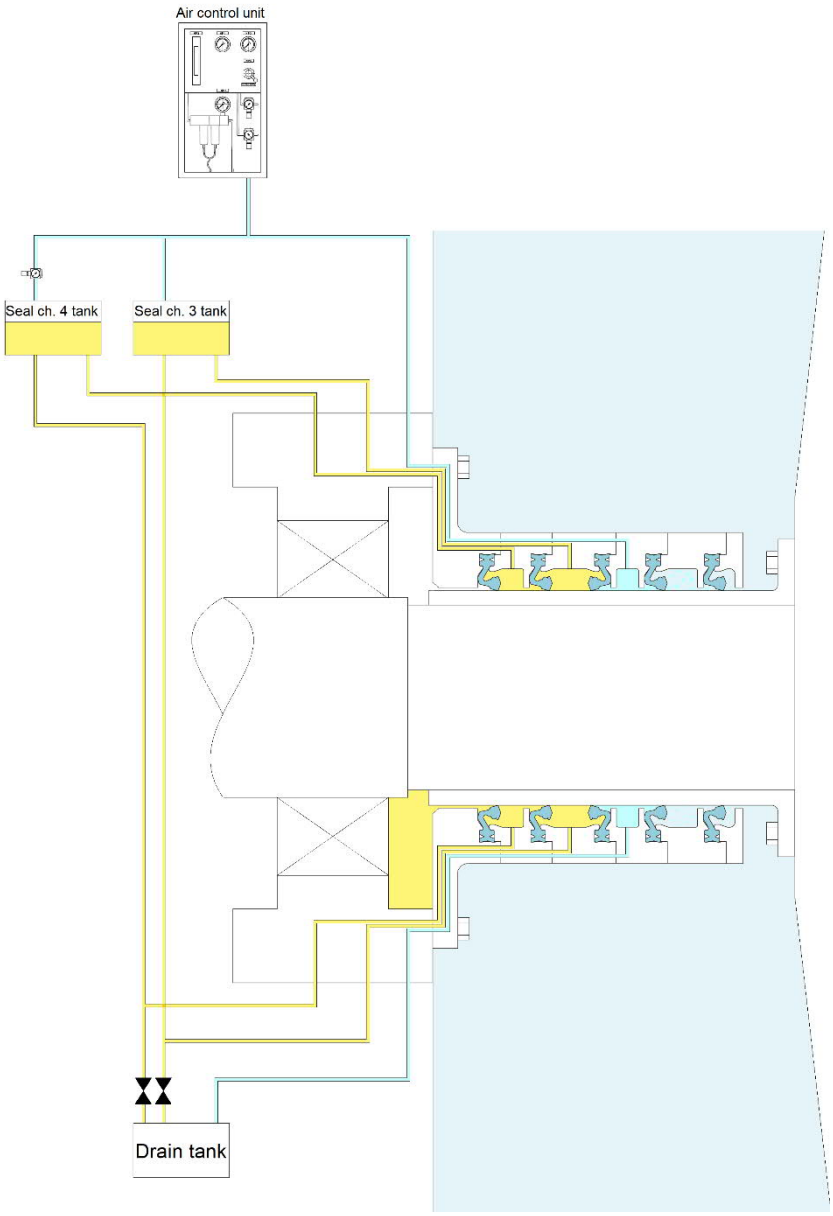

Figure 52. Schematic view of the seal system used in the case company's product.

The reason to use five sealing rings instead of four, which is typical in propeller shaft seals, is that the propeller shaft draft can be relatively large in the case company’s products and thus two sealing rings (four and five) are needed to balance the pressure difference caused by the draft. As explained earlier, air is constantly leaking to water under sealing rings one and two. The air flow is set to stay stable, and the pressure changes according to the water pressure, which will change when the draught of the ship changes, ship speed changes, or ship operation causes changes in the pressure field near the seal system. This flow-controlled system enables system response to different water pressures without pressure sensors or

logic-controlled components, and the pressure difference over the sealing rings one, two and three is the same in varying operational conditions. Pressure difference over sealing rings four and five will change when pressure in the seal chamber III changes, as the air pressure in the seal chamber IV is regulated with a pressure regulator which maintains the set pressure even if the supply pressure changes. A schematic view showing pressure differences over individual sealing rings in a stable operation condition is showed in **Figure 53**.

Item	Structure, Pressure condition, Lubricating condition					
Structure	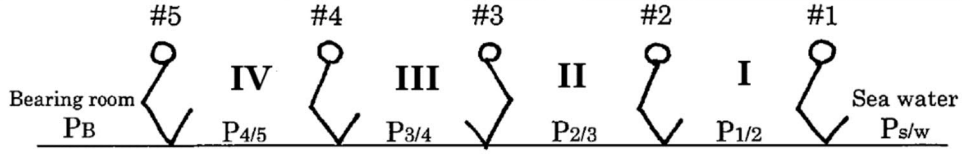					
Lubricating condition	Air / Oil	Oil	Oil	Air	Air	Sea water
Pressure condition	PB=0 bar	P4/5= 0.6 bar	P3/4= P2/3+0.36 bar	P2/3≒ Ps/w+0.2 bar	Ps/w	Ps/w
Pressure difference	△P5	△P4 =0.71bar	≒Ps/w △P3	△P2 =0.36 bar	=−0.1 bar △P1	=−0.1 bar

Figure 53. Pressure balance of the seal system.

Typically, the sealing rings are replaced on a five-year interval. As a rule of thumb, 6000 operational hours per year are expected. This means that the sealing rings should not wear or leak excessively even after 30 000 hours of use.

5.2 Operating environment

The operating environment for the seal system is very demanding. The ships that use the case company's product operate in different parts of the world, and same vessel can be operating in both icy cold waters and tropical hot waters. Thus, the water temperature can be anything between - 2 °C to + 36 °C as presented in **Figure 54**.

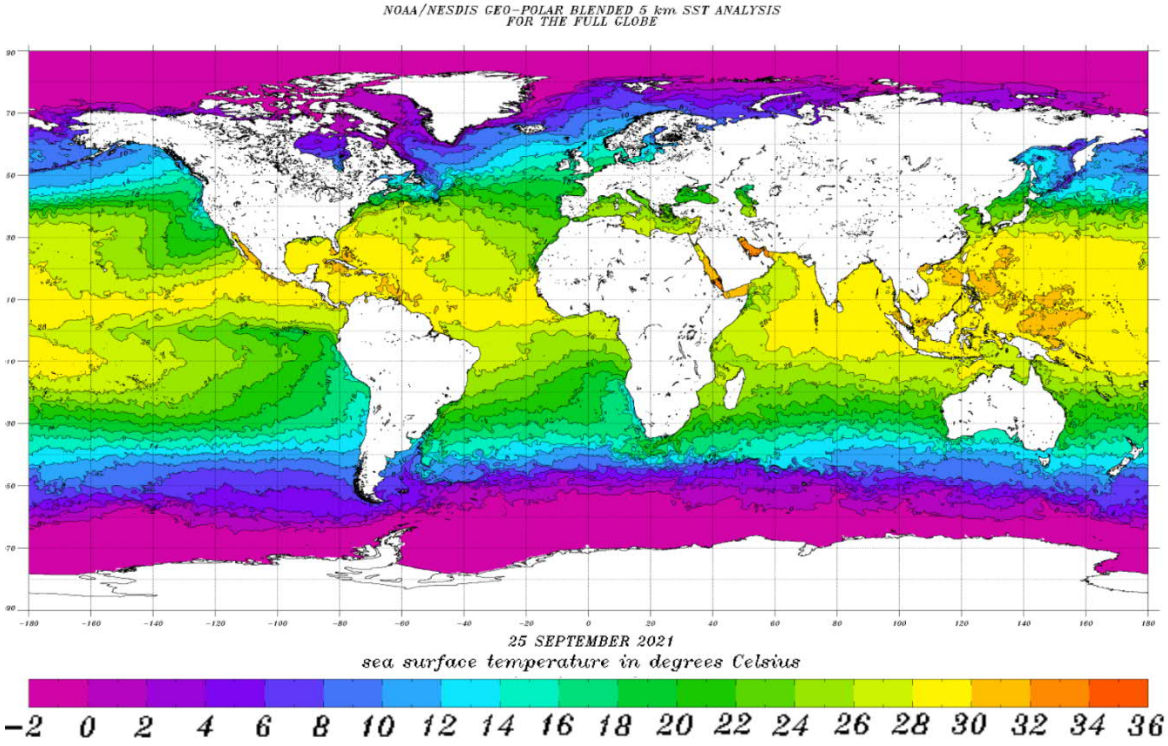

Figure 54. Sea water surface temperatures (Sea Surface Temperature Contour Charts 2013).

The water pressure typically exceeds 1 bar, and when the ship is operated at high speeds, the water pressure near the seal can be 1,2 – 1,3 bar. Maximum shaft speed in the product relevant to this thesis is more than 100 rpm, which corresponds to more than 5 m/s surface speed on the contact between the seal and the shaft. The maximum allowed dynamic runout, 0,08 mm, for the shaft is relatively small when it is compared to the shaft diameter. The case company's product can be in vessels that are operated in open water or in ice. The product relevant to this thesis operates in both ice and open water, which gives even more challenge to the seal system as on top of relatively high water pressure and shaft speed, the propeller shaft is also dynamically misaligned quite significantly when the ship is operating in ice. Measured data of the shaft displacement of one vessel was used in planning of the experiments. The highest measured values for radial displacement near the seal system are 1,01mm (peak-to-peak 1,73 mm) (VTT 2006, p. 14). The seal system can face even higher displacements in reality, when the shaft line geometry and the location of the measured displacement is taken into account. Highest measured displacements are presenter in **Figure 55**.

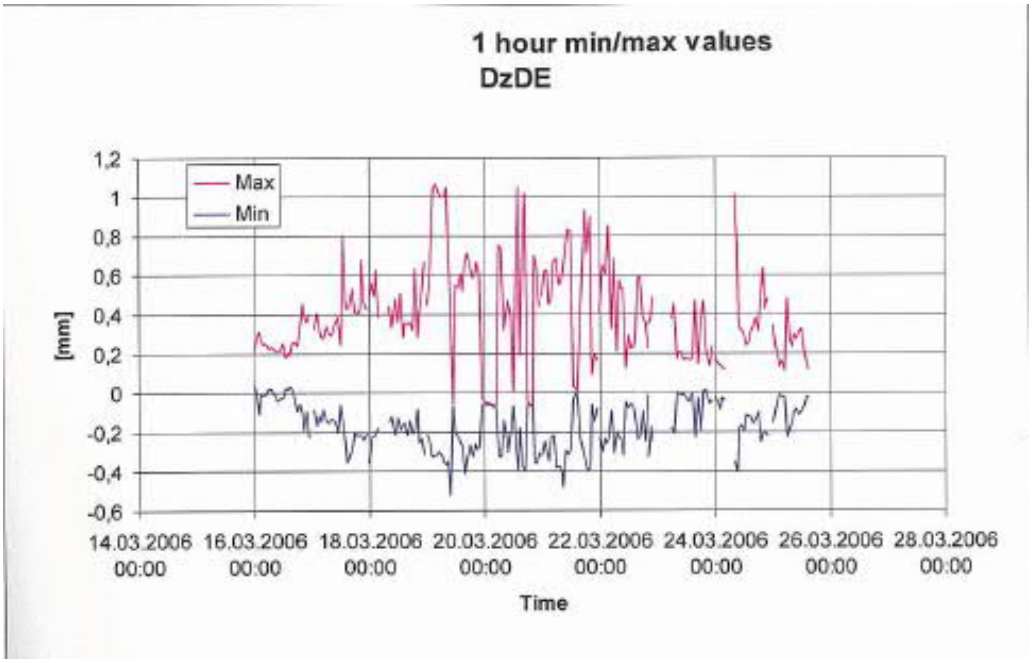

Figure 55. Highest measured displacements (VTT 2006, p. 22).

Generally, the displacements are lower even in heavy ice operation as presented in **Figure 56**. The frequency of the vibration varies in different operational conditions according to the propeller blade frequency etc., but according to a report of one of the measurements, the highest amplitudes are found when the blade frequency coincides with lowest natural frequencies of the surrounding structures, which is around 5-6 Hz in this case (VTT 2006, p. 39).

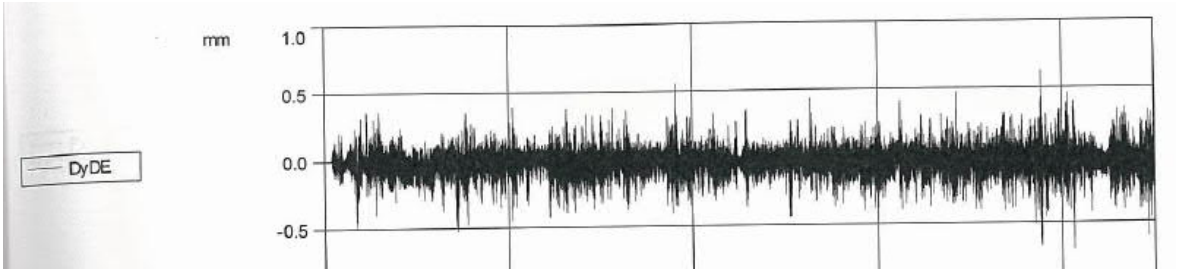

Figure 56. Radial displacement in heavy ice operation (VTT 2006, p. 45).

5.2.1 Leakage rates based on data received from operating vessels

Reports from operating vessels show that the lubricant leakage rates increase when the vessels are operating in ice. The reports also show that the leakage rates increase

significantly in all operation conditions over time, which indicates that the seals wear down. An example of increasing leakage rates is presented in **Figure 57**. The graph presents the lubricant leakage rate of a vessel with three propeller shafts.

Figure 57. Lubricant leakage rate from an operating vessel.

As can be seen from the graph, the leakage rate can be different in different shafts of the same vessel. The different shafts can encounter different operational conditions, which can explain the differences between the different shafts.

The leakage rates reported from the operating vessels are not very accurate as they are not based on sensor data but on the vessel crew estimation of filled and drained oil per month. The total operation hours are also not reported, so leakage rate per time unit cannot be accurately created. Months showing zero leakage mean that a report has not been obtained from the vessel. Graph showing the total oil leakage per vessel for 14 vessels with three propeller shafts is presented in **Figure 58**.

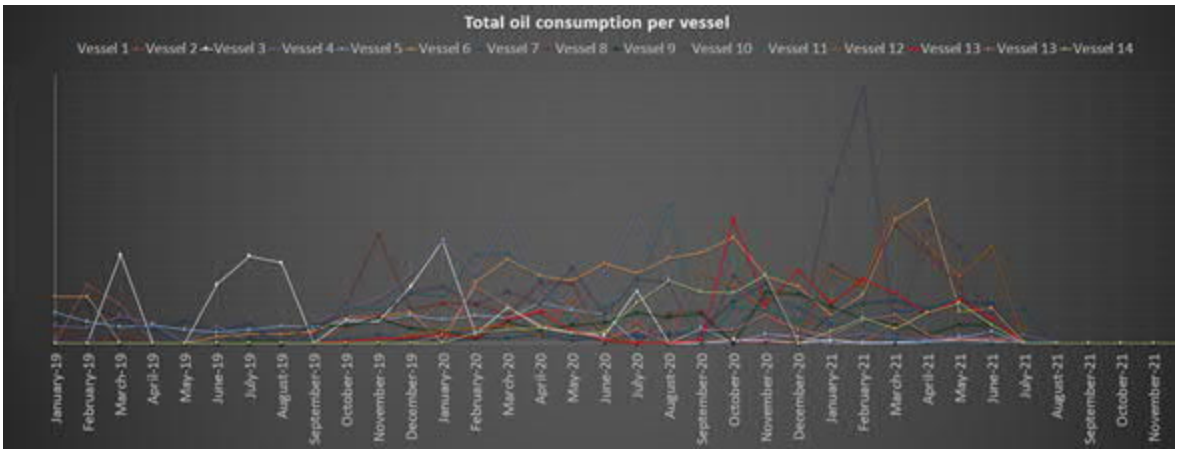

Figure 58. Leakage rates of 14 vessels.

Sensor data from the seal oil tanks of some of the vessels are also available. Based on the sensor data of one shaft of one vessel, baseline for the leakage rate with relatively new sealing rings, used sealing rings with oil leakage considered to be within normal limits, and used seals with increased oil consumption was defined. Operational conditions in the three baseline leakage rates have some variation, and not all information regarding the operation is available, but all three leakage rates were defined from an operational condition where the vessel is operating in ice conditions. Baselines for the oil leakage is presented in **Figure 59**.

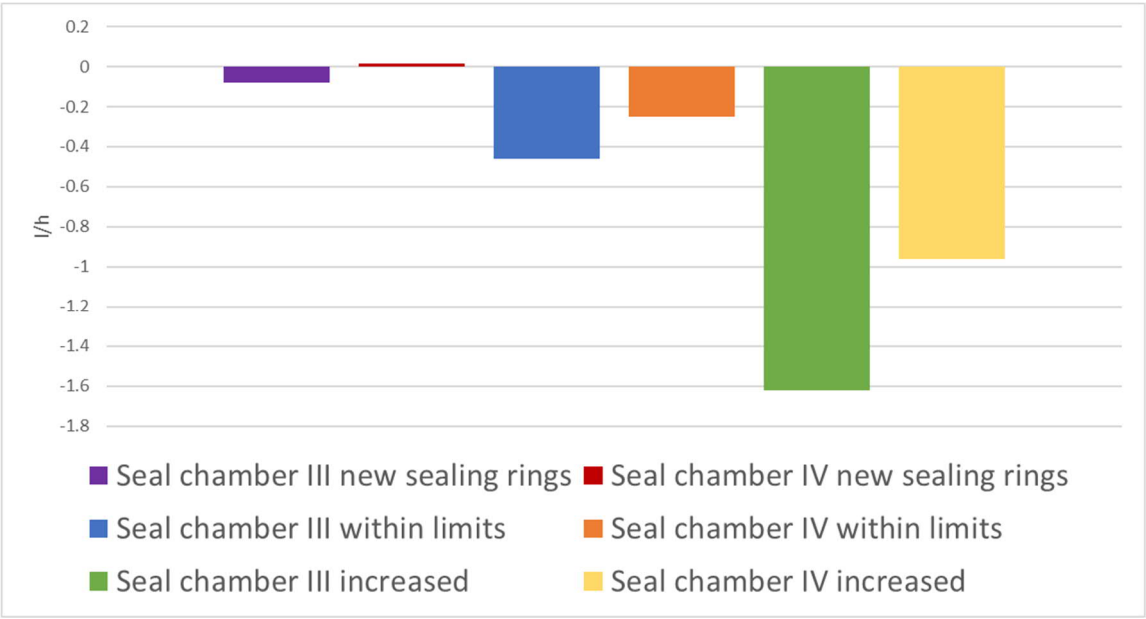

Figure 59. Baseline for oil leakage based on vessel data.

As can be seen from the figure, the leakage rate increases significantly over time, which indicates that the seals' wear rate is too large considering the required operational hours. With new sealing rings seal chamber III is losing oil and seal chamber IV is gaining it. With used sealing rings both seal chambers III and IV are losing oil in during the time from where the baselines are calculated from, but there are other time periods in the data where for example seal chamber IV tank level is rising and seal chamber III tank level is dropping. Graphs showing the sensor data can be found from Appendix I.

6 CAUSE-AND-EFFECT DIAGRAM

A cause-and-effect diagram was created from the sealing system perspective listing different potential causes for excessive oil leakage. The tests are planned so that they can confirm or rule out as many of possible causes as possible and the test results are then compared to the cause-and-effect diagram to confirm or rule out the potential causes. The upper-level diagram is divided into six sections. The sections are environment, installation and commissioning, methods and processes, people, design and materials and system and operation. An overview of the upper-level cause and effect diagram is presented in **Figure 60**.

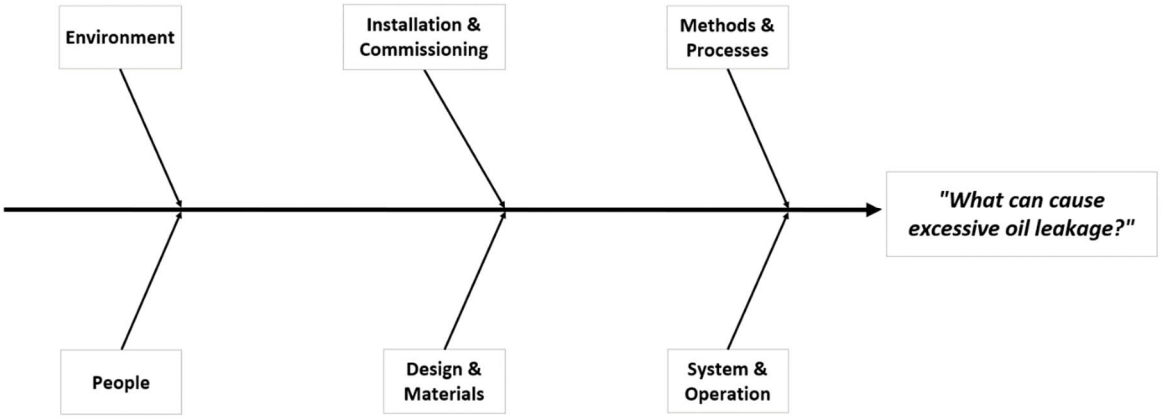

Figure 60. Upper-level cause-and-effect diagram.

The whole diagram is not being examined in this thesis, and all of the sections are not relevant regarding the tests. In this thesis, the system and operation section is being examined in more detail. The system and operation section is divided into six sub-sections: Dynamics, sealing ring wear or damage, high pressure difference, housing, shaft seal liner and air control unit. An overview of the system and operation -section is presented in **Figure 61**.

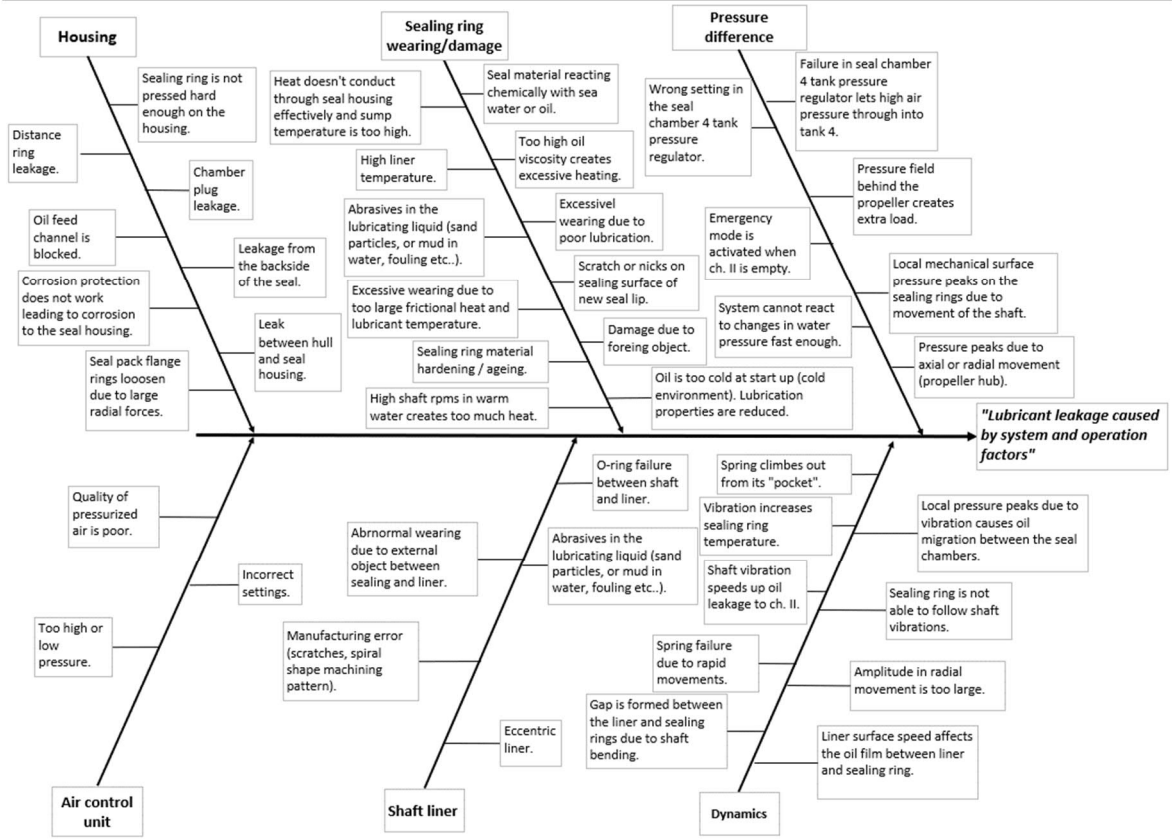

Figure 61. Cause-and-effect diagram, system and operation.

As the tests performed on the test device cannot answer all the questions in the system and operation section of the cause-and-effect diagram, at least in short term tests, it is simplified even more as presented in **Figure 62**.

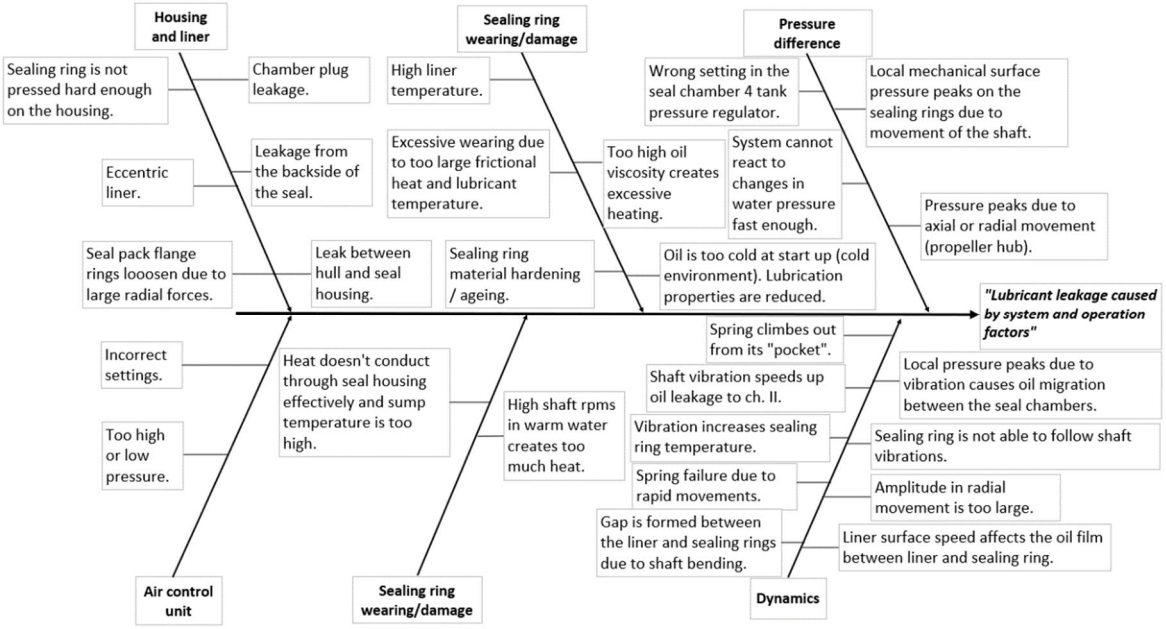

Figure 62. Cause-and-effect diagram, simplified system and operation.

Effect of some of the potential causes for leakage are still indirect, such as “Excessive wear due to too large frictional heat and lubricant temperature” as the test period is relatively short. The short-term test results can however give a reason to further investigate for example the temperature related causes. Also, some of the potential causes are not specifically tested with the test device, such as chamber plug leakage, and they are considered in case unexplained leakage is found.

7 EXPERIMENTS

The experiments were executed with a test device specially made for this purpose. The purpose of the experiments was to confirm or discard assumptions made in the cause-and-effect diagram, and to gain overall insight of the seal system behavior in different operating conditions.

7.1 Sealing rings, housing and used lubricant

Same type of seals and seal housing than used in an actual customer company application is used in the experiments. The seal packages are delivered fully assembled by the supplier and they can be installed on the propeller shaft without any additional assembly. The seal package used in the experiments is presented in **Figure 63**.

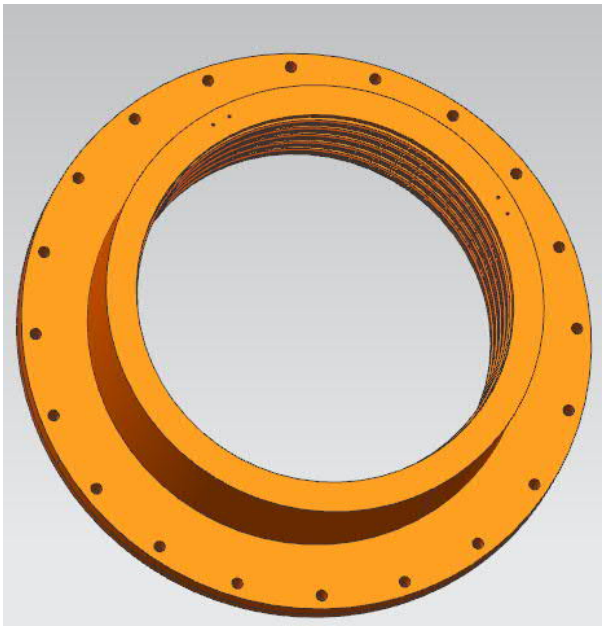

Figure 63. Seal package used in the experiments.

The material of all the seals is FKM, but more specific material properties are unknown. According to the manufacturer, the maximum long-term temperature for the material is 65 °C (Seal manufacturer 2, 2021). Short term maximum temperature is unknow, but short-term material testing is performed in 175 °C temperature by the manufacturer. According to the manufacturers statement, the liner diameter is $ø\frac{0,2}{0}$ mm and the material of the liner is

chrome steel. The surface roughness is max. Ra 0,8 according to the manufacturer. The seal inner diameter was measured from 9 sealing rings and the average of all the measurements is 788,73 mm. The air side angle is 34° and the oil side angle is 44°. The angles are measured from an assembly drawing provided by the seal supplier, so the values are approximate values. The assembly drawing can be found from Appendix II.

The seal package used in the experiments was dismantled and reassembled so that the sensors required in the experiments could be installed. Dismantling of the seal package also gave a good opportunity to inspect the quality of the manufacturing assembly. The quality of machining of each seal housing ring was good and no defects could be found from the visual inspection. However, machining chips were found from between the housing rings. The machining chips had sunken to the base material and there were no visual gaps between the housing rings. Each seal chamber was also test pressurized by the supplier. A photograph of the machining chips found from between the housing rings is presented in **Figure 64**.

Figure 64. Machining chips between housing rings.

The seal housing is an aluminum bronze alloy, and the thermal conductivity of the material is 100 $\frac{W}{mK}$. The volume of seal chambers I and IV is approximately 3,4 liters, the volume of seal chamber III is approximately 2,2 liters and the volume of the seal chamber II is approximately 1,6 liters. The volumes are calculated based on measurements on the seal pack and sealing rings made when the seal package was disassembled.

The spring constant of the garter spring was calculated by loading the spring with different weights and measuring the length of the spring with each load. Five springs were measured, and the average length of the springs were 2510 mm and calculated spring constant was 53 N/m. The diameter of the spring is 6mm. The circumferential created by the garter spring was calculated using following equation (Barnes Group Inc. 2021, p. 72).

$$P = kf \tag{8}$$

In Equation 8, P is the circumferential load, k is the spring constant and f is the deflection of the garter spring when it is assembled. When the circumferential load is known, the radial load can be calculated using the following equation (Barnes Group Inc. 2021, p. 72).

$$P_r = \frac{2P}{D_2} \tag{9}$$

In Equation 9, P_r is the radial load, P is the circumferential load and D_2 is the minimum compressed outside diameter of the spring. The circumferential load of the garter spring is 1,006 N and the radial load is 2518 N/m.

Several different lubricants are used in the seal systems of the case company's products. However, 320cSt synthetic gear oil was chosen to be used in the experiments, as majority of the case company's products use that oil.

7.2 Test device

Seal system test device allows measuring of the seal system response in different operating conditions. The shaft rotation speed, static and dynamic misalignment (2-7 Hz) both in axial and radial directions, water pressure and water temperature can be controlled. In addition, complete seal system with the same main components than in the operating vessels is installed on the test device allowing same seal system control than the ship's crew have. An overview of the test device is presented in **Figure 65**.

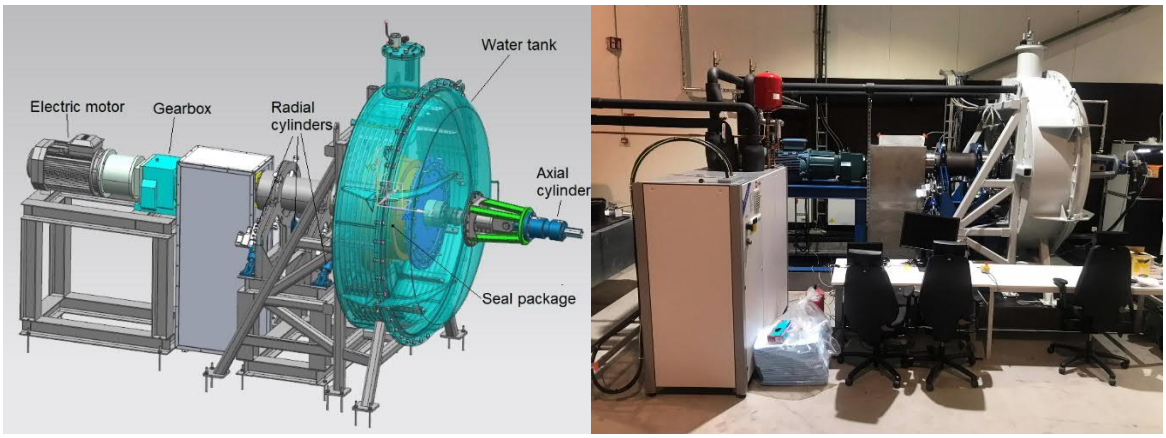

Figure 65. Seal system test device.

The shaft is driven with an electric motor that is controlled with a frequency controller. The electric motor is connected to a gearbox, which provides suitable rotation speed and required torque for the shaft that the seals are mounted on. The shaft is supported vertically with four hydraulic cylinders, which produce the required static and/or dynamic misalignment for the shaft. The liner and seal package are mounted on a part of the shaft that is inside the water tank. The shaft line is held on its place axially with one hydraulic cylinder that is mounted on the water tank cover. Pressurized air is lead to the water tank to create desired water pressure. Frictional heat is produced when the shaft is rotated, so the water tank is equipped with a cooling system. This also allows testing in different water temperatures.

7.2.1 Instrumentation

The test device and seal system are equipped with a comprehensive measurement system so that the seal system response to different operational conditions can be accurately measured. The main areas of interest were the temperature and pressure in different areas of the seal system, oil leakage, shaft misalignment, shaft speed and torque. National Instruments NI-9207 voltage and current input modules, and NI-9216 temperature input modules are mounted on NI cDAQ-9189 chassis to log the different sensor signals. The measurement data is stored on measurement PC hard drive and on an external hard drive.

The data collection is performed with on PC which uses National Instruments Flex Logger 2021 R1 -software. When performing the tests, measurement signals are visible on one monitor. A separate control software is used to control the test device. Schematic view of

the measurement system and picture showing measurement signals is presented in **Figure 66**.

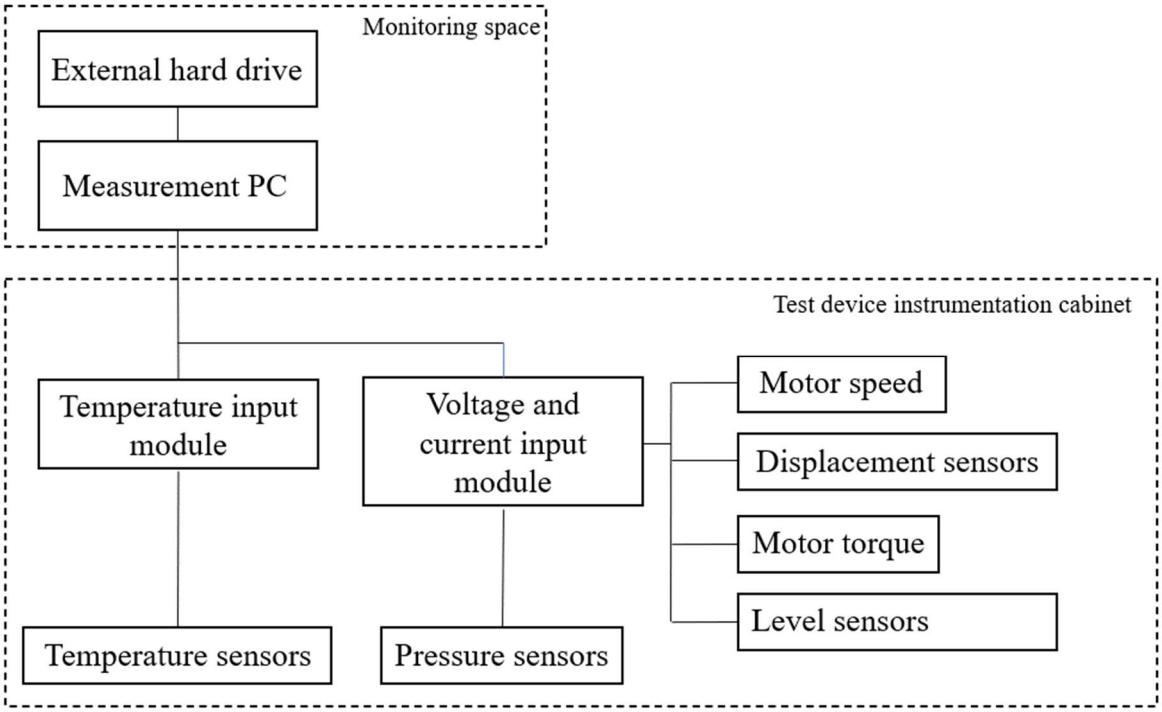

Figure 66. Schematic presentation of the test device measurement system.

Pressure in the seal chambers is measured with Müller Industrie-Elektronik GmbH PT-HL-T-C conductive pressure sensors. The location of the pressure sensors is on the bottom of each seal chamber.

Seal oil tank levels are monitored to be able to determine the leakage rate over the different sealing rings. Tank levels are monitored with Parker SCLSD level controllers.

The shaft position is measured vertically and horizontally near the cover flange of the seal package. The shaft position is measured with Contrinex DW-AD-519-M30 inductive position sensors. The axial location of the shaft is also measured with a same type of sensor.

Water tank temperature, temperature of each seal chamber and sealing ring are measured. Sensors used to measure the water and seal oil temperature are measured with Müller Industrie-Elektronik GmbH MKTS-GL Pt100 -sensors. Minco S13282PD3T120 miniature Pt100 -sensors are used to measure the sealing tip temperature. Mounting holes for the

sensors were drilled on the sealing ring as close to the contact as possible. The distance from the sensor tip to the sealing ring tip is approximately 2 mm. The temperature sensors for the sealing rings are located at the top (12 o'clock) of the sealing rings. Schematic view of the miniature pressure sensors and photographs of installed sensos are presented in **Figure 67**.

Figure 67. Sealing ring contact area temperature measurement.

The speed and torque signals are extracted from the frequency converter of the electric motor. Used frequency converter is ABB ACS 880-01. The frequency converter provides the speed and torque of the electric motor with mA signals, which is transferred to motor speed and torque readings with the measurement software. Torque given by the drive does not give fully accurate reading of the seal system torque as there are losses in other parts of the system such as the gearbox, water tank seals and rotating parts inside the water tank. The reading given by the drive itself also has some error and it cannot be used as fully accurate torque of the electric motor.

8 TEST RESULTS AND INSPECTION OF USED SEALING RINGS

Test results of the tests performed on the test device are presented in this chapter. Data obtained from the testing is mainly analyzed with National Instruments DIAdem -software. Based on the analyzed data, graphs are created with Microsoft Excel so that presenting and comparing the data from different tests is easier.

8.1 Temperature tests

The shaft speed sweep tests were performed after the test device had been operated for tens of hours and temperature readings showed only little variation when the device was operated. This ensures that the sweep tests were performed on run-in seals and thus the contact properties on the seal and the shaft have settled. The seal system response to different shaft speed with two different water pressures are presented in **Figure 68** and **Figure 69**. Temperature graphs created in the DIAdem -software from both tests can be found from Appendix III. Temperature sensor on sealing ring 5 malfunctioned already during the commissioning of the test device, so sealing ring 5 temperature behavior cannot be reported.

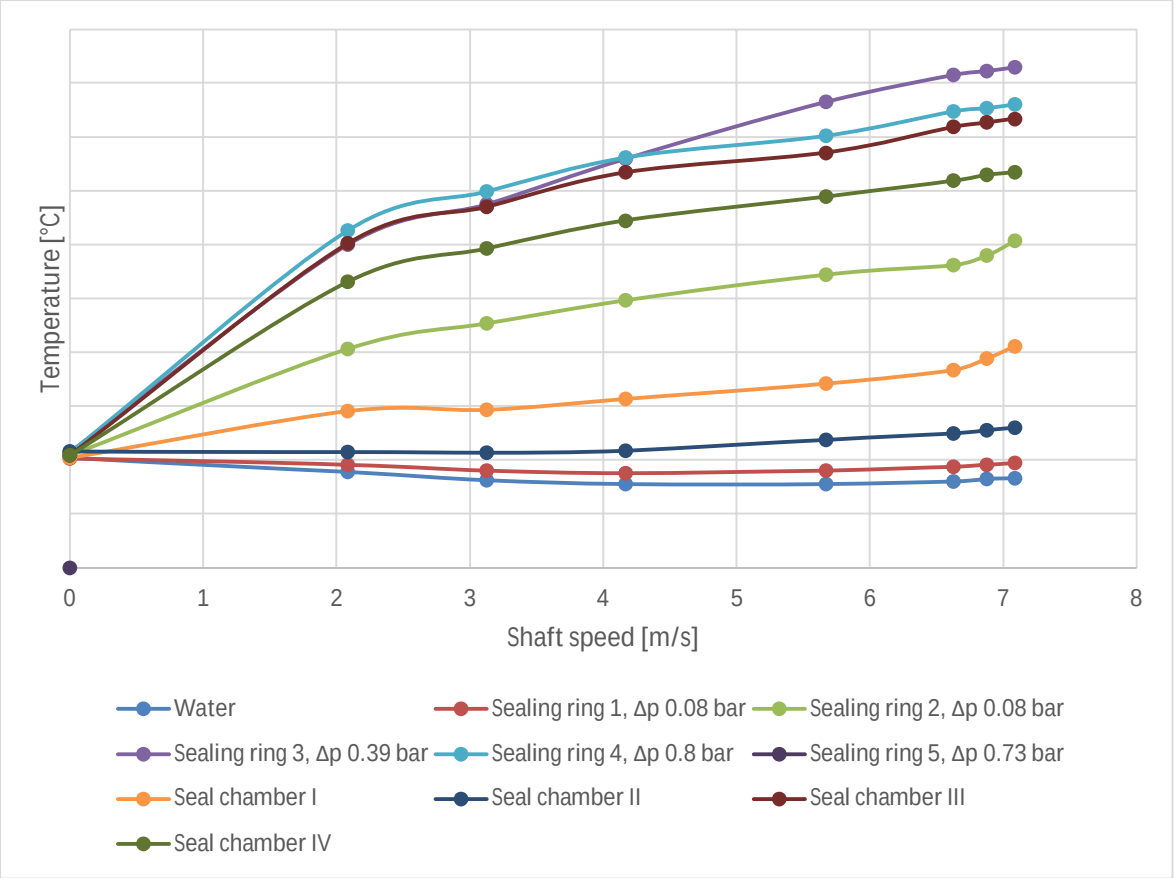

Figure 68. Seal system temperatures at different shaft speeds, water pressure 1,14 bar.

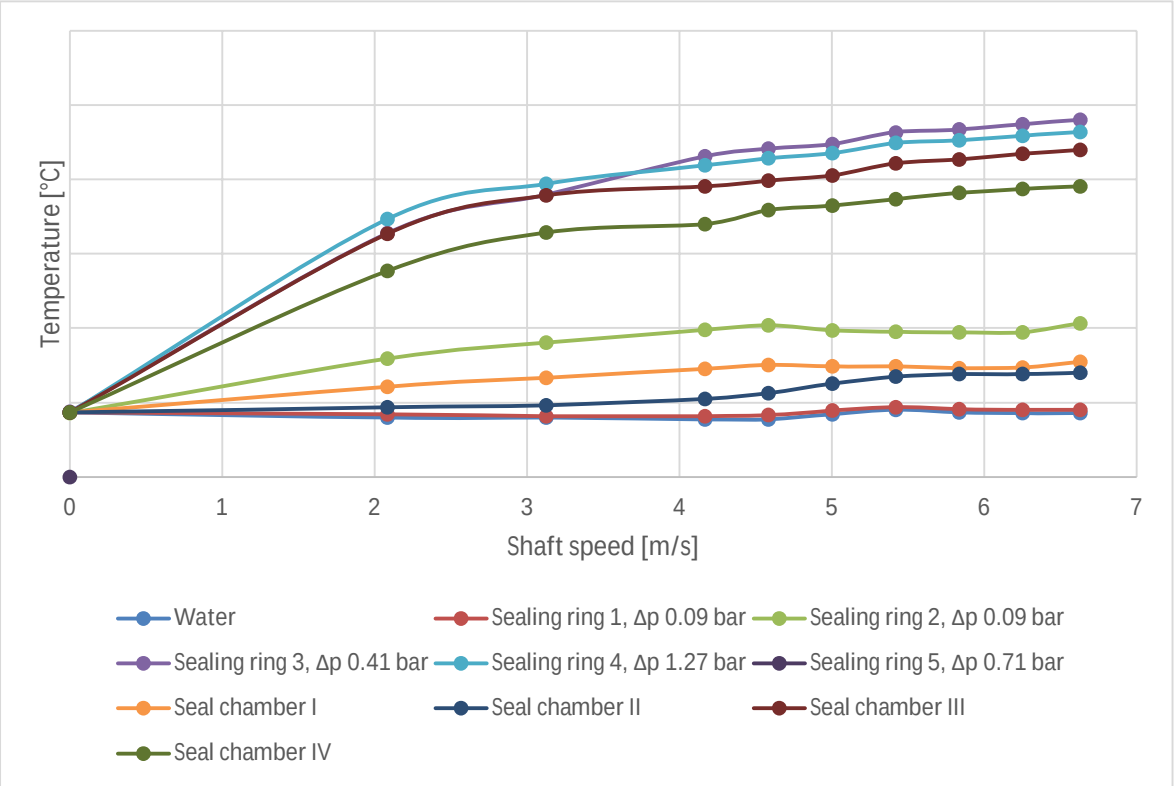

Figure 69. Seal system temperatures at different shaft speeds, water pressure 1,57 bar.

Shaft torque was also measured in the test with 1,14 bar water pressure. Shaft torque in the function of the shaft speed is presented in **Figure 70**.

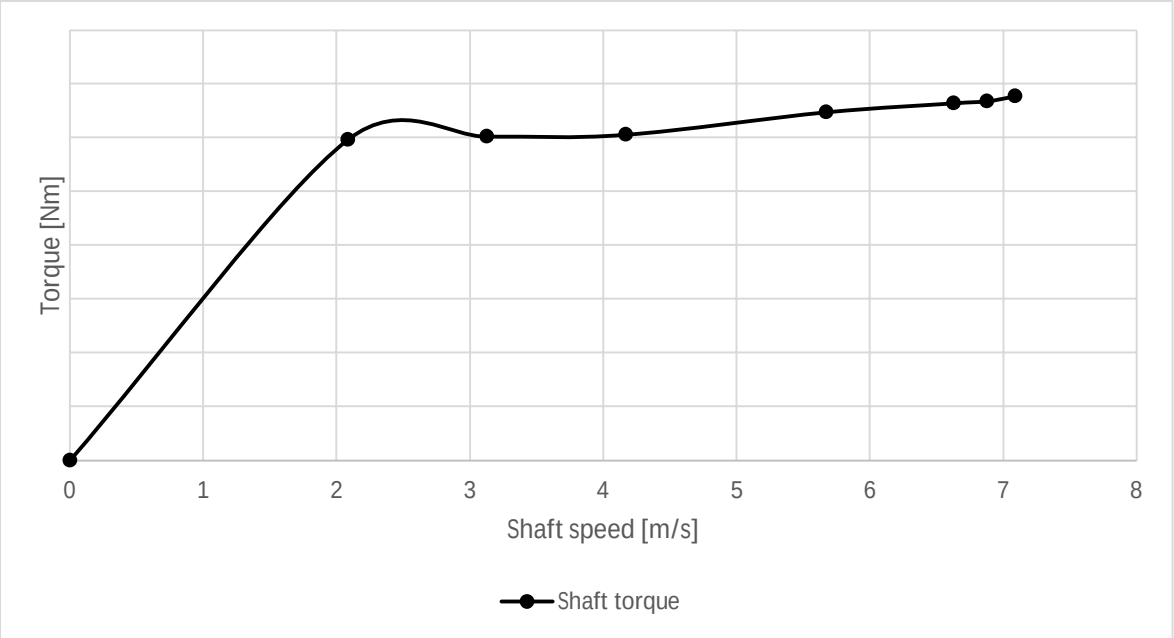

Figure 70. Shaft torque in the function of the shaft speed.

Pressure difference over sealing ring 3 was changed to find the effect of changing radial load on the sealing ring temperature and shaft torque. The results are presented in **Figure 71** and **Figure 72**.

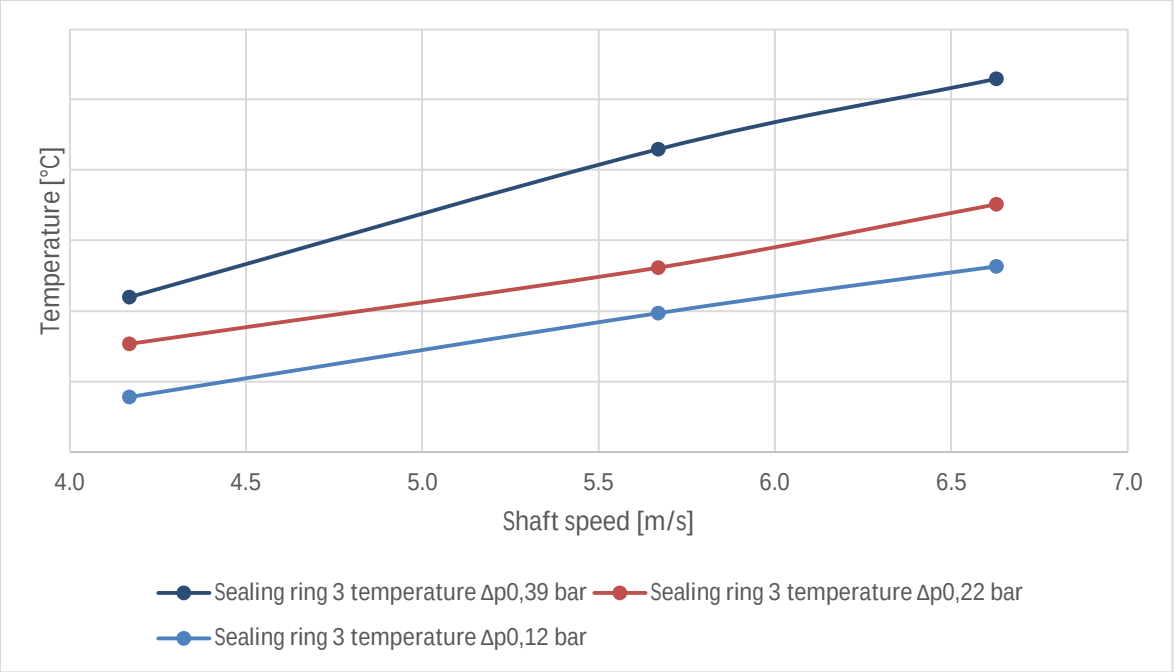

Figure 71. Sealing ring 3 temperature in the function of shaft speed with different pressure differences.

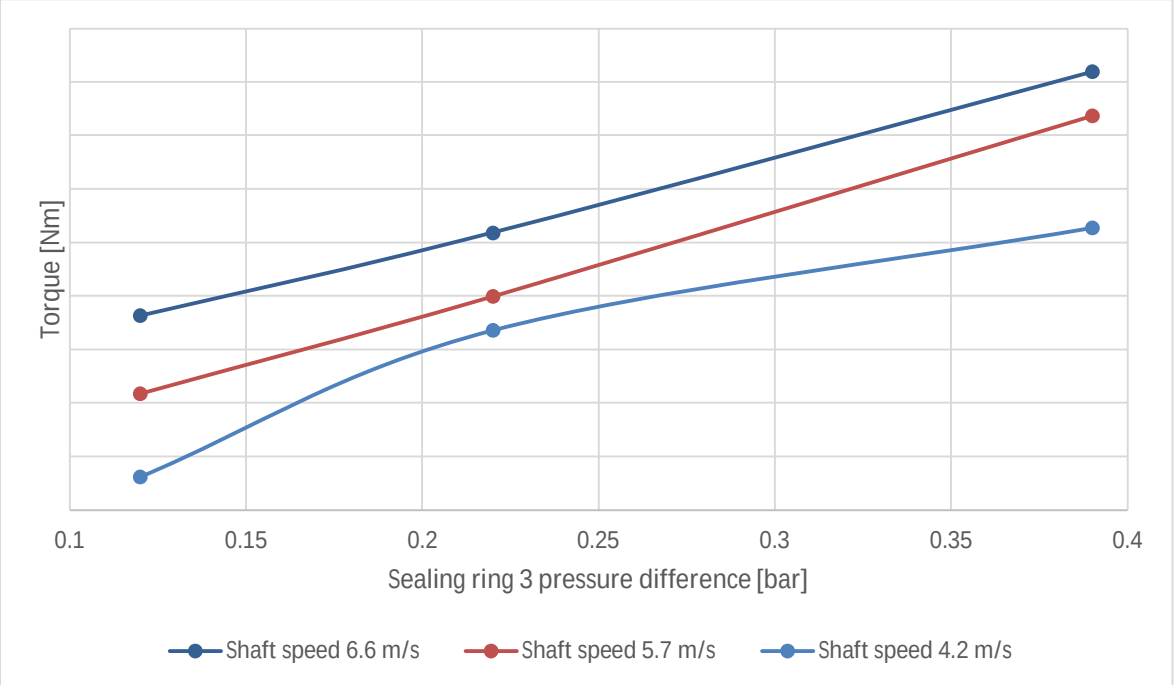

Figure 72. Shaft torque in the function of sealing ring 3 pressure difference with different shaft speeds.

Pressure difference over sealing ring 4 was changed to find the effect of changing radial load on the sealing ring temperature and shaft torque. The results are presented in **Figure 73** and **Figure 74**.

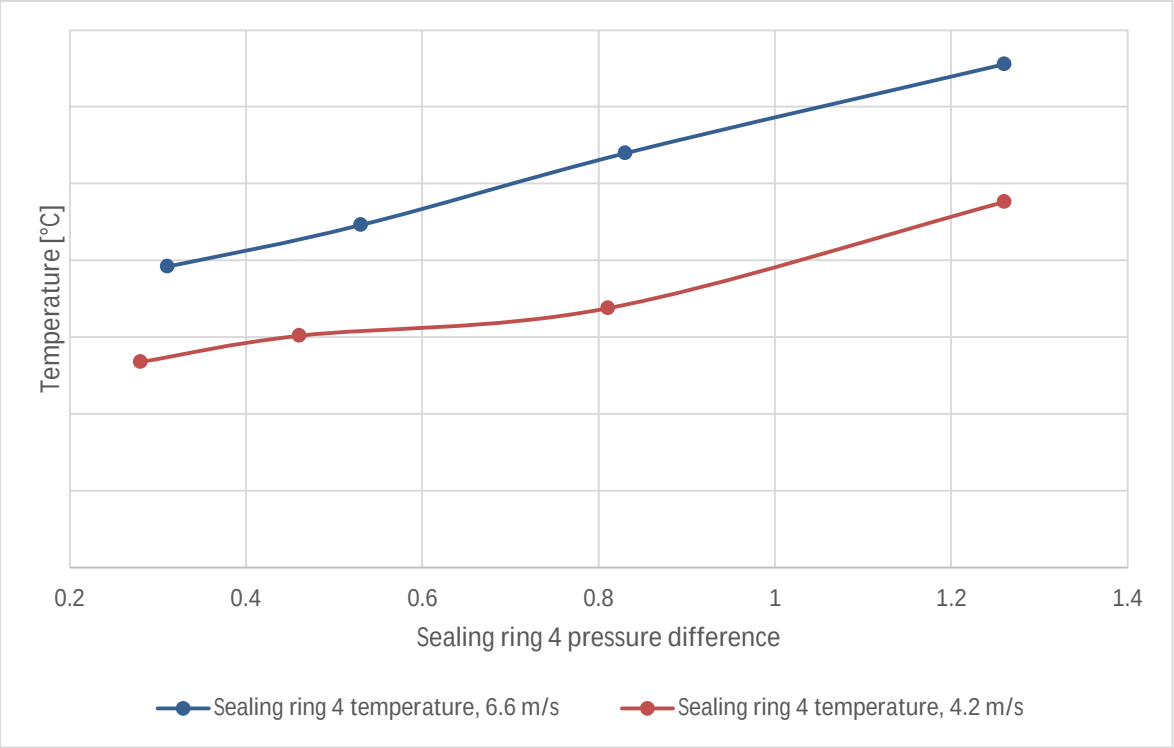

Figure 73. Sealing ring 4 temperature in the function of pressure difference on different shaft speeds.

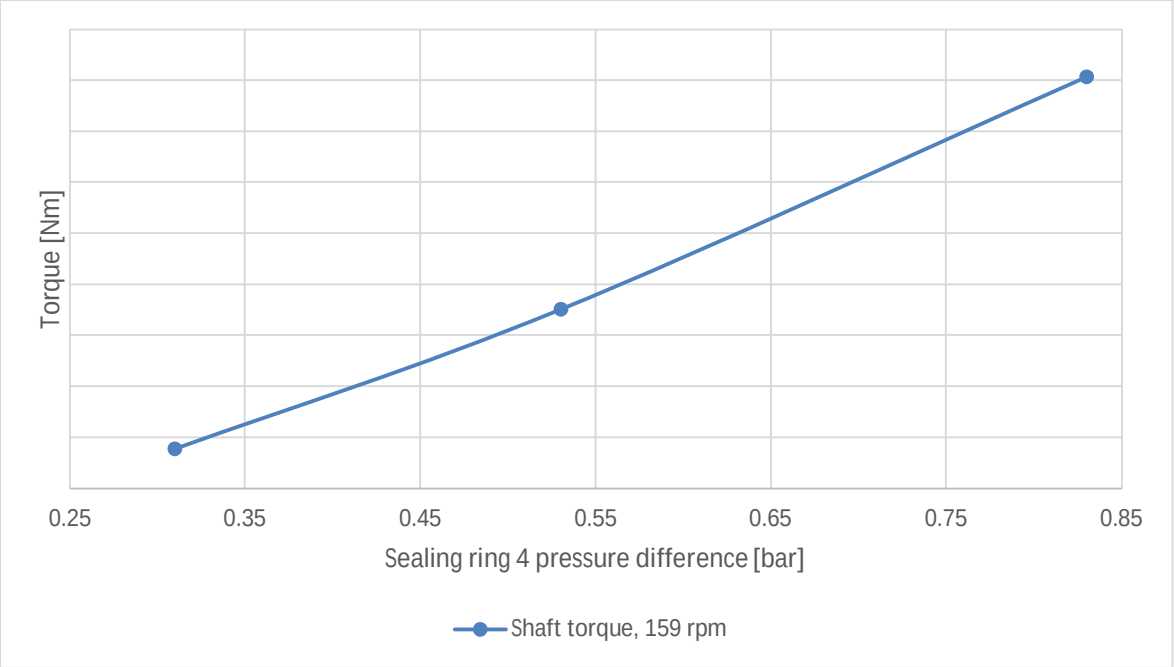

Figure 74. Shaft torque in the function of sealing ring 4 pressure difference.

Leakage rate of seal chambers III and IV was calculated based on the change on the seal oil tanks oil level. Leakage rate was calculated from the tests where sealing ring 3 pressure difference was changed with three different shaft speeds. The calculated leakage rate is presented in **Figure 75**.

Figure 75. Calculated leakage rate of seal chambers III and IV.

Only one leakage rate per pressure difference is presented because it was found that for example the system temperature has a significant effect on the oil level measurement results. To be able to calculate an accurate leakage rate, the oil level has to be recorded at the beginning of the test and after the test when the seal oil has cooled back to its initial temperature. This was learned during the testing and for that reason the leakage rate for different shaft speeds could not be calculated, as tests with one pressure difference were performed on the same day. Accurate leakage rate from the tests where sealing ring 4 pressure difference was changed could not be calculated because when these tests were performed the temperature's effect on the oil level measurements was not yet revealed.

8.2 Static misalignment tests

Seal chamber III pressure and shaft misalignment in the first static misalignment tests with standstill shaft without water in the water tank are presented in **Figure 76**. For better visual appearance, only the pressure of seal chamber III is presented. Seal chamber IV showed same behavior in the test.

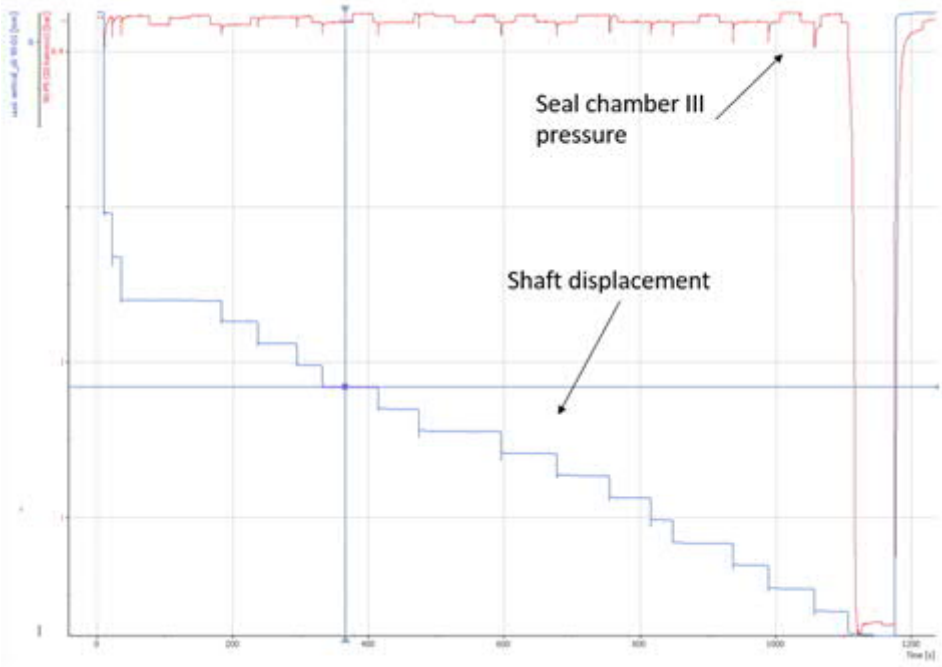

Figure 76. Pressure of seal chamber III in the static test.

Results of the second static misalignment test where there was also water in the water tank are presented in **Figure 77** and **Figure 78**. **Figure 77** shows the pressure of different seal chambers and **Figure 78** shows the temperature of different sealing rings. Further graphs can be found from Appendix V.

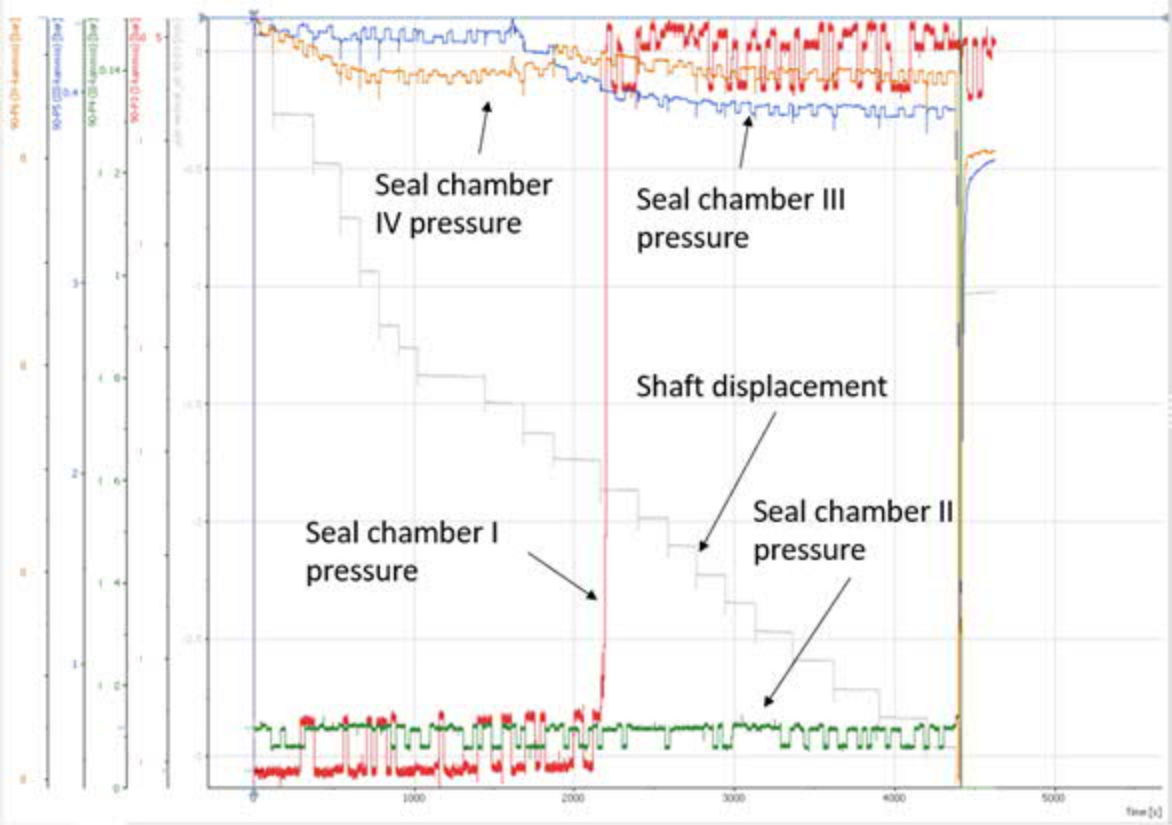

Figure 77. Seal chamber pressures in static misalignment test with standstill shaft.

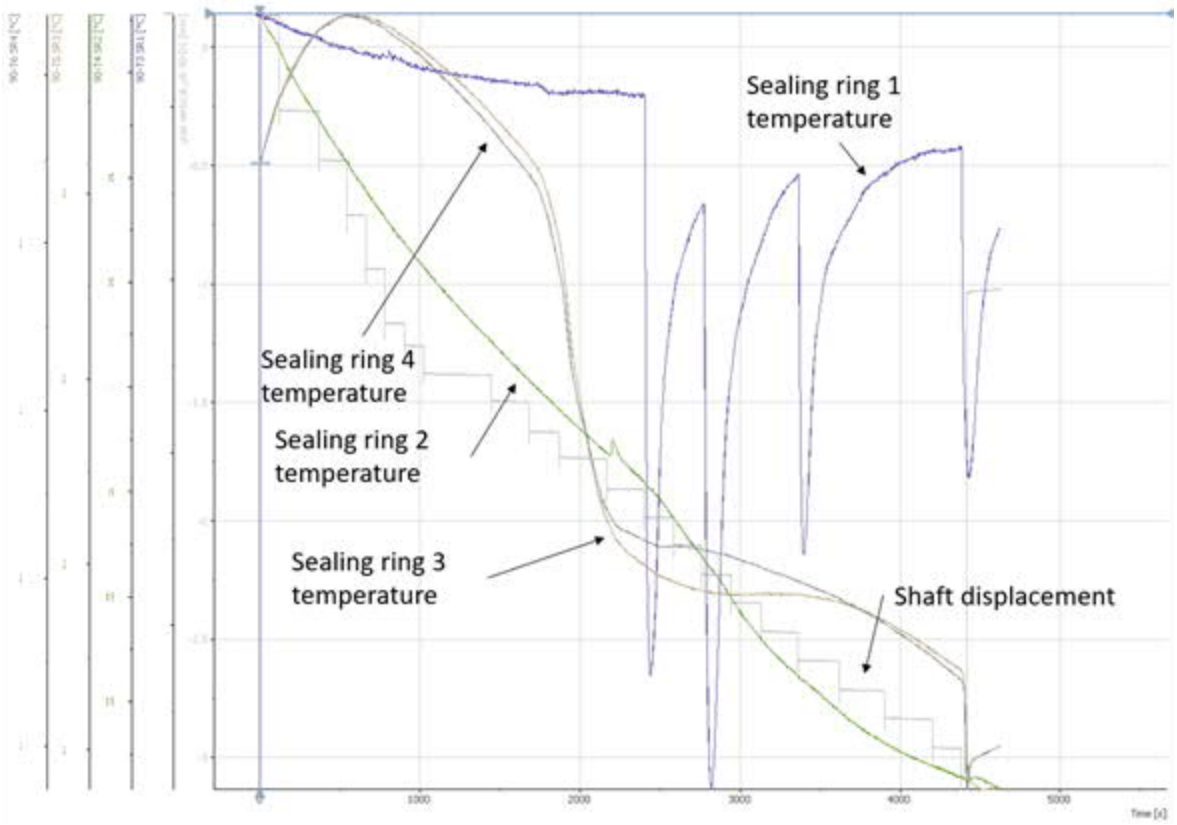

Figure 78. Sealing ring temperatures in static misalignment test with standstill shaft.

In addition to the tests with a standstill shaft, testing with different static misalignment values with a shaft rotating at 4,2 m/s shaft speed was performed. Temperature behavior of the sealing rings is presented in **Figure 79**. Further graphs can be found from Appendix V.

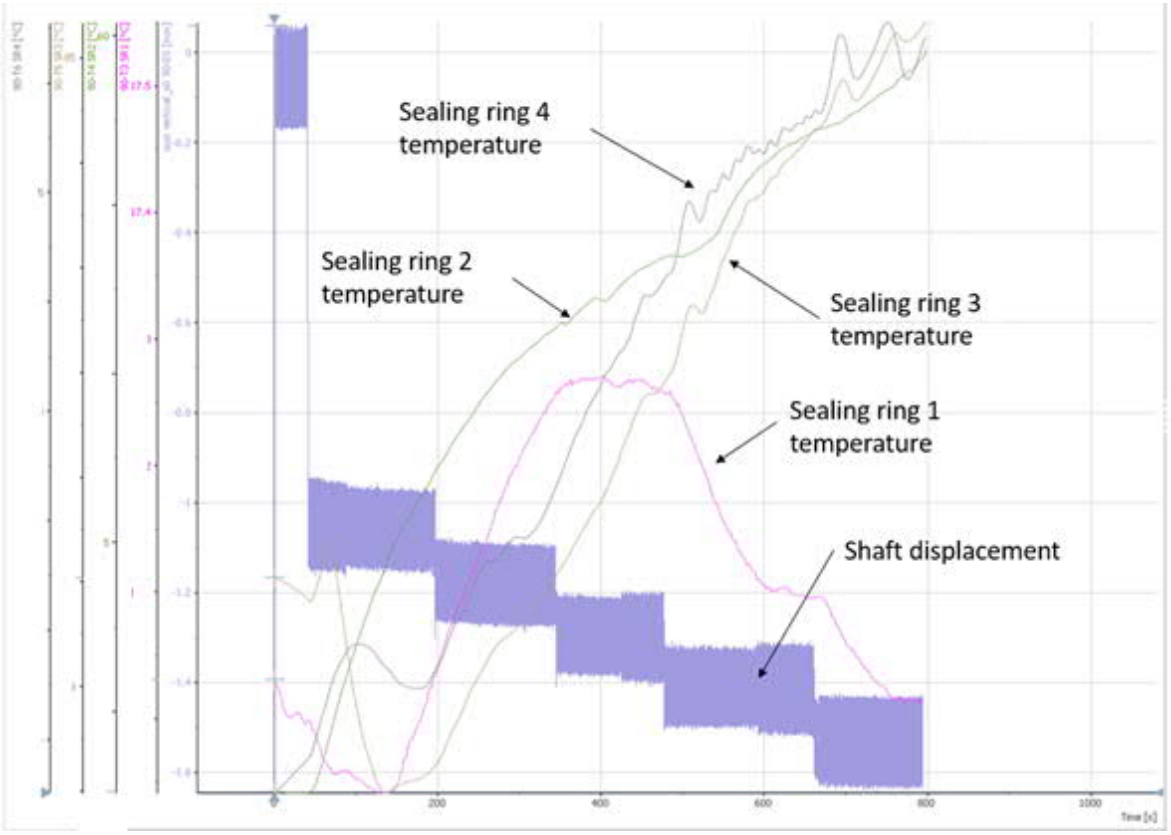

Figure 79. Sealing ring temperatures in static misalignment test with 4,2 m/s shaft speed.

8.3 Dynamic misalignment tests

Seal system response to increasing misalignment amplitude was tested in the first dynamic misalignment test. Graph showing all of the sealing rings and seal chambers temperature response to the increasing vibration amplitude is presented in **Figure 80**. More graphs can be found from Appendix VI.

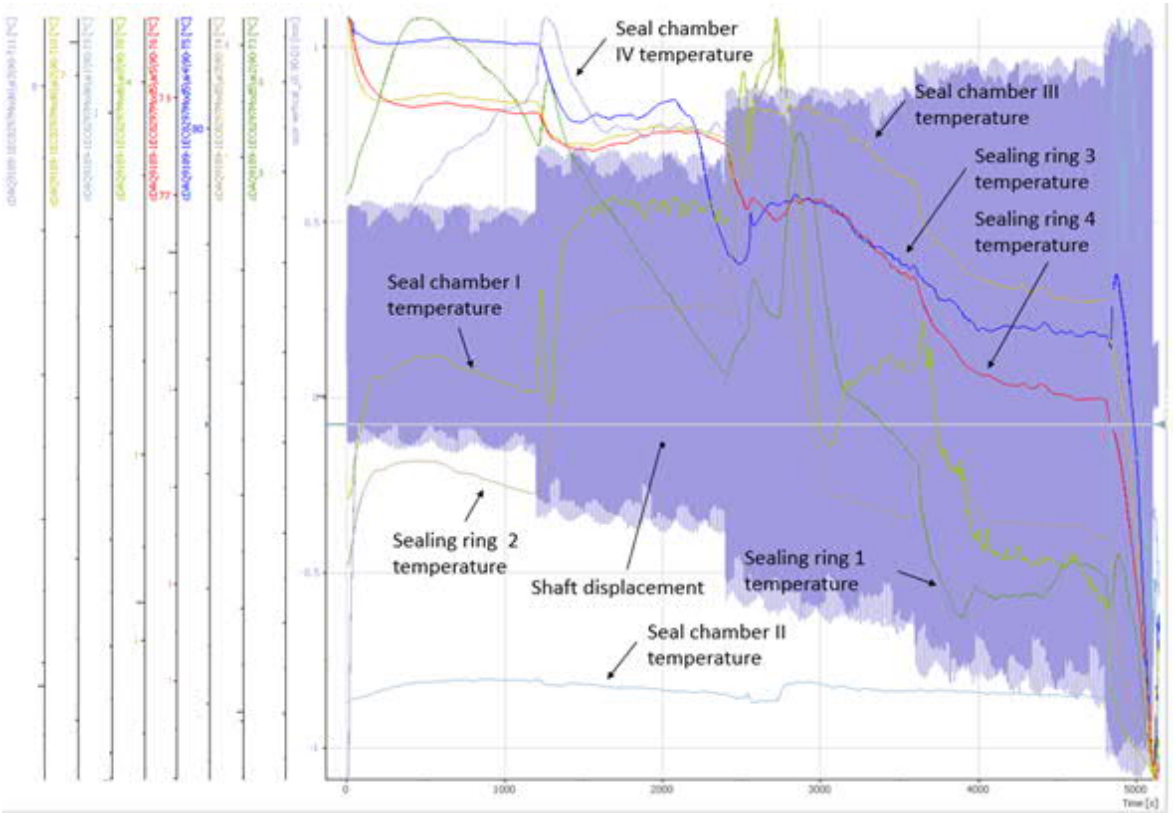

Figure 80. Seal system temperature response to increasing vibration amplitude.

Graphs showing the seal system response to changing shaft speed and pressure difference over sealing ring 3 to constant vibration amplitude is presented in **Figure 81**, **Figure 82** and **Figure 83**. More graphs can be found from Appendix VI.

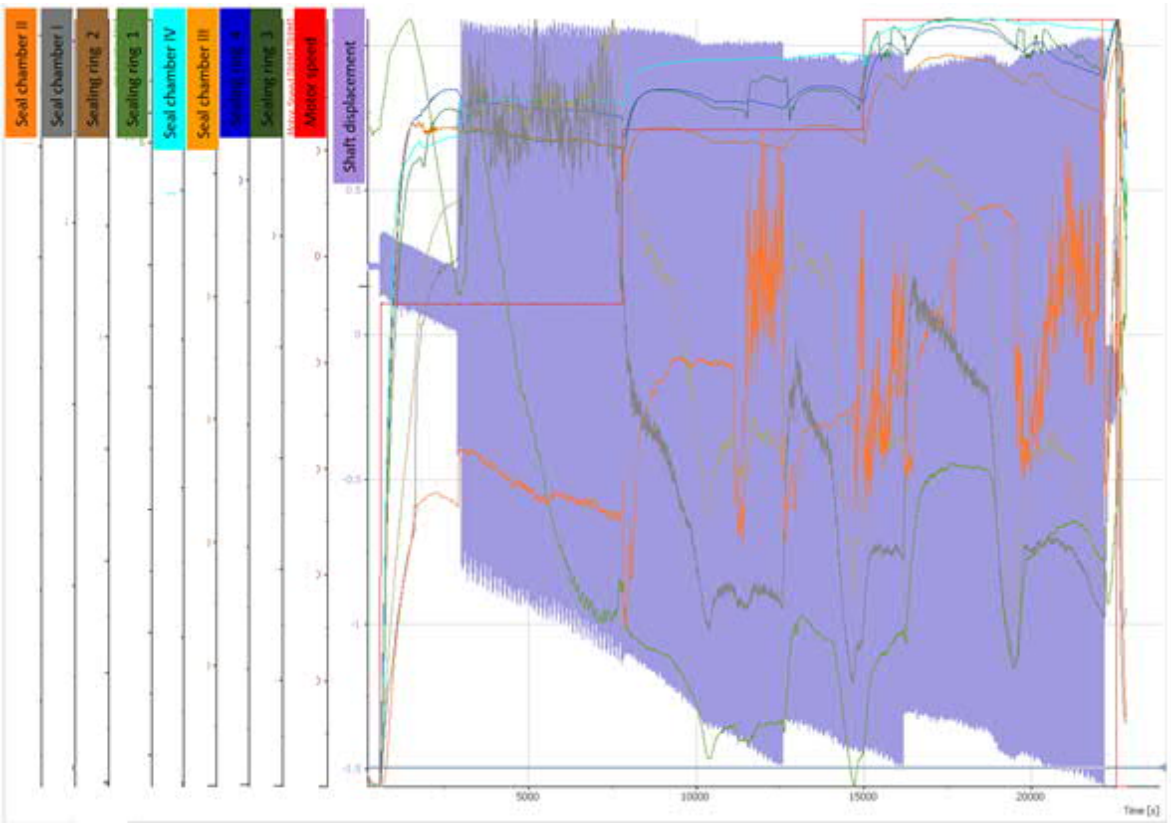

Figure 81. Seal system response to constant vibration amplitude with changing shaft speed, Δp0,4 bar over sealing ring 3.

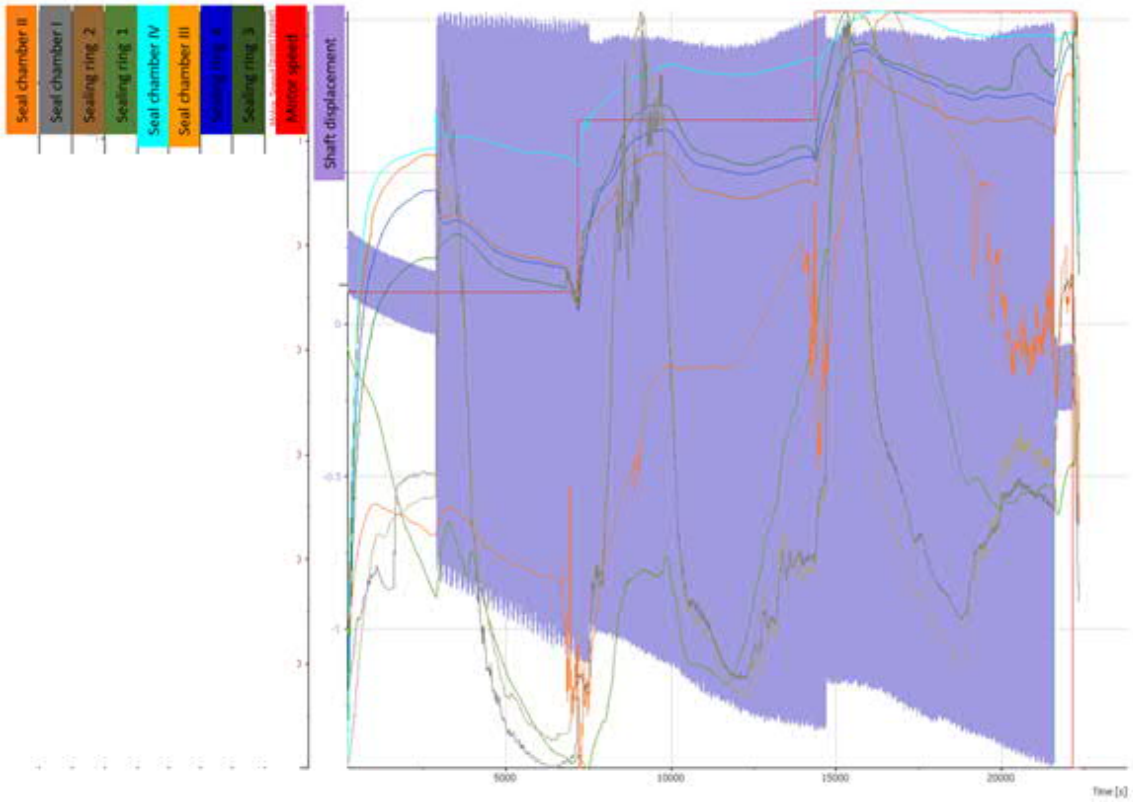

Figure 82. Seal system response to constant vibration amplitude with changing shaft speed, Δp0,14 bar over sealing ring 3.

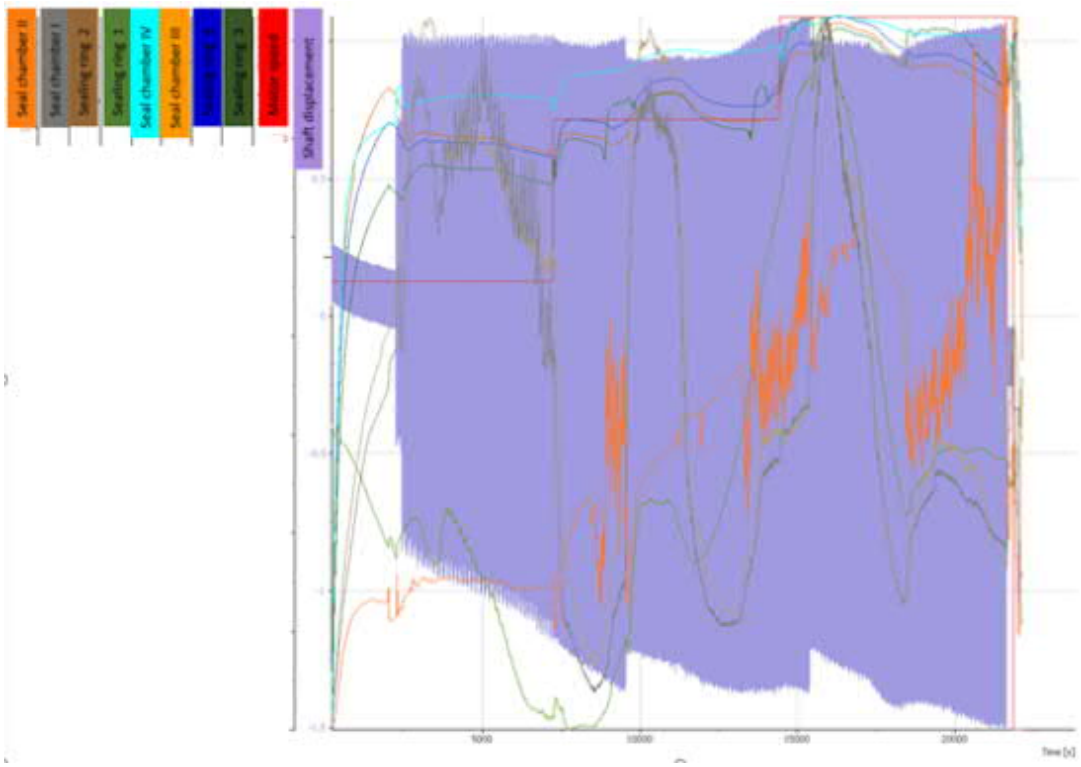

Figure 83. Seal system response to constant vibration amplitude with changing shaft speed, Δp0,22 bar over sealing ring 3.

Oil leakage rate was also measured in the tests where the sealing ring 3 pressure difference was changed. Leakage rates are presented in **Figure 84**.

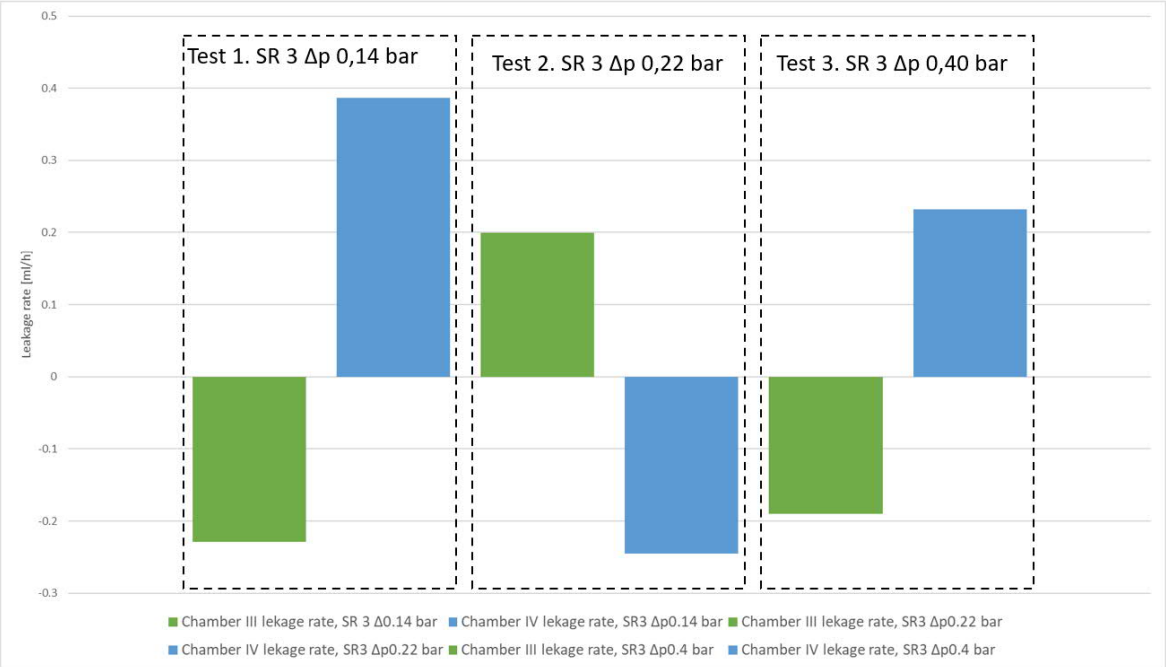

Figure 84. Calculated leakage rate of seal chambers III and IV.

8.4 Inspection of used sealing rings

Used sealing rings from three shafts of three different vessels were inspected. Vessels one and two had been operating for approximately 2,5 years, and vessel three for only less than a year. The vessels can be considered identical and same lubrication oil was used in all three vessels. Pictures of the sealing rings of vessel 1 are presented in **Figure 85**, pictures of the sealing rings of vessel 2 are presented in **Figure 86** and pictures of the sealing rings of vessel 3 are presented in **Figure 87**.

Figure 85. Used sealing rings from vessel 1.

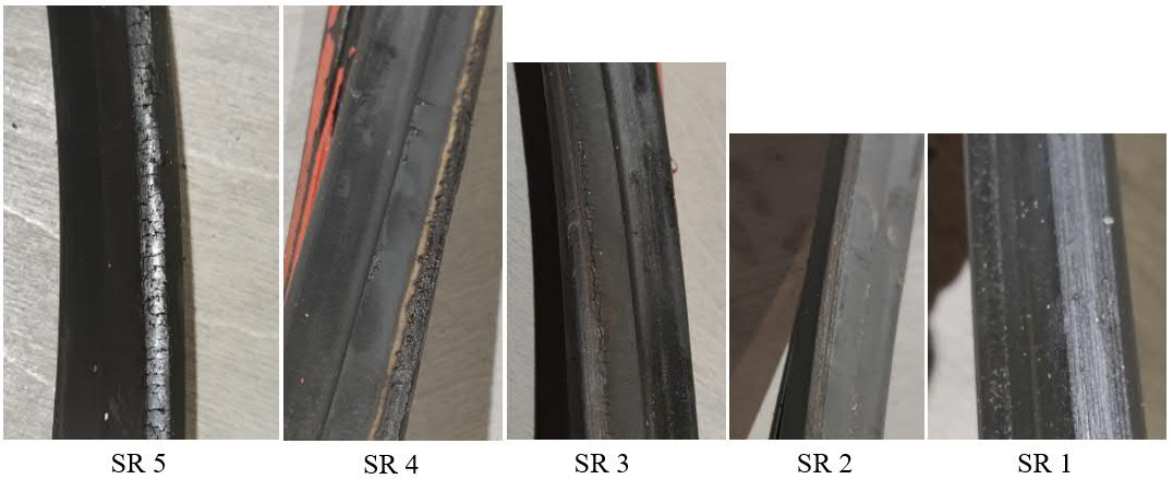

Figure 86. Used sealing rings from vessel 2.

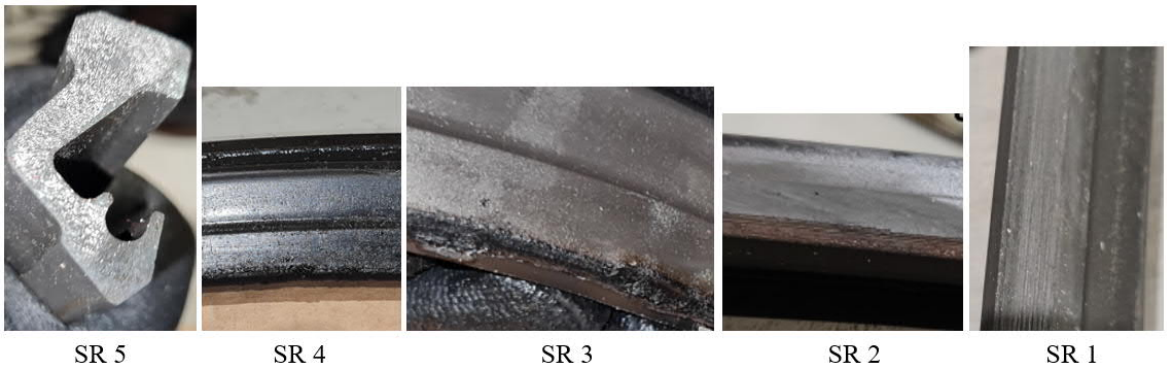

Figure 87. Used sealing rings from vessel 3.

8.5 Summary of the experiments

Highest measured temperatures of each sealing ring, seal chamber and seal system torque are presented in *Table 7*.

Table 7. Highest measured temperatures and shaft torque.

Shaft speed [m/s]	Shaft torque [Nm]	Location	Temperature [°C]	Pressure [bar]	Δp over sealing ring [bar]
7.1	338	Water	999.9	1.14	N/A
		SR 1	999.9	N/A	0.08
		SR 2	999.9	N/A	0.08
		SR 3	999.9	N/A	0.39
		SR 4	999.1	N/A	0.8
		SR5	N/A	N/A	0.73
		Chamber I	999.9	1.06	N/A
		Chamber II	999.9	1.14	N/A
		Chamber III	999.9	1.53	N/A
		Chamber IV	999.9	0.73	N/A

In static misalignment conditions with non-rotating shaft, the seals are found to leak when the misalignment is between 1,7 and 3,3 mm. Static misalignment with rotating shaft was found to increase the sealing ring temperature especially in sealing rings 1 and 2. Temperatures in the static misalignment tests with rotating shaft would have increased even further if the test would have been continued.

Oil temperature is found to be less stable in the dynamic misalignment conditions compared to a non-vibrating shaft. Calculated lubricant leakage rates show inconsistency.

Summary of the visual inspection performed on the used sealing rings is presented in *Table 8*.

Table 8. Visual inspection of used sealing rings.

SEALING RING VISUAL INSPECTION RECORD SHEET				
Vessel ID	Vessel 1	Vessel 2	Vessel 3	
Material	FKM	FKM	FKM	
Oil type and viscosity	Synthetic PAO 320 cSt	Synthetic PAO 320 cSt	Synthetic PAO 320 cSt	
Visual inspection	Points	Points	Points	Notes

Table 7 continues. Visual inspection of used sealing rings.

Color change at running track SR #1	1	1	1	
Color change at running track SR #2	1	1	1	
Color change at running track SR #3	1	2	4	
Color change at running track SR #4	1	3	2	
Color change at running track SR #5	1	1	2	
Oil carbon formation SR #3	3	2	4	
Oil carbon formation SR #4	2	4	3	
Oil carbon formation SR #5	2	4	1	
Hardening SR #1	1	1	1	
Hardening SR #2	1	1	1	
Hardening SR #3	2	3	3	
Hardening SR #4	2	4	3	
Hardening SR #5	2	4	1	
Crack formation SR #1	1	1	1	
Crack formation SR #2	1	1	1	
Crack formation SR #3	1	4	4	
Crack formation SR #4	1	4	3	
Crack formation SR #5	1	5	1	
Blistering SR #1	1	1	1	
Blistering SR #2	1	1	1	
Blistering SR #3	1	2	3	
Blistering SR #4	3	2	2	
Blistering SR #5	3	2	1	
Wear of sealing edge SR #1	1	5	5	
Wear of sealing edge SR #2	2	4	4	
Wear of sealing edge SR #3	3	4	4	
Wear of sealing edge SR #4	2	4	3	
Wear of sealing edge SR #5	2	5	1	
Chemical attack SR #1	1	1	1	
Chemical attack SR #2	1	1	1	
Chemical attack SR #3	2	4	4	

Table 7 continues. Visual inspection of used sealing rings.

Chemical attack SR #4	2	4	3	Legend for visual inspection	Points
Chemical attack SR #5	2	5	1		
Deposit on shaft SR #1	N/A	N/A	N/A	None	1
Deposit on shaft SR #2	N/A	N/A	N/A	Little	2
Deposit on shaft SR #3	N/A	N/A	N/A	Moderate	3
Deposit on shaft SR #4	N/A	N/A	N/A	Strong	4
Deposit on shaft SR #5	N/A	N/A	N/A	Very strong	5

9 ANALYSIS OF THE PERFORMED TESTS AND INSPECTED SEALING RINGS

Analysis of the test results obtained from the tests performed on the test device are presented in this chapter. The results are compared to the possible causes presented in the cause-and-effect diagram to confirm or discard causes for lubricant leakage.

9.1 Shaft speed sweeps

In the shaft speed sweep tests the sealing ring 4 temperature is rising with steepest slope when the first shaft is accelerated from 0 m/s speed to 2,1 m/s speed. Sealing ring 4 exceeds seal chamber IV temperature by approximately 3 °C after the first 100 seconds of shaft rotation. After less than seven minutes of shaft rotation, the temperature difference is already 6 °C and the difference in the slope between sealing ring 4 and seal chamber IV is constantly getting larger. The sealing ring 4 reaches its highest temperature at this shaft speed after approximately 25 minutes of shaft rotation. After the temperature reaches the highest value, it decreases by approximately 2 °C. Sealing rings 3 and 4, and seal chambers III and IV show similar behavior. This phenomenon is only present on this shaft speed. Sealing ring 4 settles to approximately °C, and seal chamber IV to °C. Sealing ring 3 and seal chamber III temperatures rise practically on the same slope on same temperature, and they settle to approximately °C. There is not a similar difference between the sealing ring 3 and the seal chamber III temperature as between sealing ring 4 and seal chamber 3. Seal chamber III has higher heat input than seal chamber IV as the heat density is largest on the sealing ring – shaft contact and thus both sealing rings 3 and 4 heat seal chamber III oil.

At the next shaft speed, 3,1 m/s the behavior is similar to the previous shaft speed. Sealing ring 4 temperature rises to approximately °C while the seal chamber IV temperature is 10 °C lower. Sealing ring 3 and seal chamber III temperature settles to approximately °C.

The next shaft speed, 4,2 m/s shows a change in the temperature balance as the sealing ring 3 reaches the same temperature with the sealing ring 4 while seal chamber III temperature stays approximately 2 °C lower. The difference between sealing ring 4 and seal chamber IV temperature stays approximately the same as before. Sealing rings 3 and 4 temperatures also

show small fluctuation at this shaft speed. The reason for the fluctuation is unclear. It could possibly be a sign of changing lubrication regime of sealing ring 3 or 4. It is difficult to say which sealing ring (or both) is causing the fluctuation as both sealing rings 3 and 4 temperatures affect the seal chamber III temperature.

Sealing ring 3 temperature increases on the steepest slope when the shaft speed is further increased to 5,7 m/s. The temperature difference between the sealing ring temperature and the oil temperature is approximately 10 °C. Temperature difference between sealing rings 3 and 4 is approximately 5 °C and the difference between sealing ring 4 and seal chamber IV has increased to 12 °C. Diverging of the sealing ring 3 temperature and the temperature fluctuation is shown in **Figure 88**.

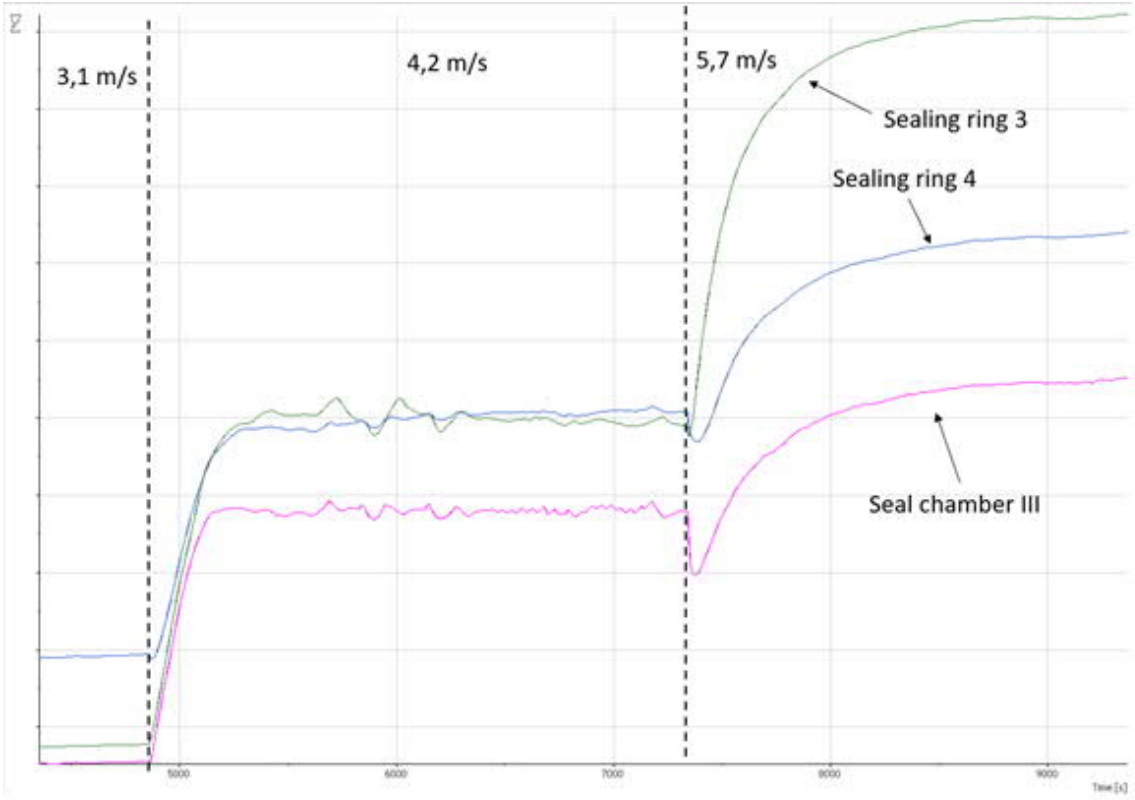

Figure 88. Sealing ring 3 temperature diverging from sealing ring 4.

The temperature balance of the oil seals and seal chambers continues similar on all following shaft speeds but the increase in the temperature flattens the higher the shaft speed gets as (Jia et al. 2014, p. 1180) explained. The torque behavior is also similar to the behavior presented by (Guo et al. 2013, p. 198) although the shaft torque did not show decreasing

even on the highest shaft speeds. The reason for this could be that the threshold value of the shaft speed when the friction torque starts to decrease was not reached in the tests. The highest temperatures of the oil seals and seal chambers are presented below.

- Sealing ring 4: °C
- Seal chamber IV: °C
- Sealing ring 3: °C
- Seal chamber III: °C

The reason for the changed behavior in the sealing ring 3 temperature after 4,2 m/s shaft speed is unclear. Based on theory focusing on the lubrication film properties, the lubrication film thickness should increase when shaft speed is increased, and the lubrication regime should be closer to elastohydrodynamic lubrication. Can the lubrication film properties of sealing ring 3 be degenerated at higher shaft speeds on this particular sealing ring design?

Sealing ring 1 temperature is approximately 2-3 °C higher than the water tank temperature and the sealing ring 1 temperature follows the water tank temperature for the entire test. Sealing ring 2 temperature increases in a similar fashion compared to sealing rings 3 and 4, but the temperature starts to fluctuate when shaft speed reaches 6,6 m/s. The fluctuation increases when the shaft speed is increased further. The fluctuation on the temperature could be a sign of increasing asperity contact between the sealing ring and the shaft or even a sign that the sealing ring is operating in boundary lubrication regime. This could be the case on sealing ring 2 as if seal chamber I is dry, the sealing ring 2 operates without any lubrication. Sealing ring 2 temperature level is still significantly lower than sealing ring 3 or sealing ring 4 temperature. Seal chamber II temperature does not follow sealing ring 2 temperature and stays within 5 °C from its initial temperature for the entire test. This was expected as constant airflow is lead through the seal chamber II. Seal chamber I temperature on the other hand roughly follows sealing ring 2 temperature and the fluctuation in the sealing ring 2 temperature can be seen in the seal chamber I temperature. Fluctuating temperature of the sealing ring 2 and seal chamber I is presented in **Figure 89**.

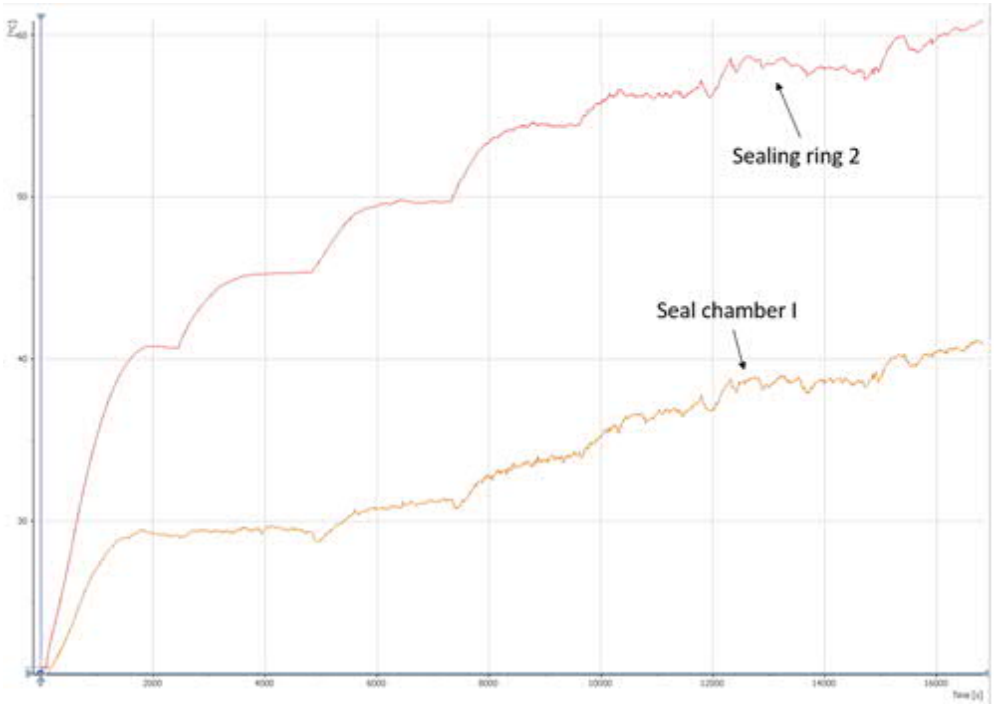

Figure 89. Fluctuating temperature of sealing ring 2 and seal chamber I.

When comparing the second shaft speed sweep performed on 1,57 bar water pressure the temperature behavior of the seal system is similar to the previous test, but the overall temperature level is a little higher. Increased temperature of the sealing ring 4 and seal chamber III is obvious as the radial load is increased. Sealing ring 3 also has higher temperature, but that too can be explained by increased temperature in the seal chamber III. Interestingly, sealing ring 3 temperature diverges from sealing ring 4 temperature at lower shaft speed, 4,2 m/s, compared to the previous test at lower water pressure. The diverging occurs at same sealing ring temperature, °C, which indicates that the diverging is more temperature and thus oil viscosity dependent than shaft speed dependent. Tests performed with different pressure differences over the sealing ring 3 points to the same direction. When the pressure difference over the sealing ring 3 is the lowest, 0,12 bar, the sealing ring 3 temperature does not exceed °C and sealing ring 3 does not diverge from the sealing ring 4 temperature. When the pressure difference is increased to 0,22 bar, sealing ring 3 temperature diverges again when the sealing ring temperature reaches roughly °C. Figures showing the seal systems temperature with different sealing ring 3 pressure differences can be found from Appendix IV.

Overall temperature level of the oil seals was significantly higher than anticipated. A common assumption in the case company was that the oil temperature in the seal chambers would be close to water temperature, a similar assumption made also by Borras (Borras, 2020, p. 110). This makes it very difficult to compare the test results to the ones obtained by Borras as in Borras' tests the oil sump temperature was kept at 20 °C. The study made by Borras is also the only study available focusing on propeller shaft seals, so comparing the obtained test results to previous tests is not possible.

Based on the obtained test results, a temperature model for the sealing ring 3 was created in the case company. The model shows that the actual contact temperature is up to °C higher than the measured value. This at the latest confirm the temperature related causes for leakage in the cause-and-effect diagram. Figure from the temperature model created by the case company showing the contact temperature with respect to the monitoring point temperature is presented in **Figure 90**.

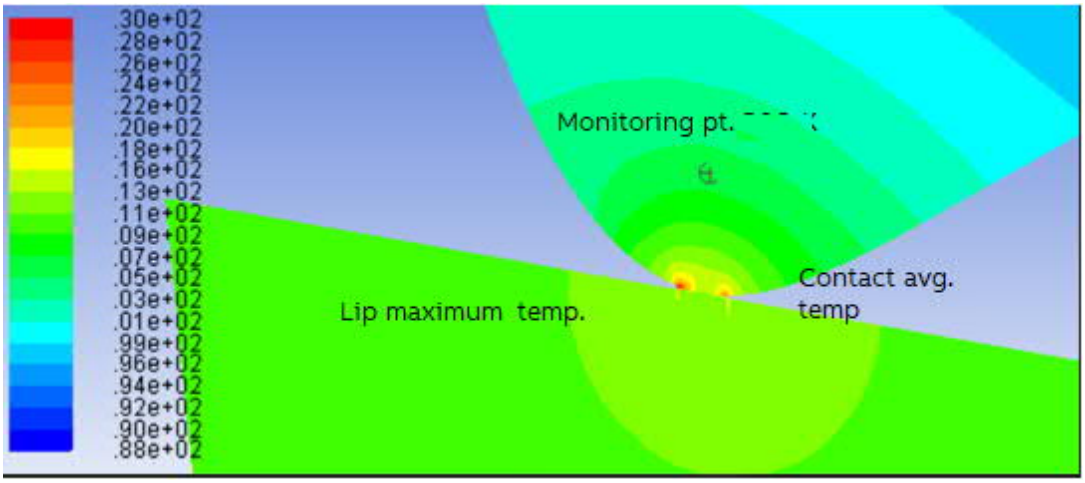

Figure 90. Calculated contact temperature of sealing ring 3.

As the testing was performed for a complete seal system with different radial loads and lubricants (oil and water), the lubrication regimes of the sealing rings cannot be defined based on the test results.

There are many temperature related causes for sealing ring wearing and damage in the cause-and-effect diagram. Based on the results excessive wearing of the sealing rings due to too high operating temperature might be one of the main reasons for lubricant leakage. Long

term effect of the temperature could not however be confirmed in the tests as the test period was relatively short.

9.2 Tests with changing pressure difference over sealing rings 3 and 4

Tests performed with different pressure differences over the sealing ring 3 show that the contact temperature increases when the pressure difference is increased, as can be easily concluded even without testing. The tests show that the increase in the temperature slope of sealing ring 3 is steeper with the highest pressure difference compared to the two lower pressure differences. Torque measurements does not show similar behavior and when examining the results more closely, the change in the slope is only between the two lower shaft speeds. It is possible that the sealing ring temperature had not yet stabilized before the shaft speed was increased.

Same applies for the test where sealing ring 4 pressure difference was changed – contact temperature and shaft torque increase when the pressure difference is increased, and the increasing in the temperature and shaft torque is linear.

Temperature balance of the seal system with different sealing ring 3 and 4 pressure differences can be found from Appendix IV.

9.3 Baseline for leakage rate

As already explained in Chapter 8.1 determining the leakage rate was more challenging than originally anticipated. The leakage can occur in both directions over the sealing ring, but unfortunately small changes in the oil level behind sealing ring 5 could not be measured. Same applies for seal chamber II as even though the seal chamber II is constantly drained, small leakages are very difficult to identify. Oil leakage to the seal chamber II could also be spouted to water with the constant air flow from seal chamber II to water. Schematic view of the problem is presented in **Figure 91**.

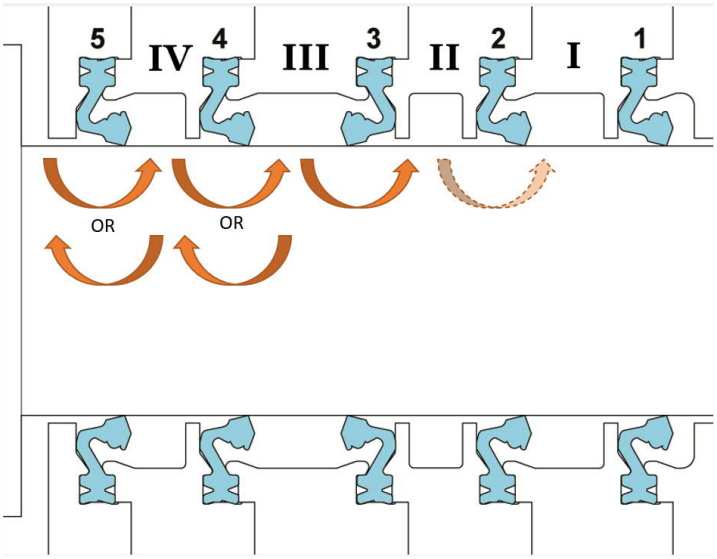

Figure 91. Possible directions of oil leakage.

Calculated leakage rates based on the tests where the pressure difference over sealing ring 3 was changed also show some inconsistency. Leakage rate of the seal chamber 4 should stay the same as pressure difference over sealing ring 3 is the only changed parameter between the three tests. When looking at the leakage rates of seal chamber III between tests 1 and 2, the change in the direction of the net leak rate could be explained by the increase in the sealing ring 3 pressure difference. Increased radial force should mean less leakage and thus the oil level in the seal chamber III tank could be increasing if the leakage rate of sealing ring 4 would be larger than the leakage rate of sealing ring 3. This would be logical as the net pump rate is normally higher from the back side of the seal to the spring side of the seal. However, when the seal chamber IV leakage rate is also taken into account, the leakage rates does not make sense as seal chamber IV loses oil slower than seal chamber III gains oil in test 2. The leakage rate of seal chamber IV is also opposite between tests 1 and 2. The direction of leakage of seal chambers III and IV are the same between tests 2 and 3, but again the results are inconsistent between the two tests. Seal chamber III leakage rate is smaller in test 3 compared to test 2 and this time seal chamber IV loses more oil than is gained by the seal chamber III.

The inconsistent behavior of the leakage rates makes it difficult to analyze the effect of the sealing ring 3 pressure difference to the leakage rate. The inconsistent behavior was not a

complete surprise, as experiences from the operating vessels show incosistent behavior in the direction of the oil leakage.

9.4 Static misalignment tests with standstill shaft

In the first test performed without water in the water tank, shaft misalignment was increased gradually. Seal chamber III pressure collapses when the misalignment increases from 3,2 mm to 3,3 mm compared to its initial position. Before that no leakage was detected by the tank level sensors or visual indication. When the seal chamber pressure collapsed leakage started immediately with high leakage rate. Pressure difference over the sealing ring 3 was 0,41 bar. The oil temperature stayed stabile for the entire test.

In the second misalignment test where there was also water in the water tank, seal chamber III temperature increases rapidly by approximately 0,8 °C when the displacement is increased from 1,7 mm to 1,8 mm, and then returns to its original temperature. This could be as sign of small oil leakage from seal chamber IV to the seal chamber III. Seal chamber III oil tank level sensor signals turned out to be unreliable in the static misalignment tests, as they reacted to the displacement of the shaft even when no leakage occurred. Seal chamber III pressure also decreased slightly simultaneously, which could indicate leakage. Seal chambers I and II temperatures decrease for the entire test and there is a clear change in the slope of the decrease when misalignment reaches 2,1 mm. The change from their initial temperature is rather small, less than 0,1 °C and the change in the temperature cannot be used to confirm water leakage. However, pressure of seal chamber increases simultaneously by approximately 0,07 bar which confirms water leakage. Seal chambers III and IV pressure collapses when misalignment reaches 3,2 mm, which corresponds well to the previous test. After the test water had mixed with oil in both seal chambers further confirming the leakage.

Pressure difference over sealing ring III was initially 0,43 bar and pressure difference over sealing ring 1 was 0,1 bar. As sealing ring 1 leakage was confirmed at 2,1 mm misalignment, and sealing ring 3 leakage at 3,2-3,3 mm misalignment, the pressure difference and/or viscosity has an effect on the sealing ring leakage when static misalignment is considered. Possible small leakage of sealing ring 4 or 3 detected in the second test much earlier at 1,8 mm misalignment was left unconfirmed.

The static misalignment tests with non-rotating shaft does not straight answer to any branch of the cause-and-effect diagram, but by comparing the results between static and dynamic misalignment test the effect of the speed of the movement on the seal followability can be seen.

9.5 Static misalignment tests with rotating shaft

In the third static misalignment test the shaft was rotating at 4,2 m/s speed. The temperature of the oil seals did not have a strong react to shaft misalignment. Sealing ring 3 temperature was actually decreased by 2 °C when the shaft misalignment was changed from 0 to 1 mm. This could be due to larger contact area of the sealing ring tip as the sealing ring is distorted when the shaft is misaligned. Sealing ring 3 temperature increased by total of 5 °C when the shaft misalignment reached 1,6 mm. Seal chamber III temperature increased by only 2,5 – 3 °C. Sealing ring 4 and seal chamber IV showed even less change in their temperatures. Temperature of sealing ring 1 did not chance during the test. Sealing ring 2 however showed rather rapid increase in its temperature. Sealing ring 2 initial temperature was °C and had already reached °C temperature at the end of the test. Rapid increase in the sealing ring 2 temperature was the reason the test was relatively short as damage of sealing ring 2 at this stage of testing was seen harmful. The temperature of the sealing ring would have increased even further if the test would have been continued, as its temperature was still increasing with relatively steep slope. Increasing temperature of sealing ring 2 can be seen as a sign of increasing asperity contact between the sealing ring and the shaft and a sign that the sealing ring is operating in boundary lubrication regime.

Looking back at the cause-and-effect diagram it seems that static bending of the shaft, or misalignment caused by component and assembly tolerances most probably won’t create big problems for the oil seals, as the theoretical maximum misalignment from the tolerance chain of different components is approximately 1 mm and it is not very likely this would ever come true. However, considering sealing ring 2 even smaller misalignment would most probably cause premature wearing in the sealing ring 2.

9.6 Gradually increasing dynamic misalignment test

The shaft speed for the entire test was 4,2 m/s, and the system had been run until oil temperature in seal chambers III and IV had stabilized before starting the test. Vibration amplitude was increased gradually until heavy leakage could be identified. Each vibration amplitude was held for approximately 20 minutes. The first vibration amplitude was approximately 0,35 mm, the second vibration amplitude was approximately 0,53 mm, fourth amplitude was approximately 0,75 mm, fifth amplitude was approximately 0,85 mm and the final sixth amplitude was approximately 1,1 mm. The final amplitude was held for only for 12 minutes as heavy water leakage to seal chamber II was identified. Leakage rate of the water was tens of liters per minute.

Looking back at the beginning of the test, a drop in temperatures of sealing rings 3 and 4 and seal chamber III can be seen. The drop of sealing ring 3 is quite small, approximately 0,5 °C, but the sealing ring 4 and seal chamber III temperatures drop for 1-2 °C. The temperatures remain stable for as long as the first vibration amplitude is held. Interestingly, seal chamber IV temperature starts to rise when the vibration starts and is still rising when the vibration amplitude is increased. The total rise of temperature in seal chamber IV during the first vibration amplitude is approximately 2 °C. Sealing ring 2 and seal chamber I temperatures also rise when the vibration is started and rise for a total of 2-3 °C. Their slopes are pointing downwards when the vibration amplitude is increased which is contrary to the seal chamber IV temperature behavior. Seal chamber II temperature stays more or less stable.

When the vibration amplitude is increased to 0,53 mm, the temperatures of sealing rings 3 and 4 and seal chamber III drops again similarly than when the vibration was started. Temperature increase of seal chamber IV also stops and seal chamber IV temperature drops close to seal chamber III temperature. Approximately 5 minutes before the vibration amplitude is further increased, the sealing ring 3 temperature drops for almost 3 °C, which could be an indication of leakage from under the sealing ring 3 to seal chamber II. Sealing ring 2 and seal chamber I show similar behavior than in the previous amplitude – both temperatures increase for a bit. Seal chamber I temperature also fluctuates, which could be an indication of water entering to the seal chamber I. Seal chamber II temperature stays stable.

When the vibration amplitude is increased again, to 0,75 mm, the sealing rings 3 and 4 temperatures starts to drop like they did in the previous amplitudes, but this time they don't stabilize and keep on decreasing until the end of the test. Same applies for the seal chambers III and IV temperatures. This could be due to loss of contact between the sealing rings and the shaft and/or oil leakage from under the sealing rings. Sealing ring 2 temperature increases for over 10 °C when the vibration amplitude is increased but then collapses for over 20 °C and then again starting to rise again. Seal chamber I temperature follows the sealing ring 2 temperature.

The answer for the relatively rapid and high increase in the temperature could be explained by hot oil leaking into the seal chamber II. Pressure behavior of the seal chamber III backs this up, as it first decreases by 0,06 bars and later rises by 0,03-0,04 bars. Pressure drop in the seal chambers III and II is presented in **Figure 92**.

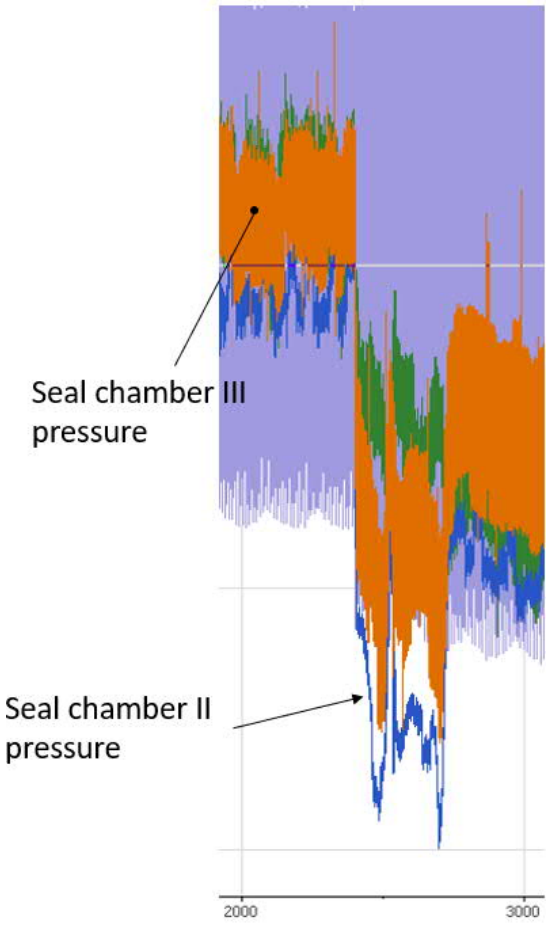

Figure 92. Pressure drop in seal chambers II and III.

The only inconsistency here is that seal chamber II pressure changes similarly, which also causes the seal chamber III pressure to change. However, seal chamber I should show similar behavior if the pressure drop in the seal chamber II would be caused by loss of contact of sealing rings 1 and 2. This behavior could not be seen. Even though the increase of temperature in the seal chamber II is relatively small, it can still be seen as a clear change compared to its earlier behavior. Also, the reason for the seal chamber II temperature not to increase as much as sealing ring 2 and seal chamber I temperatures could be explained by the relatively high air flow from under the sealing rings 1 and 2. Small oil leakage from seal chamber III could be grabbed by the air flow and be spouted to the seal chamber I and then to water without it ending up into the seal chamber II temperature sensor.

The next vibration amplitude 0,85 mm shows least changes of any of the amplitudes. Sealing rings 3 and 4, and seal chambers III and IV temperatures keeps declining. Sealing ring 2 and seal chamber I temperatures decline at first but then stay relatively stable. Seal chamber II temperature stays stable.

All of the sealing rings and seal chambers temperatures crash down when the vibration amplitude is increased to 1,1 mm except for seal chamber II temperature which increases rapidly. The rapid changes in the temperatures are a clear sign of both oil and water leakages. Pressures of each seal chamber also start to decrease, although leakage cannot be indicated by drop in the pressures.

In addition to the disturbance in seal chambers III and II pressures found in the beginning of vibration amplitude 0,75 mm, the pressures of seal chambers I, II and III drop every time the vibration amplitude is increased. As air is constantly leaking to water under the sealing rings 1 and 2, the drop in the pressures can be explained by the loosening of the contact between the seal and the shaft of sealing rings 1 and 2 in vibrating conditions allowing the air to escape to the water more easily. Seal chamber IV pressure is regulated to a constant pressure by a pressure regulator, so seal chamber IV pressure does not show similar behavior. However, the increasing amplitude can be seen also in the seal chamber IV pressure. Fluctuation of seal chamber IV pressure increases together with the vibration amplitude, which indicates that the pressure regulator is not fast enough to compensate for the changes in the seal chamber pressure.

9.7 Dynamic misalignment with changing pressure difference over sealing ring 3

The general idea of these tests where to determine a leakage rate for the sealing ring 3 with steady vibration amplitude and compare the results to the baseline leakage rate determined with a non-vibrating shaft. As presented in Chapter 9.3, defining a reliable leakage rate is surprisingly difficult. As the seal system had to be run until oil temperature had stabilized, the leak rate during the warm-up is also included in the total leakage rate. Also, other dynamic misalignment tests, that are not presented in this thesis showed that the leakage rate with a vibrating shaft is smaller than anticipated. For this reason, the vibration amplitude in these tests is set close to the amplitude where heavy water leakage was found in the dynamic misalignment test where the misalignment was increased gradually. Unfortunately, when the vibration amplitude is this high, the amplitude slowly creeps higher as can be seen from the figures presented in Chapter 8.3. Creeping of the amplitude is due to the test device hydraulics and correcting it will require changes in the test device control software. Change in the amplitude during the three tests with different shaft speeds is presented in *Table 9*.

Table 9. Creeping vibration amplitude in the leakage rate tests.

	Shaft speed [m/s]			
	4.2	5.7	6.6	Δp over sealing ring 3 [bar]
Amplitude in the beginning [mm]	0.9	1	1	
Amplitude in the end [mm]	1.1	1.15	1.2	0.14
Amplitude in the beginning [mm]	0.9	1	1	
Amplitude in the end [mm]	1.1	1.15	1.2	0.22
Amplitude in the beginning [mm]	0.9	1	1.15	
Amplitude in the end [mm]	1.1	1.15	1.25	0.4

For a reliable leakage rate, the vibration amplitude should have of course stayed stable, but fortunately the creeping is similar in all of the tests. Another disadvantage of the creeping amplitude was that it when the amplitude creeped high enough, water started to leak to seal chamber II. This occurred in all of the tests with all shaft speeds. The water leakage can be seen from the seal chamber I and II temperatures.

Temperature and pressure behavior in the tests is not analyzed as thoroughly as in the test where the dynamic misalignment was increased gradually. Similar drops and rises in the temperatures as in the gradually increasing misalignment test can be found in these test also.

Seal chamber IV temperature is also mainly higher than seal chamber III temperature in all of the test, which is opposite to the temperature tests. Overall, the seal chamber III temperatures are a few degrees lower compared to the tests without shaft vibration. This could be caused by lubricant leakage from seal chamber III to seal chamber II. Unfortunately, oil leakage could not be reliably confirmed from the seal chamber II drain line. It is possible that small oil leakage from the seal chamber can be led straight to water with the constant air flow.

Calculated leakage rates are smaller than in the tests where the shaft was not vibrating. The direction of leakage also changes like it did in the non-vibrating shaft test, but in these tests the direction of leakage was the same in tests one and three, as in the tests without vibration, the direction changed after test one and stayed the same in tests 2 and 3. As changes in the temperatures of the seal chambers indicated small oil leakages, measuring the oil level before and after the tests is not a reliable way to calculate leakage rates. It is possible that oil enters the system from behind sealing ring 5, as that space does not have an accurate oil level measurement system and thus the calculated leakage rates are not correct. It is also possible that the direction of leakage changes during the tests, which makes it difficult to calculate leakage rates at least from tests with relatively low duration.

Even though the calculated leakage rates are not accurate and most probably more leakage occurred when the shaft was vibrated compared to non-vibrating conditions, the leakage rates in vibrating conditions are still very small. The small leakage rates mean that the seal system is very robust against relatively high continuous vibration at 5 Hz amplitude at least when the seals are new and in good condition.

Considering the cause-and-effect diagram the dynamic misalignment tests leave a twofold feeling. Both oil and water leakages were found, but on the other hand the oil leakage rates are small. Very high water leakages in cases where the sealing rings are in good condition has not been reported from the operating vessels, but significantly higher oil leakage rates have been found in vibrating conditions even with new sealing rings as presented in Chapter 5.2.1. Could it be that the vibration in the actual application is different compared to the type tested?

9.7.1 Effect of misalignment on sealing ring wear-rate

Dynamic runout is known to have a significant effect on the sealing rings lifetime as explained in Chapter 4.9. Even though dynamic runout in the case company's products is very small, vibrating operational conditions could cause same effect on the sealing rings. The increase in the contact pressure in dynamic misalignment was estimated by structural modeling by the case company as presented in **Figure 93**.

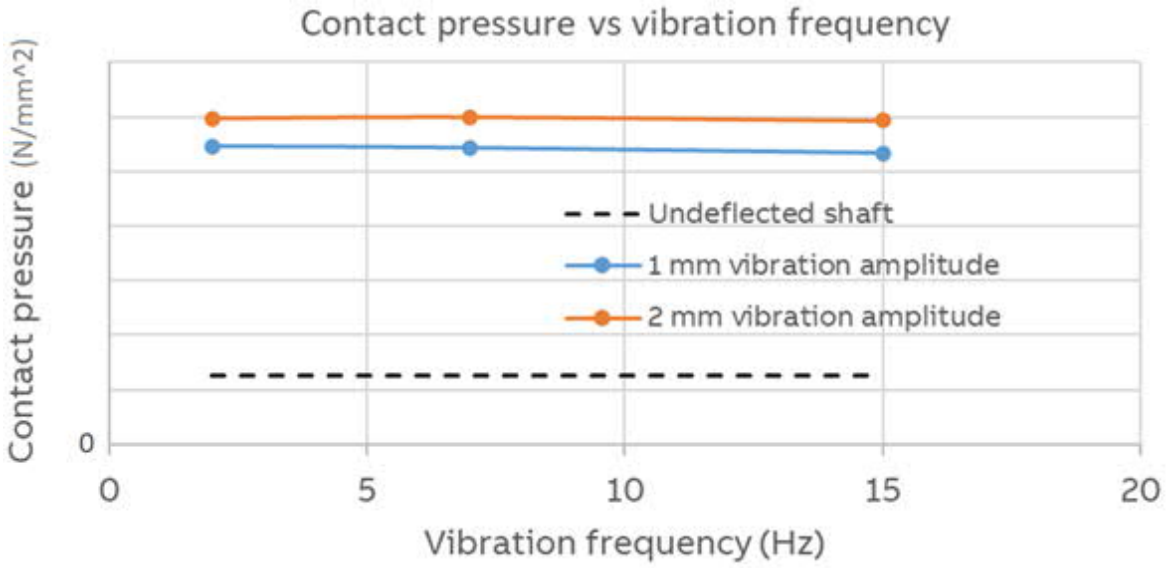

Figure 93. Increasing surface pressure due to dynamic misalignment.

Based on the results from the structural analysis, it seems that the contact pressure raises significantly when the shaft is vibrating. The increase in the contact pressure does not seem to be related to the frequency but on the amplitude. This raises a question whether the phenomenon is only related to the amount of misalignment. Effect of static misalignment on the seal contact pressure is presented in **Figure 94**.

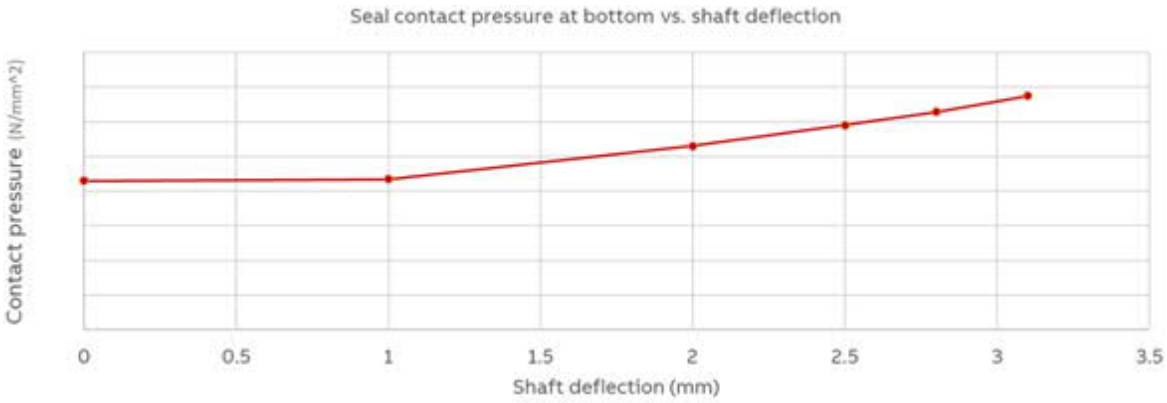

Figure 94. Effect of static misalignment on the contact pressure.

When comparing the results of the analysis for static and dynamic cases, it comes clear that the frequency also plays a significant role in the contact pressure and thus a vibrating shaft could be a factor that increases the seal wear rate. However, even though the percentual increase in the contact pressure is significant when dynamic misalignment is considered it is difficult to estimate the effect of the increase in the contact pressure on the wear rate without long term testing.

9.8 Accuracy of different variables

As can be imagined there is variation in the different input and output variables. According to the measured electric motor speed, the speed oscillates constantly, but stays within 2 rpm of the set speed in the tests. When the gearbox ratio is taken into account, the rotation speed in the seal system stays within 0,22 rpm, which can be considered very small. The electric motor torque also oscillates in a similar fashion compared to the motor speed. The oscillation stays within approximately 0,5 – 0,6 Nm, when it is measured from the electric motor. When the gearbox ratio is taken into account, the oscillation is 4,6 – 5,5 Nm. It is unclear, whether the oscillating torque is a cause or result of the oscillating shaft speed. The torque in the seal system could vary as the sealing rings operate in the mixed lubrication regime.

The third decimal of the measured pressures fluctuates occasionally even when testing is ongoing. It is unclear whether the fluctuation is due to minor air pressure changes in the system or is it due to the sensor signal itself. In any case the fluctuation can be considerd very small.

Small 1 – 2 °C changes in the temperature of the water tank was observed during the tests, which will naturally have a small effect on the results. However, the changes in the temperature are relatively slow.

Creeping amplitude in the vibration testing was observed and the magnitude can be seen from *Table 9*. The displacement sensors were calibrated with mechanical dial indicators. Still it is reasonable to assume that mesured displacement values are not absolute especially in the dynamic misalignment tests.

9.9 Analysis of used sealing rings

Making correct assumptions of the inspected sealing rings is very difficult, because typically if the oil leakage rate is increased over a certain threshold, the seal system is operated in various special operation modes which reduces the oil leakage but increases the radial load of the sealing rings 1 and 2, and/or sometimes also sealing rings 3, 4 and 5. Fortunately, the leakage rate in vessel 1 had been within normal limits and special operation modes had not been activated.

9.9.1 Sealing rings of vessel 1

Sealing rings 1 and 2 are generally in good condition, only small wearing that can be considered normal found in the contact area.

Sealing ring 3 contact surface is rough, and carbon build-up can be found from the back side of the seal, which indicates that the operating temperature of the seal has been high. Blisters, cracks or other defects were not found. As the oil leakage rate reported from the vessel was within normal limits, the carbon build-up had not disrupted the seals normal operation significantly. The contact width was measured with a vernier caliber, and it was approximately 2,5 mm. Some areas of the sealing ring were in better condition than others, which indicates that the lubrication conditions are not uniform in all areas of the contact.

Sealing ring 4 contact surface was not as rough as sealing ring 3 surface but small amount carbon build-up was found from the back side of the seal. There are also blisters on the back side of the seal near the contact surface. Blistering also indicate that the seal has been subjected to high temperatures. However, blisters can also be caused by chemical

incompatibility of the lubricant and the seal material or if the seal has been exposed to other chemicals, such as cleaning solvents. Static and dynamic oil – material tests have been performed by the manufacturer, but chemical incompatibility cannot still be ruled out as the dynamic test period is relatively low, and it is performed in lower temperature than the temperature found in the experiments. The contact width was measured with a vernier caliber, and it was approximately 2 mm. Contact width is smaller than in the sealing ring 3, which indicates that sealing ring 3 has worn more than sealing ring 4 even though the radial force on the sealing ring 4 is higher. Lower wearing of sealing ring 4 can be explained by better lubrication conditions of the sealing ring 4 as it has oil on both sides of the seal. Some areas of the sealing ring were in better condition than others as was the case with sealing ring 3 also.

Sealing ring 5 condition was very similar to sealing ring 4. Same un-uniform surface condition was also present in sealing ring 5.

9.9.2 Sealing rings of vessel 2

Sealing ring 1 showed high wearing and the contact surface has several deep radial scratches. The high wear rate and the scratches can be explained by the use of a special operation mode of the seal system where sealing ring 1 has very high pressure difference.

Sealing ring 2 showed signs of excessive wearing similar to sealing ring 1. The high wear rate of sealing ring 2 can be also explained with the special operation mode.

Sealing ring 3 showed only small signs of carbon build-up, which is different compared to the sealing ring 3 of vessel 1. Instead, relatively deep axial cracks were found on the contact surface. Axial cracking can be caused by various different reasons, for example high temperature, high pressure difference or poor lubrication. The measured contact width is 5mm, which is also high compared to vessel 1. High contact width can be explained by the use of a special operation mode where the sealing ring 3 pressure difference is increased. Measured contact width was approximately 3 mm.

Sealing ring 4 has a lot of carbon build-up in the contact area. The amount of the build-up is significantly higher than the amount found from vessel 1. Axial cracking was also found

from the contact surface. It is easy to conclude that this high carbon build-up has lifted the sealing ring off from the shaft. In addition, the surface color was not consistent with the rest of the material. Reason for the change in the color is unknown. Special operation modes also increase the pressure difference over sealing ring 4, which can explain some of the damage.

Sealing ring 5 has very deep axial cracks on the contact surface. Again, special operation modes can explain the magnitude of the damages for some extent. Measured contact width of sealing ring 5 is 5 mm.

The condition of sealing rings 3, 4 and 5 was poor across the whole contact area, but still some areas showed less damage than others.

9.9.3 Sealing rings of vessel 3

Sealing rings 1 and 2 are in very similar condition compared to vessel 2, which can be explained by the use of same special operation modes as in vessel 2.

Sealing ring 3 shows signs of carbon build-up on the air side of the seal. The color of the contact surface has also changed, and the surface looks “burned”. Again, this indicates that high temperatures are present in the contact area. The contact width is 4 mm. Special operation modes has also been used in vessel 3. The surface condition was un-uniform in this sealing ring also.

The condition of sealing ring 4 was relatively good at some areas, but poor on other areas. On the poor areas both carbon build-up, axial cracking and blistering was found. Measured contact width is 1,5 mm on the good areas and 4 mm on poor areas.

Sealing ring 5 is in the best condition of any of the oil seals inspected. A stripe of brownish color is present on the back side of the seal near the contact surface, which could be an indication of early-stage carbon build-up. Measured contact width is 1,2mm.

9.9.4 Summary of inspected sealing rings

Overall condition of the sealing rings of vessel 2 was the worse of all of the inspected sealing rings. Vessel 1 had been in operation for the same duration as vessel 2, but the seal condition was significantly better, even though damage could also be found from the oil seals of vessel 1. For some reason the seals of vessel 3 were quite heavily damaged when considering the much shorter duration of operation. The overall operational profile of the vessels is similar, so it cannot alone explain the differences between different vessels. However, different vessels are not necessarily operated the same and thus shaft speeds and other operational conditions can vary between the vessels. The seal material itself might have variance in its composition, which could also explain this kind of behavior at least partly.

When considering the progression of the wearing and damage of the oil seals, it seems that the deterioration starts on some sections of the sealing rings and progresses to other areas while they deteriorate even more on the areas that were first deteriorated. This suggests that in addition to excessive temperature, the lubrication conditions are not uniform on all areas of the seals. It is difficult to say how much the special operation modes have influenced on the oil seal's damage. In other words, the sealing ring condition of vessel 1 could be close to the point when the oil consumption reaches the threshold limit where the special modes are being put to use and the further damage is caused by the increased radial load.

Sealing rings 1 and 2 wearing seems to be connected to the use of the special operation modes and when they are not used, the wear-rate of the sealing rings is well within limits.

9.10 Summary of Chapter 9

Temperature levels in the seal system were found to be higher than anticipated earlier. The temperature behavior of the seal system was found to correspond to the theory behind seal lubrication and heat generation and the temperature-related phenomena could be explained logically.

Measuring of the leakage rates was found to be more difficult than expected during the testing. Calculated leakage rates also seem inconsistent and variation between the different tests could not be fully explained logically. However, lubricant leakage in the static and dynamic misalignment conditions can be seen in the temperature balance of the seal system.

Leakage can also be identified from the pressures of each seal chambers, at least when the leakage is heavy.

Inspected used sealing rings show progressing wear and damage behavior. The wearing and damage seem to be at least partly temperature related. Some of the wear and damage can be explained by the use of special operation modes of the seal system.

10 DISCUSSION

At first glance radial shaft seals seem as very simple, even secondary components in rotating machines. However, when the sealing mechanism and the seal performance is examined a little closer, it is obvious that radial shaft seals are actually quite sophisticated and complex components with a numerous number of different factors effecting on their performance. In general, finding the affecting factors for leakage rate in large radial shaft seals is a subject much larger than can be covered in a master's thesis as for example several studies could only focus on the sealing ring materials.

10.1 Comparison of test results with literature

Large radial shaft seals, let alone seal systems with several sealing rings with different radial loads, lubricants etc., are also a very difficult topic to study as 100 % of the published studies or textbooks focus to examine systems with one sealing ring. In addition, only a few studies were found where propeller shaft seals are being examined, and actually all of those studies are covered in a doctoral thesis made by Borras (2020). Borras also focuses on one sealing ring, and the diameter is his studies is also 4 times smaller than the diameter relevant for this thesis. Lubricant leakage rates reported by Borras (2020, p. 167) are significantly smaller than the leakage rates obtained from the tests even when the leakage rate is converted to unit of volume per unit of length. Leakage rates reported by Jia et al. (2014, p. 1180) are closer to the leakage rates of measured in some of the tests, but as the leakage rates in the tests had quite large deviation, it is very hard to tell whether the leakage rates are comparable or not.

Sealing ring contact temperatures have been studied in numerous studies but typically only with oil – air interface. These studies are thus comparable with the test results of sealing ring 3. When comparing the results with for example results presented by Horve (1996, p. 188), the contact temperatures with similar shaft speeds are considerably higher in Horve's tests even though the pressure difference over the sealing ring is zero in Horve's tests. This could be explained by the difference in the sump temperature with lower shaft speeds as Horve used relatively high (93 °C), stable sump temperature. When comparing the tests results presented by Horve and the results presented in this thesis where the sump temperatures and shaft speeds are similar, the temperatures are relatively close to each other. Unfortunately,

the tests were not performed with exactly same shaft speeds and sump temperatures, so the comparison can only be done on a general level. Considering the sealing ring 4, the temperature levels can only be compared with the results presented by Borras (2020, p. 168). With low shaft speeds the contact temperatures presented by Borras are very close to the temperatures obtained from the tests. With higher shaft speeds, the temperatures in Borras's study are significantly higher. As Borras used similar pressure differences, the results are quite well comparable. However, Borras used relatively low 20 °C sump temperature with all shaft speeds. This implies that the heat generation in the seals used by Borras is higher than the heat generation of the seals used in the tests of this thesis.

Considering static and dynamic misalignment, comparable studies are not available. Borras et. al. (2020, p. 26) found that seals will leak if the static misalignment is increased enough, but he does not provide comparable values for the misalignment. Static misalignment is also found to influence the seal lifetime (SKF, 2019, p. 50; R.L. Hudson & Company, 2005, p. 236). As the duration of the performed tests was relatively short, this cannot be confirmed based on the tests. Vibrating shafts have not been thoroughly studied, as typically dynamic misalignment is conceived as dynamic runout of the shaft, which is different compared to the operating environment of the customer company's products as usually dynamic runout creates a lot higher vibration frequency. Horve (1996, pp. 227-228) studied the effect of dynamic runout on the seal lifetime and found that the larger the dynamic runout, the shorter the seal lifetime. Unfortunately, Horve's study did not include oil leakage data with different dynamic runout conditions. The lack of good baselines for the study makes it difficult to reflect obtained test results to existing studies.

Failure mechanisms presented in literature were found from the visually inspected used sealing rings.

10.2 Objectivity

The purpose of all tests was to monitor the seal system response to changing input parameters. The seal system operating parameters were not adjusted during the tests. The test arrangements reported in this thesis can be repeated in the case company relatively easily as the same test device is available for the case company. The input parameters in the tests were recorded and the process was monitored with numerous sensors to provide an objective

and comprehensive understanding of the seal system response to different input parameters. The obtained results can be seen to be in good accordance with literature findings.

10.3 Reliability and validity of the results

The same test conditions used in the tests reported in this thesis are well reproducible with the test device. Temperature measurements are found to be valid and reliable as variance in the temperatures was relatively small. The temperature levels in the system were monitored in several locations of the seal system, and inconsistency between the sensor readings were not detected. Temperature levels in the seal system were also found to correspond well with the related theory and no temperature related phenomenon were found that could not be explained.

Measured leakage rate's reliability and validity cannot be considered as good as the temperature measurements. There are quite a lot of inconsistency between different measurements and some of the results seem quite unreliable when they are examined closely. With the used methods it can be said that the leakage rates are relatively small compared to the preconceptions, but the accuracy of the measurements is relatively poor.

Visual inspection of the used sealing rings is in accordance with the cause-and-effect diagram, and also the theory behind seal wear and damage.

10.4 Key findings

The literature review revealed that subject seen as relatively simple has a lot more complexity than one might imagine. A relatively small change in the operation parameters or seal material and lubricants can lead to large changes in the seals long term performance. Also, in general the operating hours presented in the literature are much smaller compared to the requirements in the case company's product.

Based on the tests, temperature levels in the seal system are significantly higher than anticipated in the case company or seal manufacturer. It was also thought that pressure difference over the sealing ring would contribute to the temperature more than it did based on the tests. The leakage rates in vibrating conditions were smaller than originally

anticipated, which indicates that when the seal condition is good, the seal system performance in vibrating conditions is good.

10.5 Novelty of the results

A thorough summary of the theory behind radial shaft seals was not available in the case company before. There were also no measurements of the temperature levels in the seal system before the performed tests, so all temperature related results have high value for the case company when novelty is considered. Leakage rates from operating vessels were available already before the tests, but the operating conditions from which the leakage rates could be calculated were only know on a general level. The test also revealed that the leakage rates are relatively small when the seal condition is good.

10.6 Generalization and use of the obtained results

The obtained results from both the literature review and the performed tests helps the case company to improve the seal system design to minimize seal wear and leakage rate. Knowledge regarding the seal performance in vibrating conditions is very useful when evaluating different sealing solutions for vibrating operating conditions.

The results cannot be generalized in that extent that for example exact temperatures of sealing rings in different operating conditions would be known for different seal designs. However at least a rough estimation could be formed based on the results presented in this thesis in case different seal designs are evaluated. Same applies for the leakage rates – each seal design has its own characteristics and leakage rates in non-vibrating or vibrating conditions cannot be concluded based on the obtained test results. Considering the visual inspection of the used sealing rings, the picture is a bit foggy as even though similar phenomena could be seen on all the inspected sealing rings, the magnitude of the phenomena was different between different vessels when the operating hours are considered. To be able to generalize the results, the operating conditions should be known better.

10.7 Topics for future research

Considering the possible causes presented in the cause-and-effect, especially the temperature related causes could be verified at that extent that high temperature levels are present in the seal system. Inspected used sealing rings indicate longer term effects of the heating, but

endurance testing should be executed to fully verify the temperature related causes. Abrasive particles in the lubricant could also cause excessive wear. Impurities from outside of the seal system should pass the sealing rings 1 and 2 so they could end up in the lubrication oil. This could be possible is large amounts of water enter the system even though the seal chamber II is constantly drained. Obviously sealing rings 1 and 2 are prone to abrasive wearing as water will have relatively high particle content. The oil seals could also be damage due to hydrolysis if water is able to enter the seal system. The seal materials capability to withstand water in oil could be studied by laboratory or long-term testing. Abrasive particles could also come loose from the seal material itself – a topic that should definitely be further studied. Causes related to the dynamics could not be fully verified and leakage rates measured from the dynamic misalignment tests does not correlate with real life experiences. Some of the causes could be disqualified, such as “chamber plug leakage”, “leakage from backside of the seal” and “leak between hull and seal housing” at least when considering the seal pack that was used in the tests. Considering a larger sampling, there could still be cases where those causes would cause leakage. When individual cases are being examined, the cause-and-effect diagram will still be a good tool in troubleshooting.

Overall, the seal system of the case company’s product needs a significant amount of further studying to be able to first define sufficient understanding of the performance of the system and the different factors affecting it. There is a numerous number of different topics for further studies in addition to those already mentioned. Running a series of tests with only one sealing ring would make it possible to determine the lubrication regimes of different sealing rings, which would be beneficial in gaining a thorough understanding of the system. Tests run with different types and viscosities of oils would show the lubricant types and viscosities effect on the temperature balance and leakage rate. Speaking of leakage rates, more reliable baseline for the leakage rate could be determined by enhancing the oil level measurement accuracy in the space behind sealing ring 5. The test duration should also be increased significantly to be able to determine a reliable baseline for leakage as the effect of the oils heat expansion would be reduced when the test time increases. Running a series of high-duration tests with different radial loads, oil types, water temperatures etc. and comparing the seal condition between the tests would help to understand which parameters effect the seal wear the most.

11 SUMMARY

Radial shaft seals are very common components in rotating machines. They are often considered as simple secondary components that does not need much focus when machines are designed. However, when radial shaft seals performance is not sufficient, and they leak more than can be tolerated it is obvious that they are many times one of the key components of the machine in question. For example, excessive lubricant leakage in a ship's propeller shaft can end up to marine waters, which should oncourse be avoided.

Thorough literature review was performed to find key factors that influence radial shaft seal performance and leakage rate. A cause-and-effect diagram was created based on literature findings to give the case company a tool to recognize the factors behind the seal performance.

Series of tests were performed to answer the questions presented in the cause-and-effect diagram. The tests revealed that some assumptions, such as the assumption that the general temperature level of the seal system has to be low, were not true. It was also thought that change in the pressure difference would contribute more to the seal temperature than it actually does, which makes it easier to develop the system in the future. Lubrication regimes of the sealing rings could not be defined as the tests were performed for a full seal system with different radial loads and lubricants, but the temperature behavior of sealing ring 3 indicate that the lubrication of the sealing ring is deteriorated when the seal temperature reaches a certain threshold. Overall, managing the temperature in the seal system could extend the sealing rings lifetime and maintaining the system performance.

Static and dynamic misalignment tests showed that the seal system preforms well with relatively high static misalignment and relatively high constant vibration amplitudes at 5 Hz frequency. Reports from operating vessels show that the leakage rates are higher in the real application even with new sealing rings, which indicates that the test setup for the dynamic misalignment tests did not fully replicate actual vessel conditions. In fact, more detailed information of the displacements of the propeller shafts of the customer company's application were obtained after the tests of this thesis were completed. The new information shows that constant vibration is present in the system, single load strikes creating much

higher displacements are present. Naturally, testing the effect of high amplitude load strikes would be very beneficial as they could answer the question why the leakage rate in the tests was smaller than the leakage rates reported from the operating vessels. Dynamic misalignment was also found to cause the contact pressure to raise significantly in simulations made by the case company and increasing contact pressure could affect the sealing ring wear rate.

Inspection of used sealing rings from operating vessels also suggest that high temperatures are present in the seal system, confirming the test results. Inspected seals showed relatively high variation between different vessels and some of the seals where operated in conditions that they were not designed to be operated (special operation modes of the seal system). Thus, it is difficult to draw accurate conclusions of the magnitude of the wearing where excessive oil consumption starts.

REFERENCES

Adler, M., Walker, J., Sascha Grasshoff, C. D. & Pfadt, M. 2018. Understanding the Dynamic Influences of Gear Oils and Radial Shaft Seals. Power Transmission Engineering, Vol. 12, No. 1, pp. 30-37.

Bavel, P. v. 1997. The Leakage Free Operation of Radial Lip Seals. Eindhoven University of Technology. 126 p.

Barnes Group Inc. 2021. Engineering Guide to Spring Design [web document]. [Referred 20.9.2021]. Available: https://www.asbg.com/engineering-guide-to-spring-design.aspx

Bhushan, B. 2013. Introduction to Tribology. Second edition. New York: John Wiley & Sons Ltd. 711 p.

Borras, F.-X. 2020. Rotary Lip Seal Operation with Environmentally Acceptable Lubricants. University of Twente. 367 p.

Borras, F. Bazrafshan, M., Rooij, M. d. & Schipper, D., 2020. Stern tube seals under static condition: A multi-scale contact modelling approach. Proceedings of the Institution of Mechanical Engineers, Part J: Journal of Engineering Tribology, Vol. 235, No. 1, pp. 181-195.

Borras, F., Rooij, M. d. & Schipper, D. 2020. Misalignment-induced macro-elastohydrodynamic lubrication in rotary lip seals. Tribology International, Vol. 151, p. 10.

Brown, R. 2018. Physical Test Methods for Elastomers. Cham: Springer. 387 p.

Burkhart, C., Emrich, S., Kopnarski, M. & Sauer, B. 2020. Excessive shaft wear due to radial shaft seals in lubricated environment. Part I: Analysis and mechanisms. Wear, Vol. 460-461, p. 12.

Cardarelli, F. 2018. Materials handbook. 3rd edition. Cham: Springer. 1339 p.

Carter, C. D. 2009. Elimination of a Ship Source Pollutant - STOP (Stern Tube Oil Pollution) [web document]. [Referred 1.9.2021]. Available: imare.in/media/30645/paper-no-7b-3-mr-craig-carter.pdf

Drobny, J. 2016. Fluoroelastomers Handbook. 2nd edition. Oxford: Elsevier. 584 p.

Etkin, D. S. 2008. Worldwide Analysis of In-Port Vessel Operational Lubricant Discharges and Leakages. Proceedings of the 33. AMOP technical seminar on environmental contamination and response. Halifax, Nova Scotia, Canada. 7-9 June 2010. Pp. 529-553.

Flitney, R. 2005. Extending the application of fluorosilicone elastomers. Sealing Technology, Vol. 2005, No. 2, pp. 6-11.

Flitney, R. 2007. Seals and sealing handbook. 5th edition. Oxford: Elsevier. 620 p.

Freudenberg Sealing Technologies 2015. Technical Manual: Simmerrings and Rotary Seals [web document]. [Referred 15.8.2021]. Available: https://www.fst.com/-/media/files/fst,-d-,com/technical-manuals/en/fst_technical_manual_2015_sec01_simmerrings_and_rotary_seals.pdf

Frölich, D., Magyar, B. & Sauer, B. 2014. A comprehensive model of wear, friction and contact temperature in radial shaft seals. Wear, Vol. 311, No. 1-2, pp. 71-80.

GESAMP 2007. Estimates of Oil Entering the Marine Environment from Sea-based Activities. Rep. Stud. GESAMP No. 75, 96 p.

Guo, F., Jia, X., Lu, M., Wang, L., Salant, R., Wang, Y. 2014. The effect of aging in oil on the performance of a radial lip seal. Tribology International, Vol. 78, pp. 187-194.

Guo, F., Jia, X., Suo, S., Salant, R., Wang, Y. 2013. A mixed lubrication model of a rotary lip seal using flow factors. Tribology International, Vol. 57, pp. 195-201.

Hanhi, K., Poikelispää, M. & Tirilä, H.-M. 2007. Elastomeric materials. Tampere University of Technology [web document]. [Referred 1.9.2021]. Available: https://laroverket.com/wp-content/uploads/2015/03/Elastomeric_materials.pdf

Horve, L. 1996. Shaft seals for dynamic applications. New York: Marcel Dekker. 463 p.

ISO 6194-1 2007. Rotary shaft lip-type seals incorporating elastomeric sealing elements - Part 1: Nominal dimensions and tolerances. Geneve: International Organization for Standardization. 13 p.

ISO 6194-2 2009. Rotary shaft lip-type seals incorporating elastomeric sealing elements — Part 2: Vocabulary. Geneve: International Organization for Standardization. 37 p.

ISO 6194-3 2009. Rotary shaft lip-type seals incorporating elastomeric sealing elements — Part 3: Storage, handling, and installation. Geneve: International Organization for Standardization. 10 p.

ISO 6194-4 2009. Rotary shaft lip-type seals incorporating elastomeric sealing elements — Part 4: Performance test procedures. Geneve: International Organization for Standardization. 17 p.

ISO 6194-5 2008. Rotary-shaft lip-type seals incorporating elastomeric sealing elements — Part 5: Identification of visual imperfections. Geneve: International Organization for Standardization. 9 p.

James Walker 2017. Elastomer Engineering Guide [web document]. [Referred 11.7.2021]. Available: https://www.jameswalker.biz/de/pdf_docs/148-elastomer-engineering-guide

Jia, X., Guo, F., Huang, L., Wang, L., Gao, Z., Wang, Y. 2014. Effects of the radial force on the static contact properties and sealing performance of a radial lip seal. Science China, Volume 57, pp. 1175-1182.

Kemel Eagle Industry 2021a. Kemel Air Seal [web document]. [Referred 12.9.2021]. Available: http://www.kemel.com/product/images/001/a/airseal.pdf

Kemel Eagle Industry, 2021b. Kemel Compact Seal [web document]. [Referred 12.9.2021]. Available: http://www.kemel.com/product/images/001/b/compactseal.pdf

Kim, C. K. & Shim, W. J. 1996. Analysis of contact force and thermal behavior of lip seals. Tribology International, Vol. 30, No, 2, pp. 113-119.

Lagersmit, 2020. Maritime seals [web document]. [Referred 13.7.2021]. Available: https://www.lagersmit.com/products/supreme-standard/?utm_campaign=Brochure&utm_source=Maritime%20brochure&utm_term=suprsup-standard

Müller, H. K. & Nau, B. S. 1998. Fluid Sealing Technology principles and applications. New York: Marcel Dekker. 485 p.

Sea Surface Temperature Contour Charts 2013. [National Oceanic and Atmospheric Administration website]. Updated June 19, 2013. [Referred 26.8.2021]. Available: https://www.ospo.noaa.gov/Products/ocean/sst/contour/

Parker Hannifin 2018. Rotary seal design guide [web document]. [Referred 3.5.2021]. Available: https://www.parker.com/literature/Engineered%20Polymer%20Systems/5350.pdf

Pavlakis, P., Tarchi, D., Sieber, A., Ferraro, G., Vincent, G. 2001. On the monitoring of illicit vessel discharges. A reconnaissance study in the Mediterranean Sea [web document]. [Referred 1.7.2021]. Available: https://publications.jrc.ec.europa.eu/repository/handle/JRC21936

R.L. Hudson & Company, 2005. Shaft seal design & materials guide [web document]. [Referred 9.5.2021]. Available: https://rlhudson.com/wp-content/uploads/2018/04/rlhudson-shaft-seal-guide.pdf

Salant, R. 1997. Modeling rotary lip seals. Wear, Vol. 207, No. 1-2, pp. 92-99.

Salant, R. 2009. Soft elastohydrodynamic analysis of rotary lip seals. Proceedings of the Institution of Mechanical Engineers, Part C: Journal of Engineering Tribology, Vol. 224, No. 12, pp. 2637-2647.

SKF 2005. SKF Seal Handbook. 436 p.

SKF 2016a. Simplex Airspace - aft seal [web document]. [Referred 3.6.2021]. Available: https://skf-simplex.com/pdfs/SKF16037_DB_SimplexAirspace_web_161214.pdf

SKF 2016b. Simplex Multisafe M - aft seal [web document]. [Referred 3.6.2021]. Available: https://skf-simplex.com/pdfs/SKF16080_DB_SimplexMulltisafe_M_aft_seal_web_160506.pdf

SKF 2019. CR Seals handbook [web document]. [Referred 25.4.2021]. Available: https://www.skf.com/binaries/pub12/Images/0901d196807662c1-810-701_CRSeals_Handbook_Jan_2019_tcm_12-318140.pdf

Stakenborg, M. 1988a. On the sealing mechanism of radial lip seals. Tribology International, Vol. 21, pp. 335-340.

Stakenborg, M. 1988b. On the sealing and lubrication mechanism of radial lip seals. Eindhoven University of Technology. 98 p.

Stakenborg, M. J. L. & Leeuwen, H. J. v. 1990a. Visco-Elastohydrodynamic (VEHD) Lubrication in Radial Lip Seals: Part 1 - Steady-State Dynamic Viscoelastic Seal Behavior. Journal of Tribology, Vol. 112, No. 4, pp. 578-583.

Stakenborg, M. J. L. & Leeuwen, H. J. v. 1990b. Visco-Elastohydrodynamic (VEHD) Lubrication in Radial Lip Seals: Part 2 - Fluid Film Formation. Journal of Tribology, Vol. 112, No. 4, pp. 584-592.

Stakenborg, M. & Ostaijen, R. v. 1988. Radial lip seals, thermal aspects. Tribological design of machine elements. Proceedings of the 15th Leeds-Lyon symposium of tribology, pp. 79-88.

Seal manufacturer 1 2012. Statement regarding lubricant leakage. [Not publicly available].

Seal manufacturer 2 2021. Statement regarding seal oil temperature. [Not publicly available].

Thornhill, J. 2014. The Challenge of Stern Tube Bearings and Seals. Proceedings of the 14th propeller and shafting symposium. September 15–16, 2015. Norfolk, Virginia, USA. 6 p.

VTT 2006. Research report VTT-R-05380_07. [Not publicly available]. 46 p.

Wärtsilä 2020. Wärtsilä Airguard seal [web document]. [Referred 22.7.2021]. Available: https://www.wartsila.com/docs/default-source/product-files/seals-bearings/business-white-papers/w%c3%a4rtsil%c3%a4-airguard_business-white-paper.pdf?sfvrsn=5b86ad44_6

Wenk, J. F., Stephens, L. S., Lattime, S. B. & Weatherly, D. 2016. A multi-scale finite element contact model using measured surface roughness for a radial lip seal. Tribology International, Vol. 97, pp. 288-301.

Wennehorst, B. 2016. On lubrication and friction in soft rough conformal sliding contacts. University of Hanover.

APPENDIXES

APPENDIX I, 1

Figure 1. Oil consumption with new sealing rings.

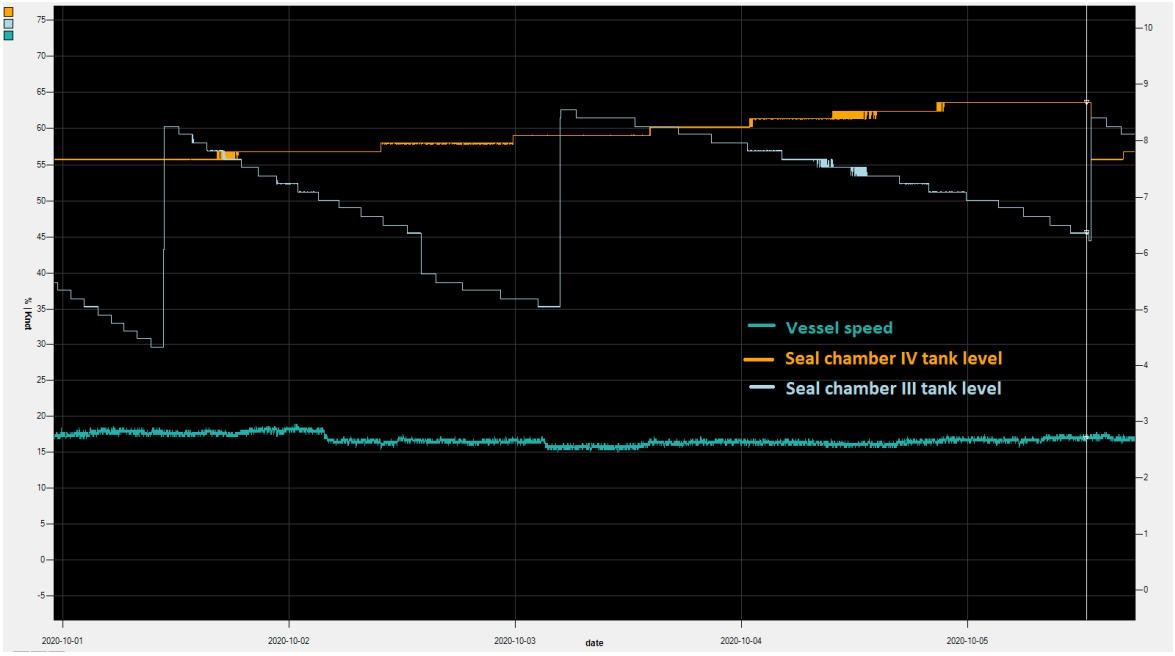

Figure 2. Normal oil consumption with used sealing rings.

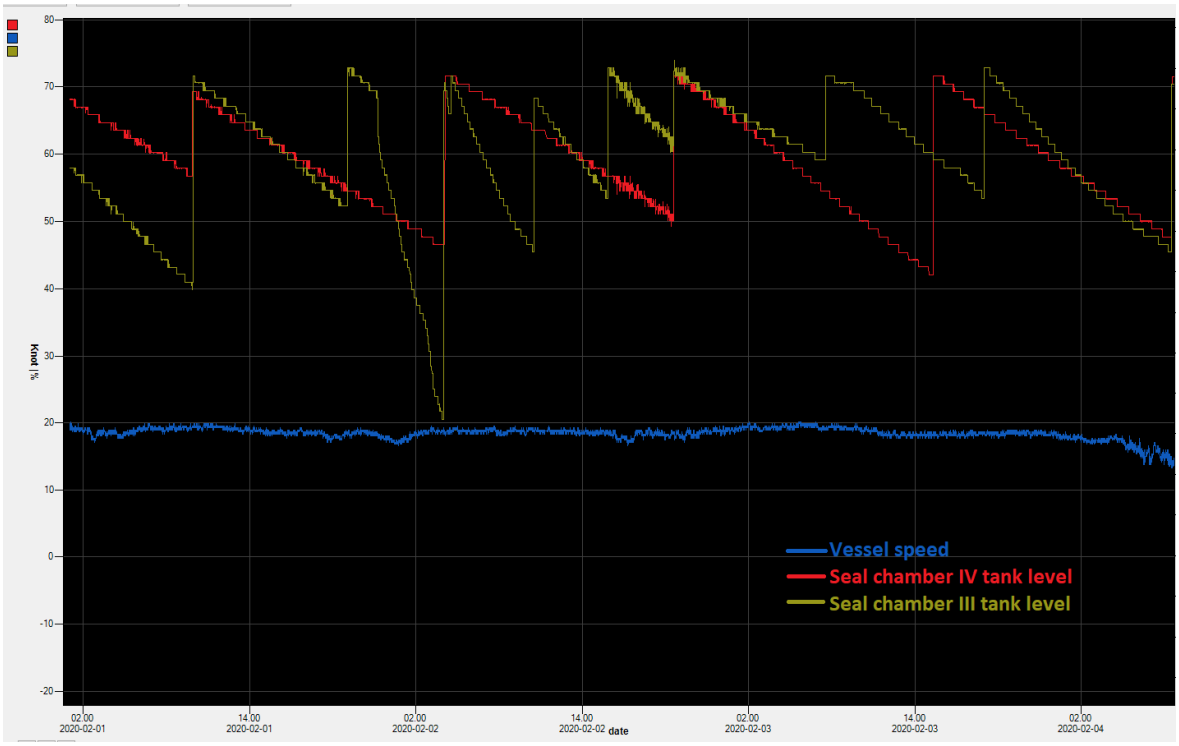

Figure 3. Increased oil consumption with used sealing rings.

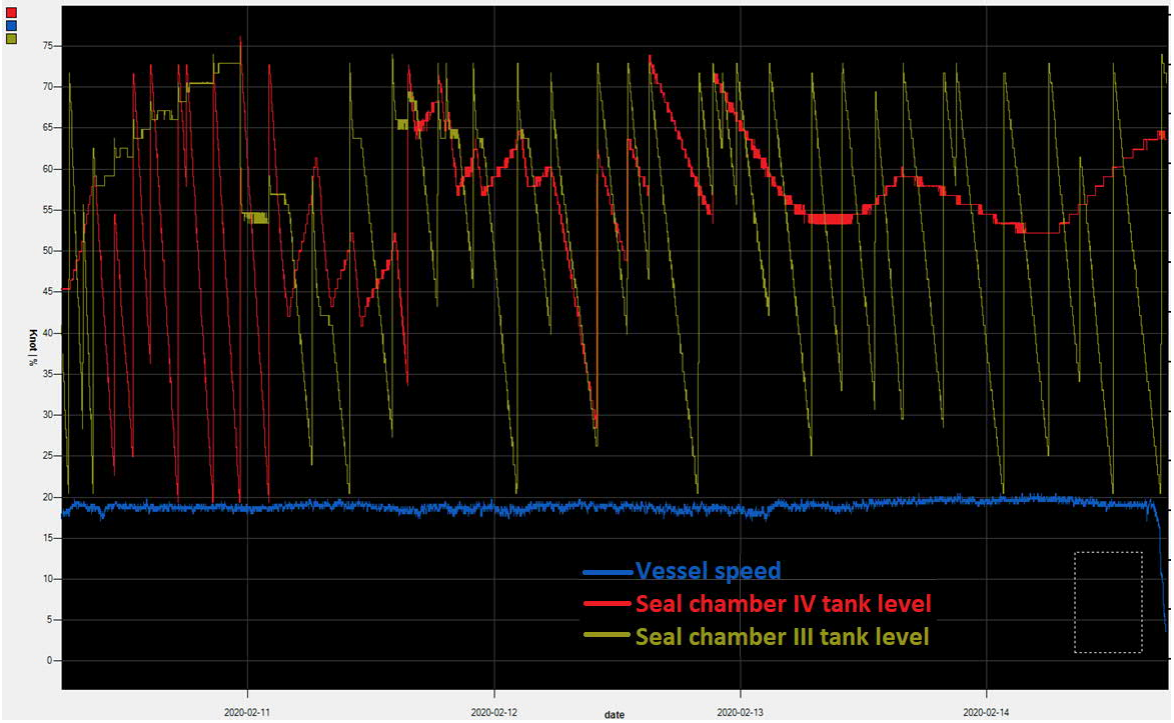

Figure 4. Rising seal chamber IV tank level and dropping seal chamber III tank level.

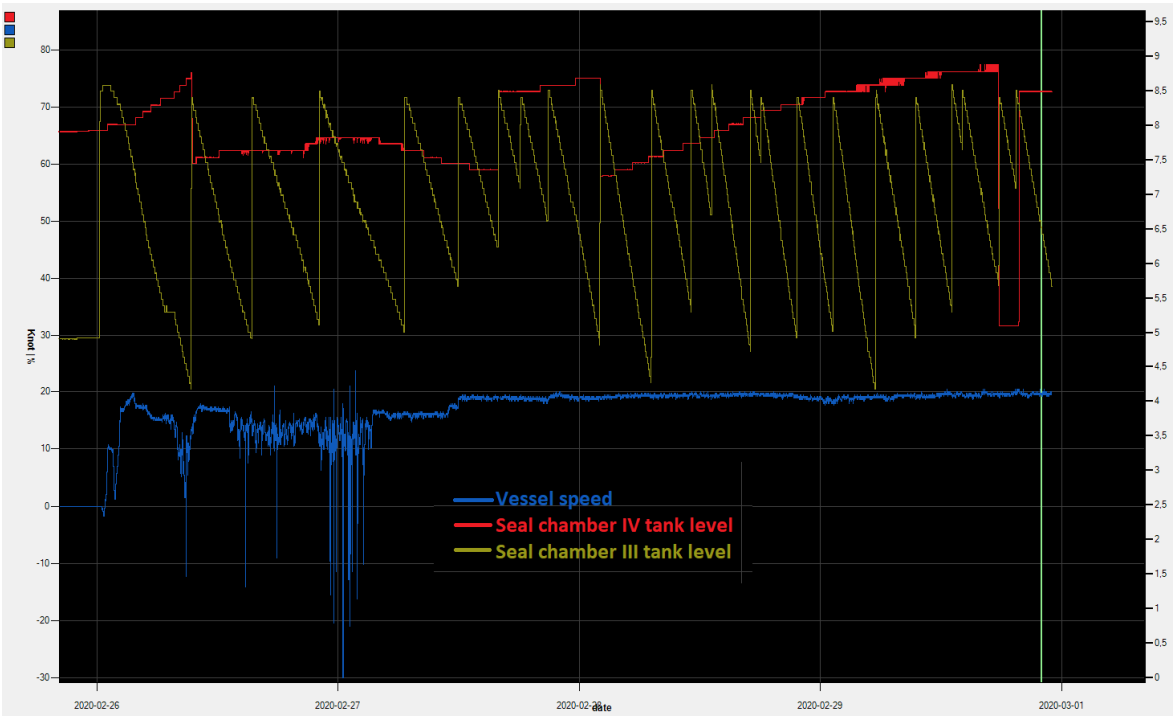

APPENDIX II

Seal manufacturer assembly drawing

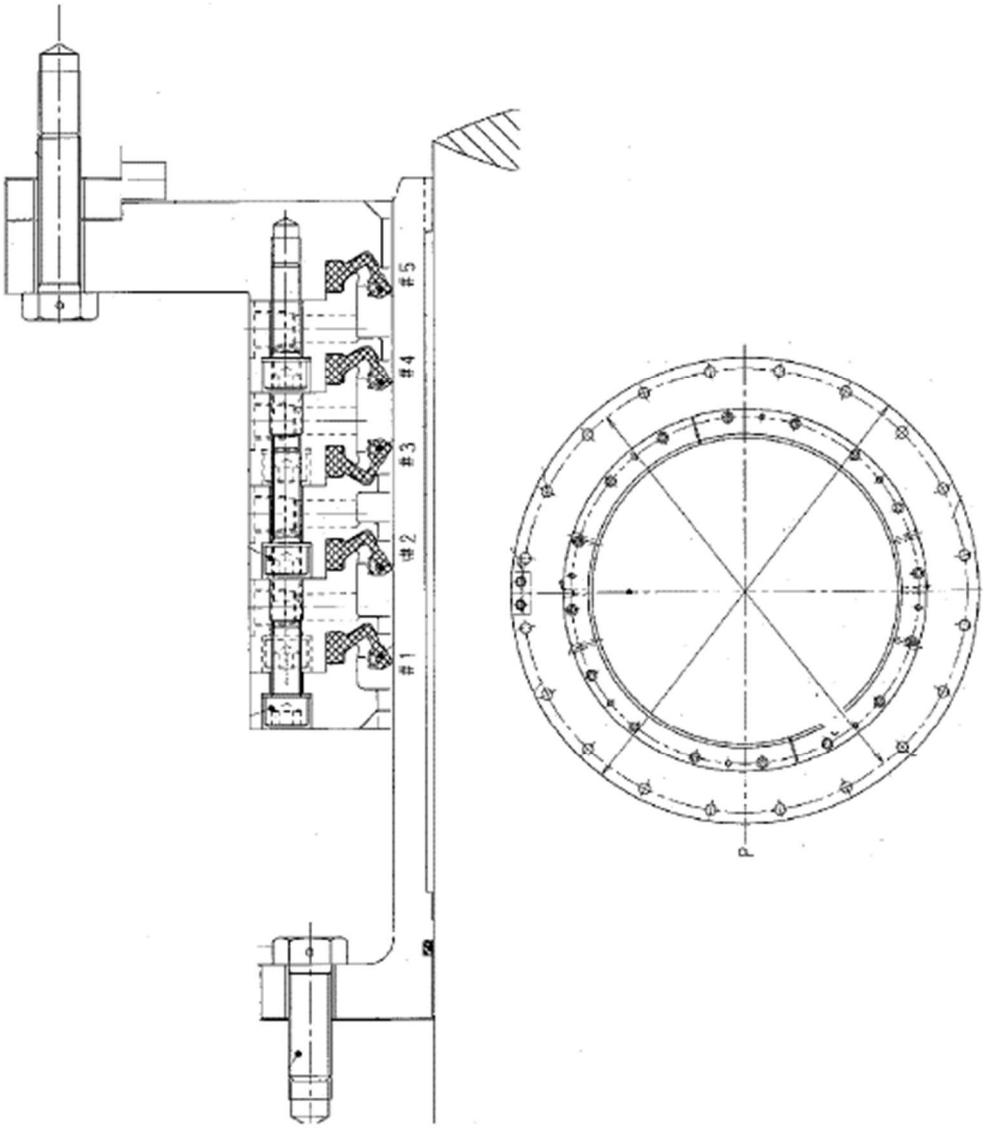

APPENDIX III

Figure 1. Sealing ring and chamber temperatures from 1,14 bar water pressure shaft speed sweep test.

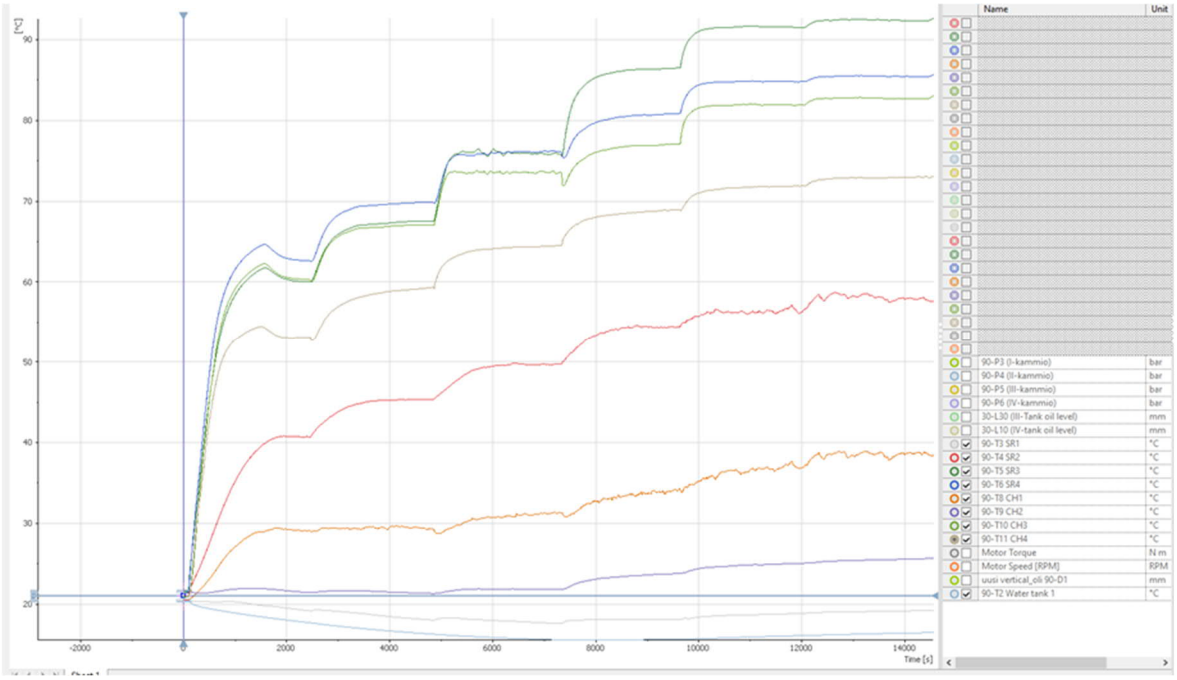

Figure 2. Sealing ring and chamber temperatures from 1,57 bar water pressure shaft speed sweep test.

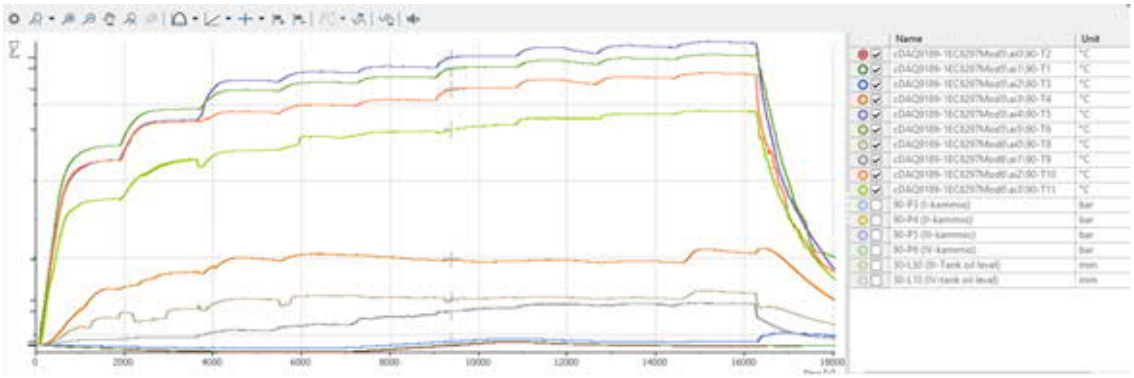

Figure 1. Seal system temperature balance with 0,12 bar pressure difference over sealing ring 3, 4,2 m/s, 5,7 m/s and 6,6 m/s shaft speeds.

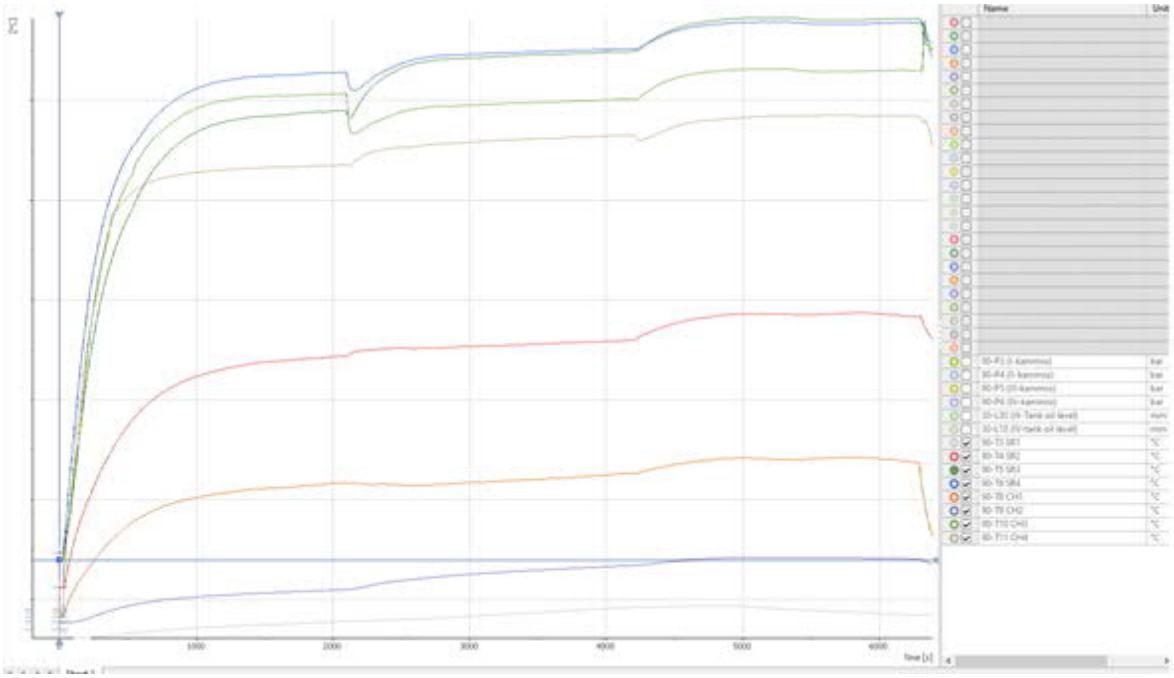

Figure 2. Seal system temperature balance with 0,22 bar pressure difference over sealing ring 3, 4,2 m/s, 5,7 m/s and 6,6 m/s shaft speeds.

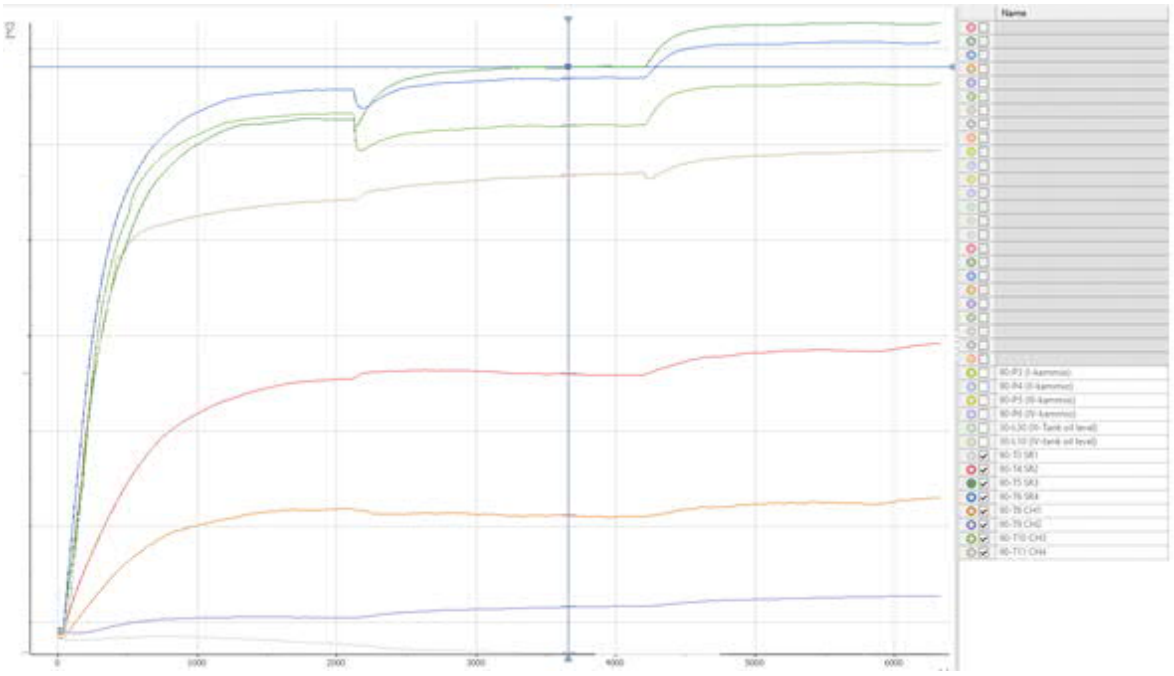

Figure 3. Seal system temperature balance with 0,4 bar pressure difference over sealing ring 3, 4,2 m/s shaft speed.

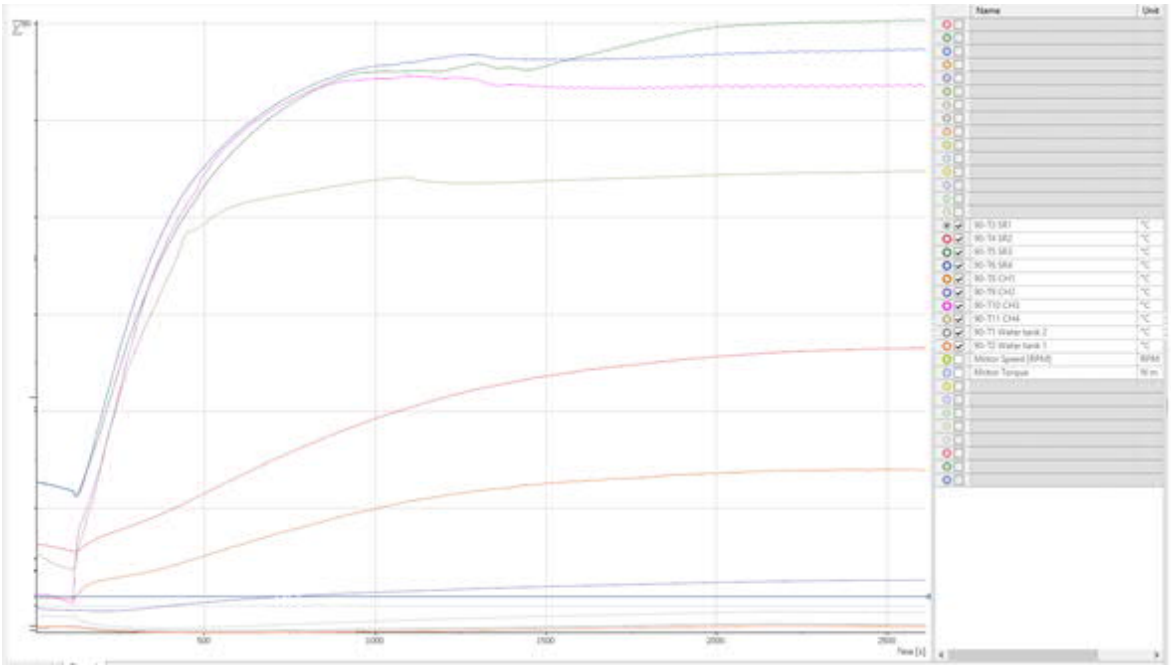

Figure 4. Seal system temperature balance with 0,4 bar pressure difference over sealing ring 3, 5,7 m/s shaft speed.

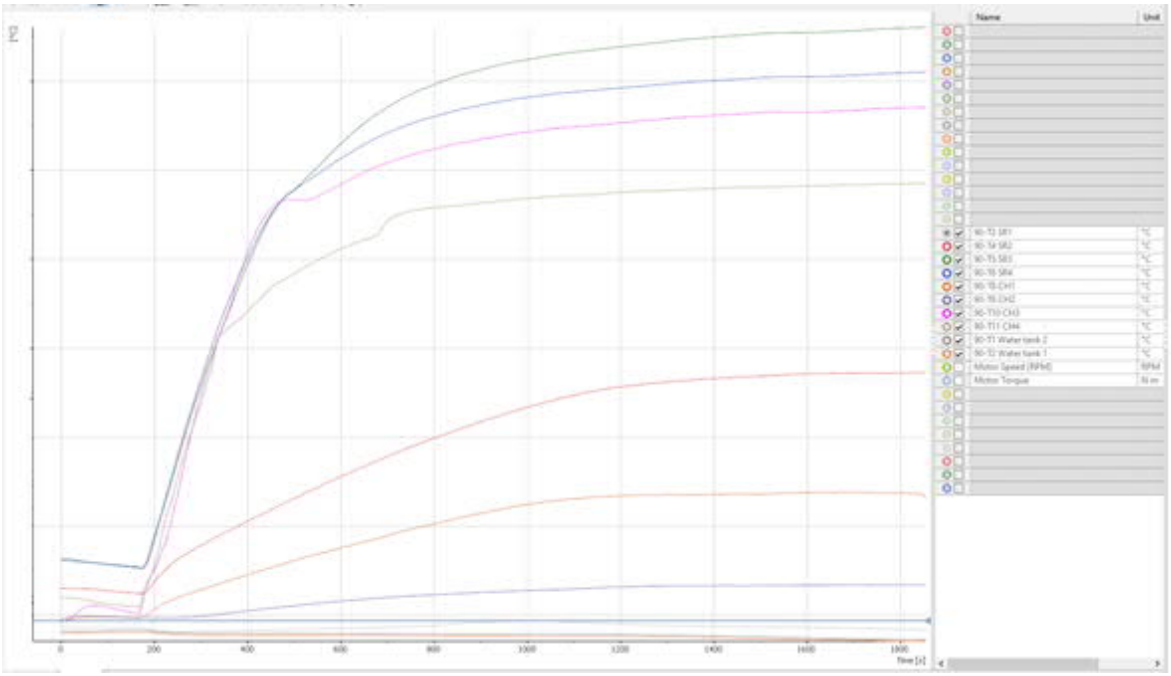

Figure 5. Seal system temperature balance with 0,4 bar pressure difference over sealing ring 3, 6,6 m/s shaft speed.

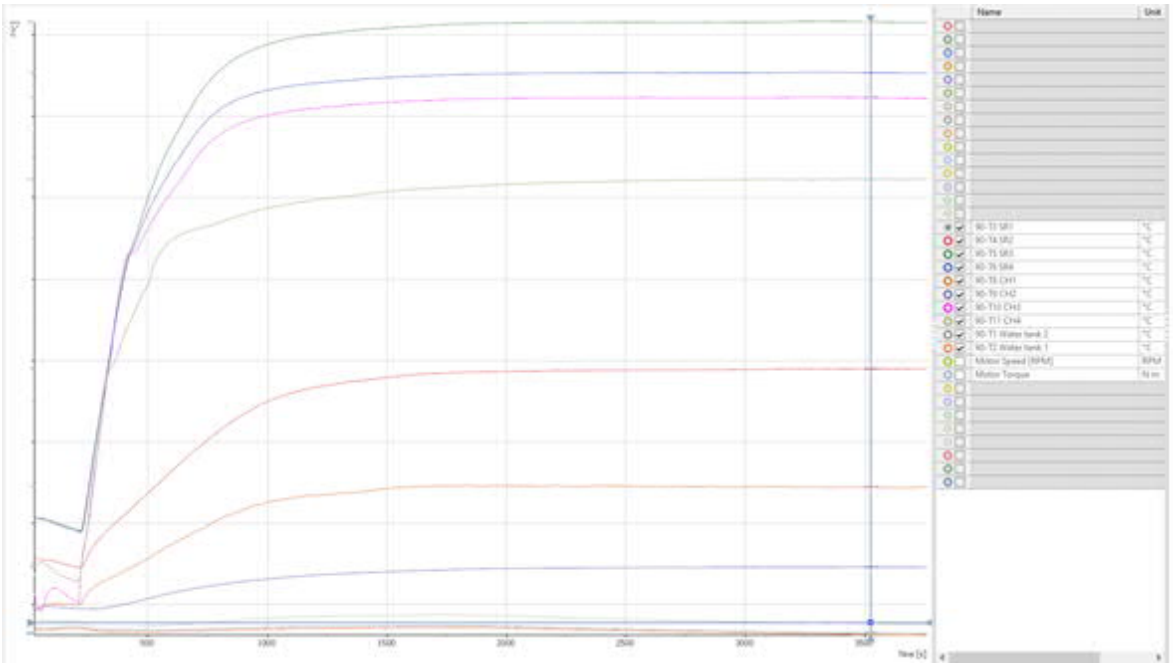

Figure 6. Seal system temperature balance with different pressure difference over sealing ring 4, 4,2 m/s shaft speed.

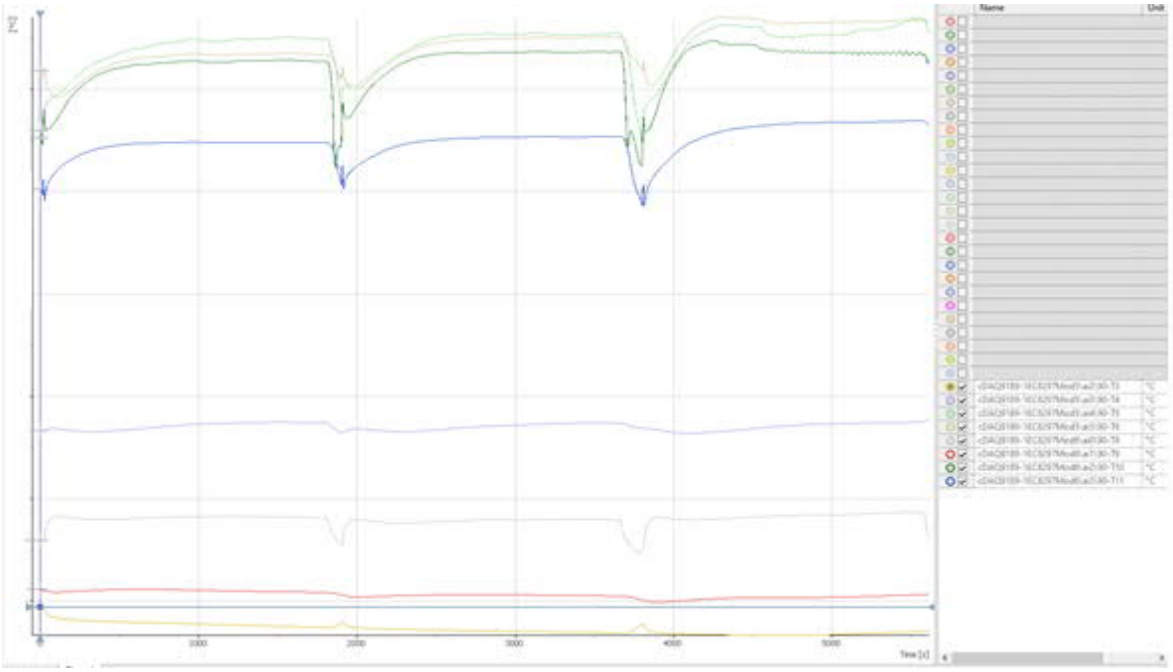

Figure 7. Seal system temperature balance with different pressure difference over sealing ring 4, 6,6 m/s shaft speed.

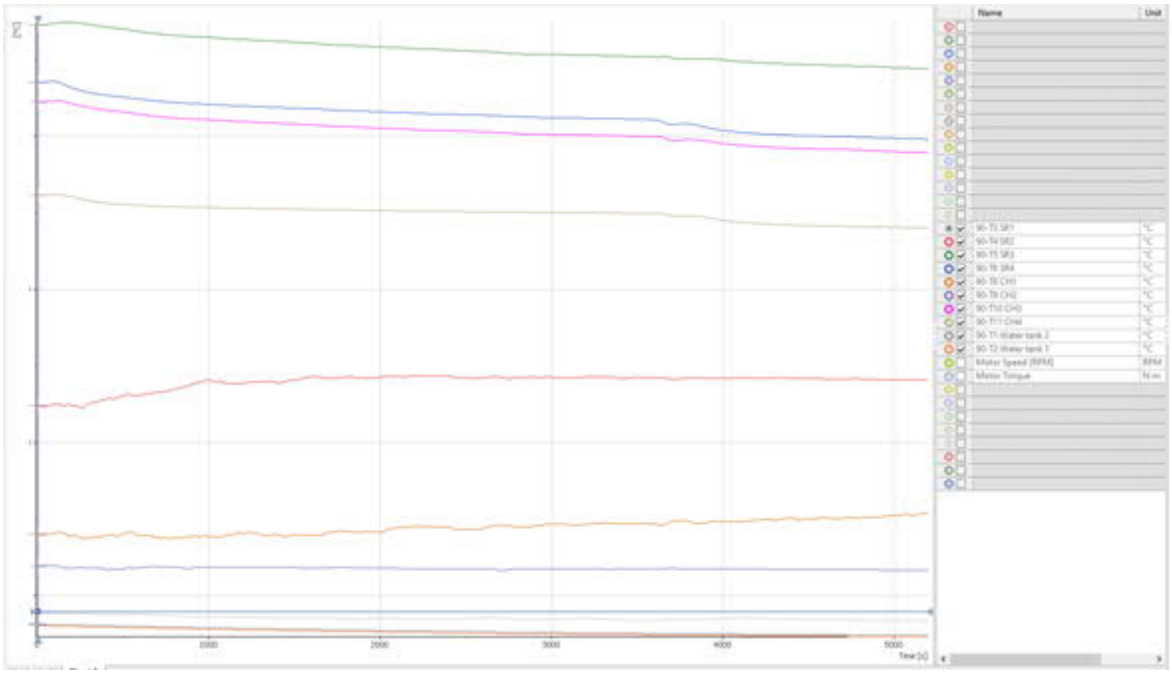

Figure 1. Temperature and pressure behavior in the first static misalignment test.

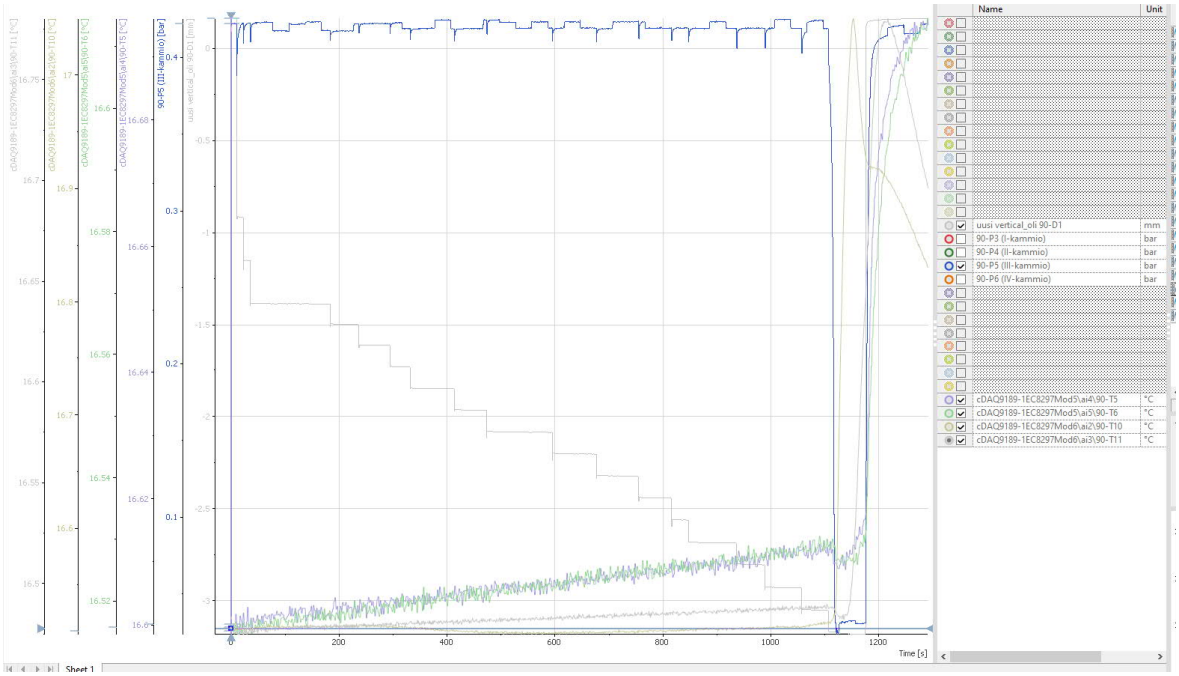

Figure 2. Seal chamber III and IV temperatures in the second static test.

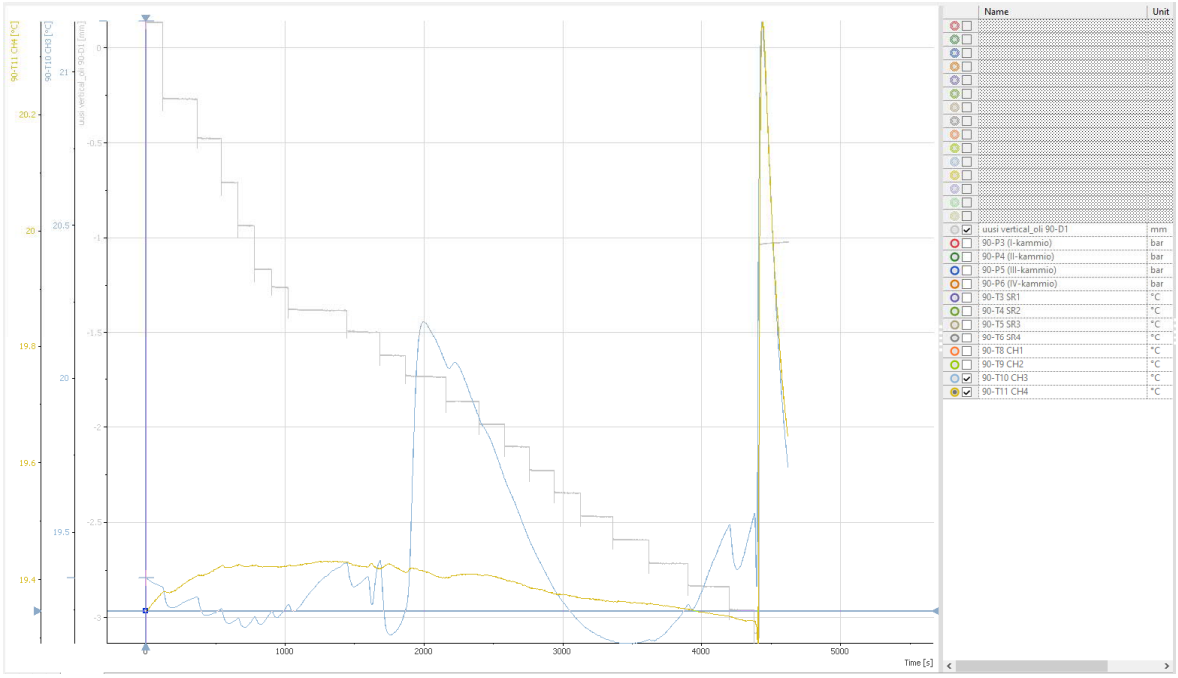

Figure 3. Sealing rings 1 and 2, and seal chambers 1 and 2 temperatures in the second static misalignment test.

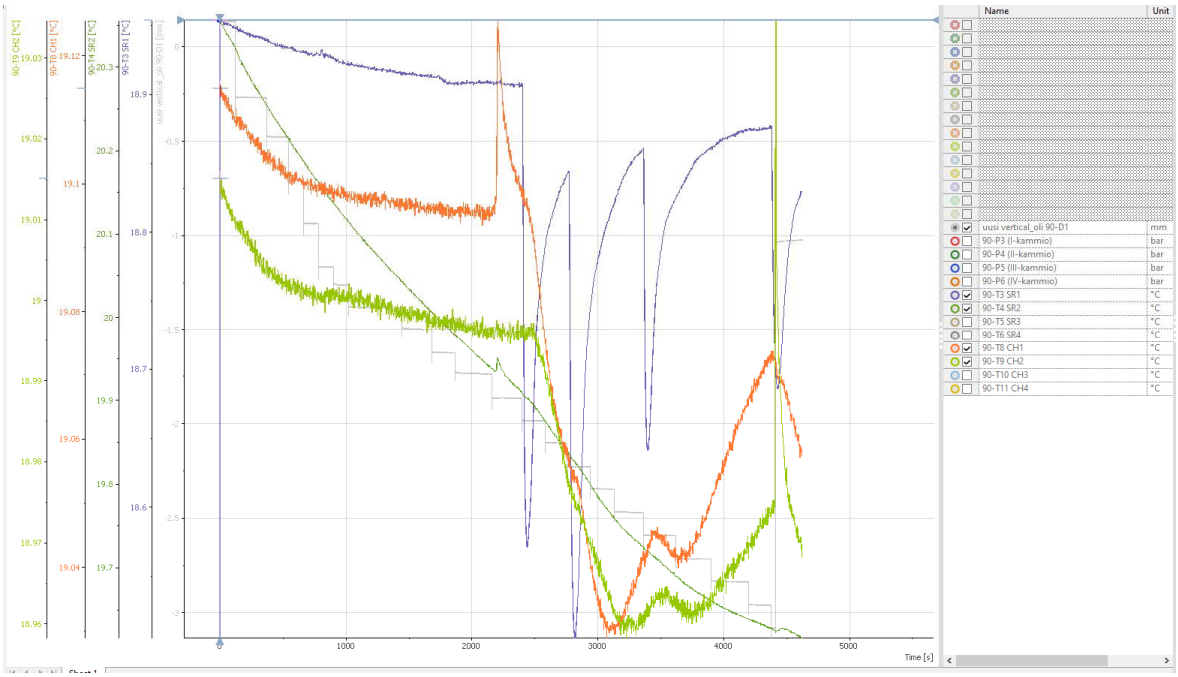

Figure 4. Sealing rings 1, 2, 3 and 4 temperatures in the third static misalignment test with 4,2 m/s shaft speed.

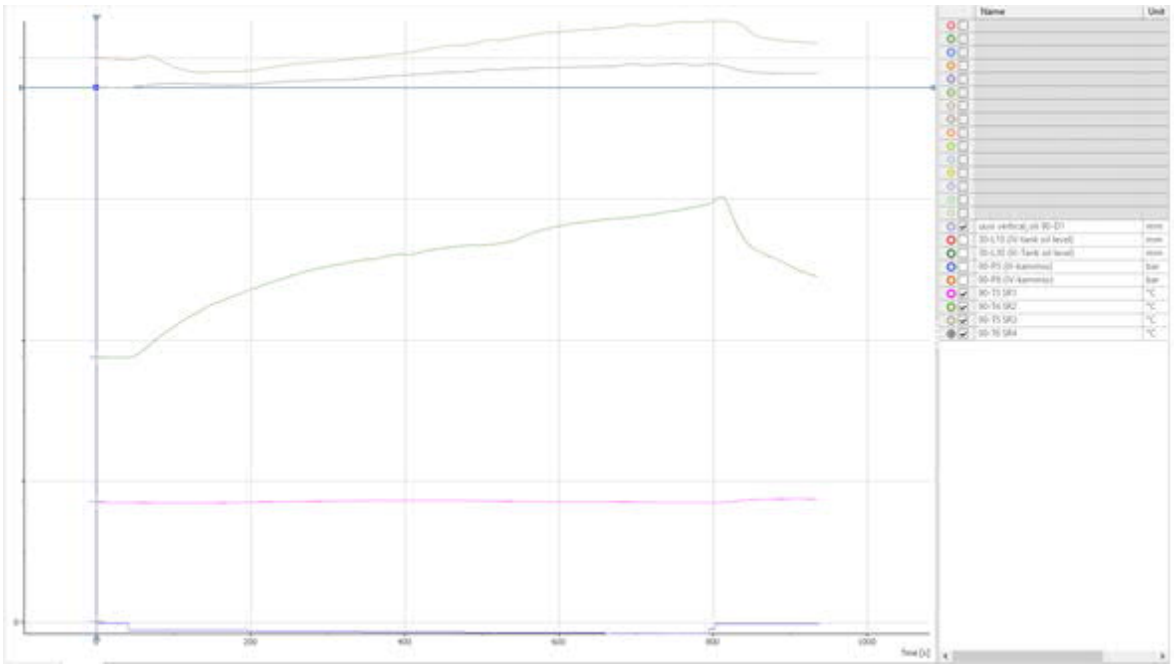

Figure 1. Pressure behavior of seal chamber I in the first dynamic misalignment test.

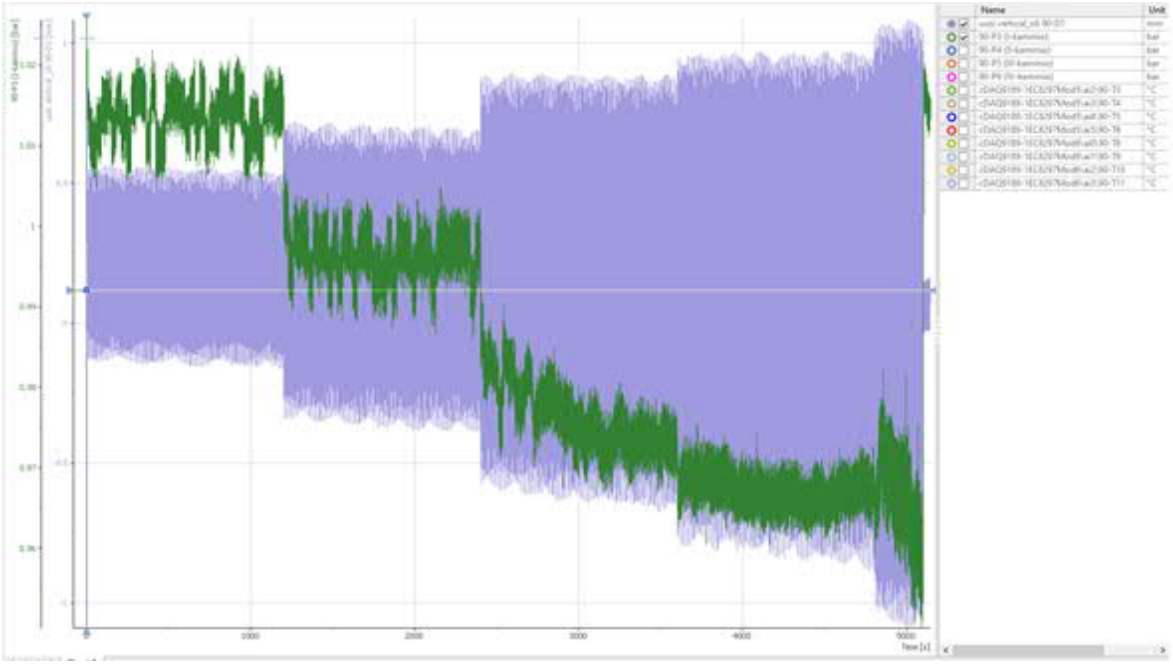

Figure 2. Pressure behavior of seal chambers I and II in the first dynamic misalignment test.

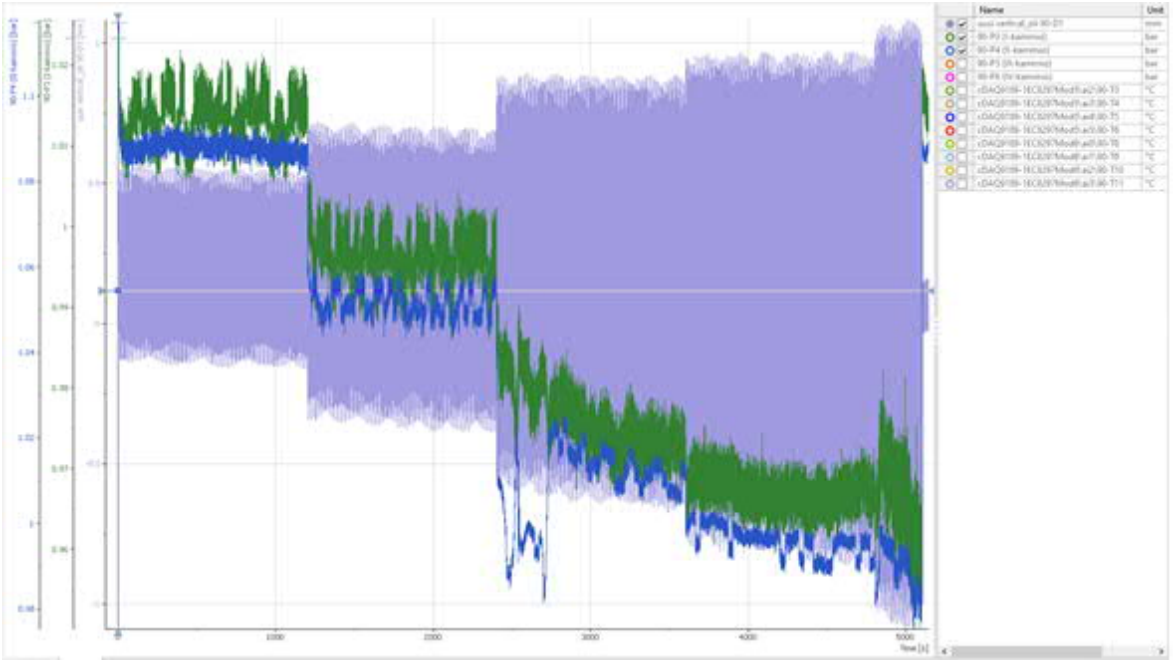

Figure 3. Pressure behavior of seal chambers I, II and III in the first dynamic misalignment test.

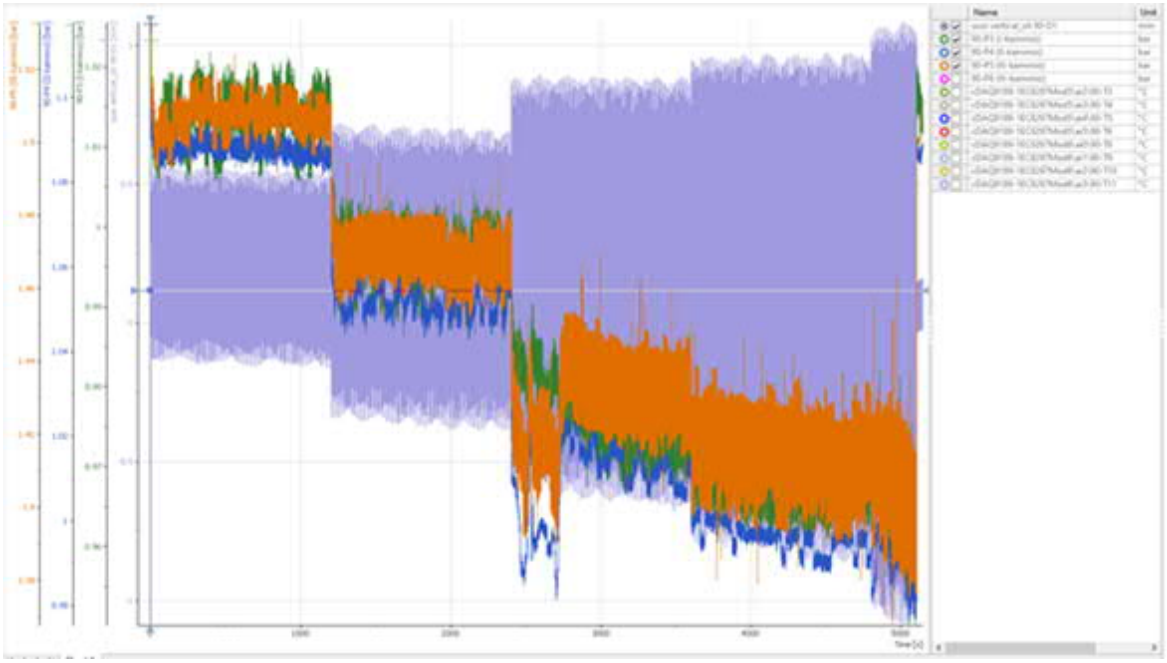

Figure 4. Pressure behavior of seal chambers I, II, III and IV in the first dynamic misalignment test.

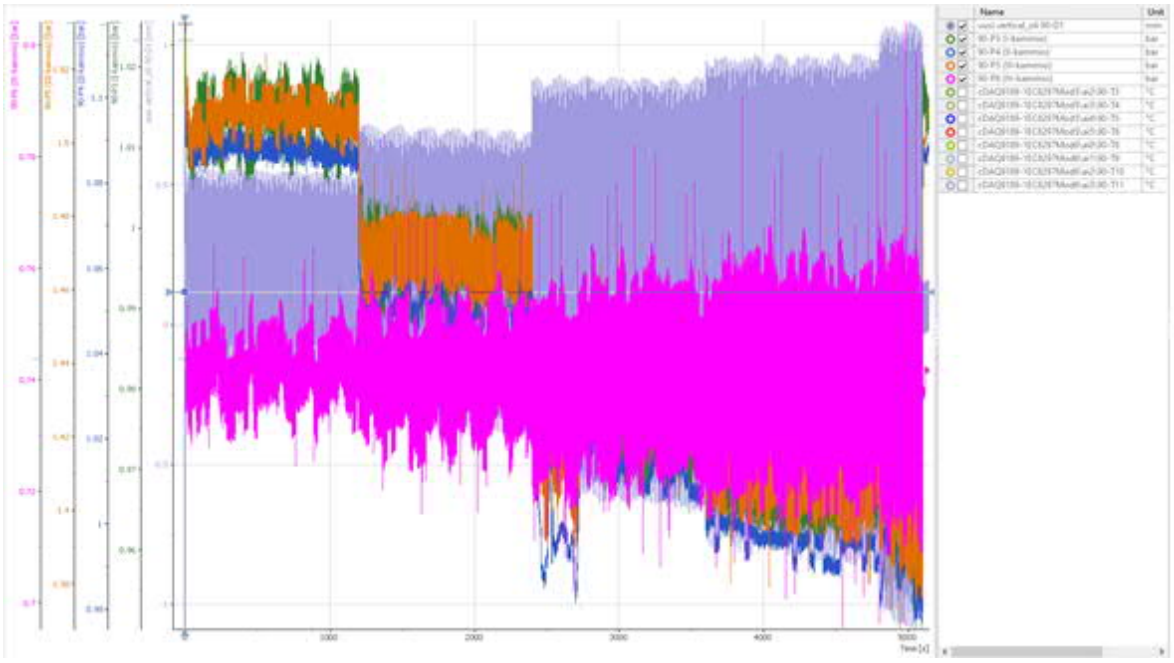

Figure 5. Pressure behavior of seal chambers I, II and III and temperature behavior of sealing rings 3 and 4, and seal chamber III in the first dynamic misalignment test.

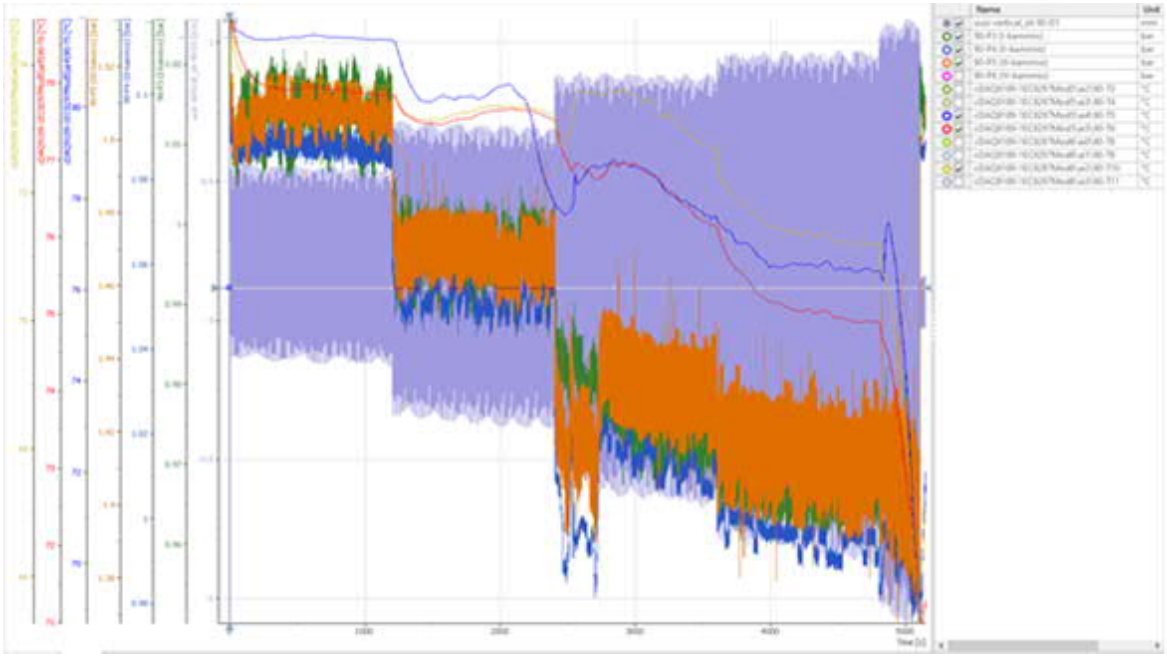

Figure 6. Overall system behavior in the second dynamic misalignment test, Δp0,4.

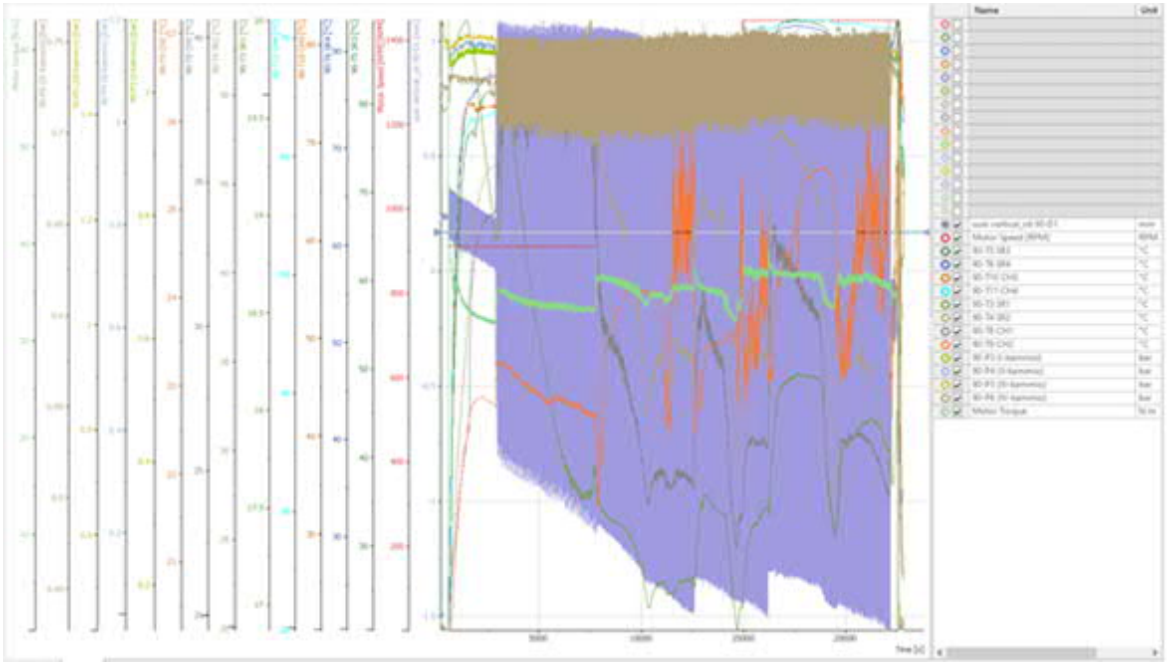

Figure 7. Overall system behavior in the second dynamic misalignment test, Δp0,22.

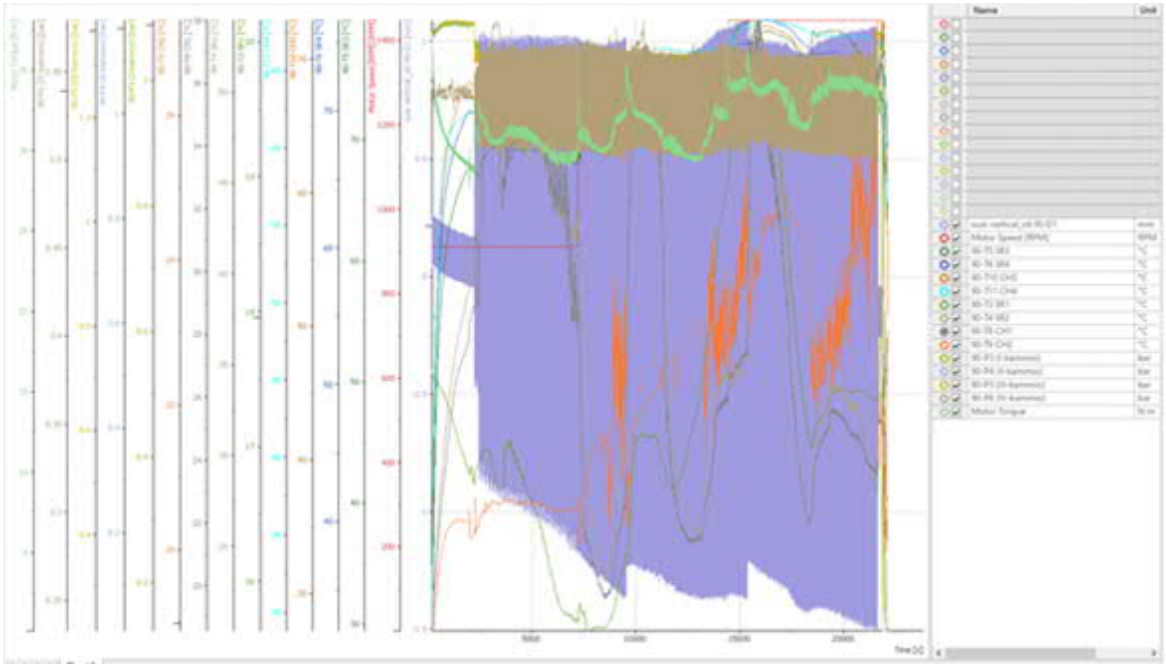

Figure 8. Overall system behavior in the second dynamic misalignment test, Δp0,14.